View metadata, citation and similar papers at core.ac.uk
brought to you by CORE
provided by Bilkent University Institutional Repository

CONJUGATED POLYMERS BASED on POLYFLUORENE DERIVATIVES and POLYPYRROLE

A THESIS
SUBMITTED TO THE DEPARTMENT OF CHEMISTRY
AND THE INSTITUTE OF ENGINEERING AND SCIENCES
OF BILKENT UNIVERSITY
IN PARTIAL FULFILLMENT OF THE REQUIREMENTS
FOR THE DEGREE OF
MASTER OF SCIENCE

By
ÜNSAL KOLDEMİR
JULY 2007

I certify that I have read this thesis and in my opinion it is fully adequate, in scope and in quality, as a thesis of the degree of Master of Science

Asst. Prof. Dr. Dönüş Tuncel

I certify that I have read this thesis and in my opinion it is fully adequate, in scope and in quality, as a thesis of the degree of Master of Science

Assoc. Prof. Dr. Ulrike Salzner

I certify that I have read this thesis and in my opinion it is fully adequate, in scope and in quality, as a thesis of the degree of Master of Science

Prof. Dr. Günay Kibarer

I certify that I have read this thesis and in my opinion it is fully adequate, in scope and in quality, as a thesis of the degree of Master of Science

Asst. Prof. Dr. Volkan Demir

I certify that I have read this thesis and in my opinion it is fully adequate, in scope and in quality, as a thesis of the degree of Master of Science

Asst. Prof. Dr. Emrah Özensoy

Approved for the Institute of Engineering and Sciences

Prof. Dr. Mehmet Baray
Director of Institute of Engineering and Sciences

ABSTRACT

CONJUGATED POLYMERS BASED on POLYFLUORENE DERIVATIVES and POLYPYRROLE

ÜNSAL KOLDEMİR

M.S. in Chemistry

Supervisor: Assist. Prof. Dr. Dönüş Tuncel

July 2007

In this thesis, a series of polyfluorene based copolymers have been prepared via Suzuki Coupling for use in light emitting diodes (LEDs). Polyfluorene based polymers are synthesized from different monomers. These polymers are characterized with spectroscopic techniques including FT-IR, UV-VIS, Fluorescence and ^{1}H, ^{13}C NMR.

Conjugated polymers are attractive chemical structures inherently allowing charge transport. However, in the solid state, conjugated polymers lack stability and form aggregates. To overcome this problem, conjugated polymers can be converted to insulated molecular wires. This can be achieved by separation of the conjugated polymer chains by a macrocycle.

In this study, encapsulation of conjugated polymers is tried with two methods. First method is to encapsulate the polymer main chain by macrocycles. Polypyrrole based polypseudorotaxane is prepared in this way. Pyrrole is complexed with the cucurbit[6]uril (CB(6)) and following chemical oxidation by $FeCl_3$ in acidic medium yields the desired polypseudorotaxane. Spectroscopic investigations such as FT-IR, UV-VIS, Fluorescence and ^{1}H-NMR confirm the formation of polypyrrole based polypseudorotaxane.

The second method involves the rotaxanation of the polymer side chains. For this purpose, fluorene based monomers are chosen because the 9^{th} position of fluorene can be easily functionalized. After attaching suitable groups to the 9^{th} position of fluorene, the rotaxane formation was attempted via 1,3 dipolar cycloaddition in the presence of CB(6).

A white light emitting diode is prepared using a hybrid inorganic and organic material based system. Prepared conjugated polymers were used in white light generation. Good results are obtained with high CRI indices. Also the thermal stability of the conjugated polymers is studied by FT-IR, UV-VIS and Fluorescence spectroscopic techniques under heat exposure.

Keywords: Pseudopolyrotaxanes, cucurbit[6]uril, Suzuki Coupling, conjugated polymers, polyfluorene, polypyrrole, white light emitting diode.

ÖZET

POLİFLOREN TÜREVLERİ ve POLİPİROL TABANLI KONJUGE POLİMERLER

ÜNSAL KOLDEMİR

Kimya Bölümü Yüksek Lisans Tezi

Tez Yöneticisi: Doç. Dr. Dönüş Tuncel

Temmuz 2007

Bu tezde, ışık yayan diyotlarda kullanılması amacıyla Suzuki Birleştirme yöntemi ile bir seri polifloren tabanlı kopolimerler hazırlanmıştır. Polifloren tabanlı polimerler farklı bant aralığına sahip monomerlerden sentezlenmiştir. Bu polimerler FT-IR, UV-VIS, Floresans ve ^{1}H, ^{13}C NMR spektroskopi yöntemleri ile analiz ve karakterize edilmiştir.

Konjüge polimerler doğal olarak yük taşıyabildiklerinden çok ilgi çekicidir. Ama, katı halde, konjüge polimerler kararlılıklarını kaybedip bir araya toplanırlar. Bu sorunu aşmak için, konjüge polimerler molekül düzeyde izole olmuş tel haline getirilebilir. Bunu sağlamak için, konjüge polimerler, büyük içi boş kovan yapılarla sarmalanır.

Bu çalışmada, konjüge polimerlerin sarmalanması iki metod izlenerek yapılmıştır. İlk metodda, polimerin temel zincirleri büyük içi boş kovan yapılar içine sokulmuştur. Polipirol tabanlı südopolirotaksanlar bu yöntemle hazırlanmıştır. Pirol, CB(6) ile kompleks oluşturduktan sonra asidik ortamda $FeCl_3$ ile kimyasal olarak yükseltgenerek istenilen südopolirotaksan üretilmiştir. FT-IR, UV-VIS, Floresans ve ^{1}H-NMR spektroskopi yöntemleri polipirol tabanlı südopolirotaksan oluşumunu kanıtlar.

İkinci metodda ise, polimerlere bağlanmış yan zincirlerin rotaksanlanması vardır. Bu amaçla, floren tabanlı monomerler seçilmiştir. Çünkü florenlerin 9. pozisyonuna istenilen fonksiyonel gruplar kolayca eklenebilir. Florenin 9 pozisyonuna uygun gruplar eklendikten sonra, rotaksan oluşumu,CB(6)'nın katalizlediği 1,3-dipolar katılma reaksiyonu kullanılarak denenmiştir.

Beyaz ışık diyotu inorganic-organik tabanlı iki malzemeden oluşan melez sistem ile hazırlanmıştır. Hazırlanan polimerler beyaz ışık üretiminde kullanılmıştır. Yüksek CRI indisli sonuçlar elde edilmiştir. Ayrıca, konjüge polimerlerin sıcaklığa maruz bırakıldıklarındaki kararlılılıkları FT-IR, UV-VIS ve Florasans spektroskopi yöntemleri ile incelenmiştir.

Anahtar Kelimeler: Südopolirotaksanlar, kukurbit[6]yuril(CB6), Suzuki Birleştirme Yöntemi, konjüge polimerler, polifloren, polipirol, beyaz ışık yayan diyot.

ACKNOWLEDGEMENT

I would like to express my sincere appreciation to my advisor Assist. Prof. Dr. Dönüş Tuncel for her clear guidance, insight, encouragement and supervision throughout the research.

I am thankful to Prof. Dr. Günay Kibarer, Assoc. Prof. Dr. Ulrike Salzner, Asst. Prof. Dr. Emrah Özensoy and Asst. Prof. Dr. Hilmi Volkan Demir for reading my thesis and their valuable feedbacks.

I wish to thank Ali Turan Görgü, Dr. Fikret Koç for their valuable comments and encouragement.

I would like to express my special thanks to my roommate, Levent Subaşı for his understanding throughout my studies.

I want to send my sincere thanks to Hasan Burak Tiftik, Oğuzhan Çelebi, Mustafa Fatih Genişel, Sedat Nizamoğlu, Adnan Hazar, İ. Erkin Gönenli, Olga Samarskaya, İbrahim Karaman, Caner Ünlü, Abidin Balan, İbrahim Hocaoğlu, Emine Yiğit, and all present and former members of Bilkent University Chemistry Department for their patience and kind supports during my study.

Special thanks due to Fatma Ayhan for her deepest love, never ending supports.

Lastly, I am grateful to my parents and my sister who encouraged and listened to me throughout my studies.

TABLE OF CONTENTS

LIST OF FIGURES

LIST OF SCHEMES

LIST OF TABLES

ABBREVIATIONS

^{13}C-NMR	Carbon13-Nuclear Magnetic Resonance
CDT	Cambridge Display Technology
CRI	Color Rendering Index
CIE	Commission Internationale de l'Eclairage
CB(6)	Cucurbit[6]uril
CD	Cyclodextrin
$CDCl_3$	Deuterated Chloform
D_2O	Deuterated Water
DMF	Dimethyl Formamide
DMSO	Dimethyl Sulfoxide
FT-IR	Fourier Transform-Infrared
T_g	Glass Transition Temperature
GPC	Gel-Permeation Chromatography
HOMO	Highest Occupied Molecular Orbital
IMW	Isolated Molecular Wires
LED	Light Emitting Diode
LUMO	Lowest Unoccupied Molecular Orbital
MMC	Montmorillonite Clay
M_n	Number Average Molecular Weight
OLED	Organic Light Emitting Diode
PANI	Polyaniline
PPV	Poly Para(Phenylene vinylene)
PPy	Polypyrrole
^{1}H-NMR	Proton-Nuclear Magnetic Resonance
Py	Pyrrole
rt	Room Temperature
UV-VIS	Ultra Violet-Visible
WLED	White Light Emitting Diode
M_w	Weight Average Molecular Weight

CHAPTER 1

INTRODUCTION

1.1 General Considerations:

Polymers like plastics dominate our daily life as they are light and easily manufactured. Two cornerstone events namely, that of observation of electrical conductivity and that of discovery of the remarkable optical properties, stimulated research on polymers starting up new applications. Traditional polymers are treated as insulator materials until it was seen that doped polyacetylene shows dramatic changes in electrical conductivity.[1] By doping, electrons are added or removed with strong oxidizing or reducing agents forming polaron or soliton states causing high electrical conductivity. Studies on the electrical conductivity properties were followed by the research on investigation of optical properties. Besides, conjugated polymers attracted great interest for Organic Light Emitting Diode (OLED) applications as they show interesting optical features after the pioneer work of Friend *et. al*. obtaining green-yellow light from poly(*p*-phenylene-vinylene) (PPV).[2]

Utilization of conjugated polymers is quite feasible in large-area micrometer size devices because polymers can be processed from solution. So far applications of conjugated polymers to display technology[2,3,4,5,6] (OLED applications), solar cell systems[7] (photovoltaics), biosensors[8] and lasers[9,27] were presented. Because of their inherent electrical and optical properties conjugated polymers are called organic semiconductors. Their structural properties lead them to be comparable to inorganic semiconductors in terms of their electrical and optical properties. Figure 1.1 shows some examples of conjugated polymers.

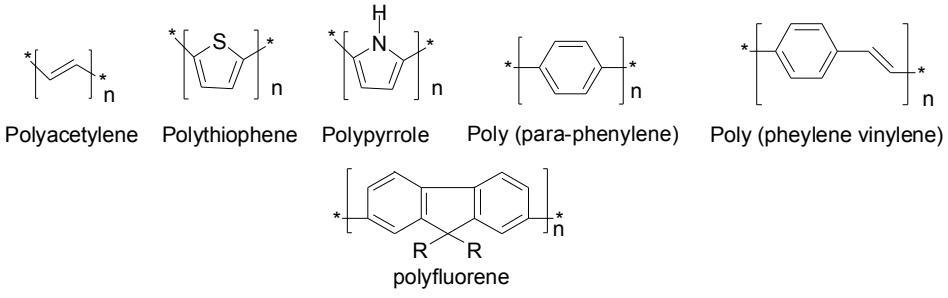

Fig. 1.1- Examples of conjugated polymers

1.2 The Importance of π Bonding

The unique structure of the conjugated polymers comes from the conjugated bonds, which are composed of alternating double and single bonds. The alternating double and single bonds are essential to these structures. Single bonds keep the molecule intact upon excitation of the delocalised π electrons. Delocalised π bonds form throughout the polymer chain enhancing the conduction of the charge carriers.

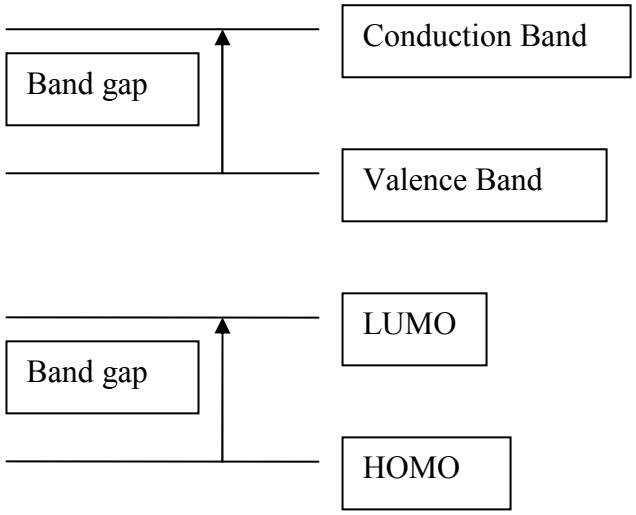

Fig. 1.2- Depiction of band structure in inorganic and organic semiconductors

In a conjugated polymer, the combination of π bonding levels and π* antibonding levels form a band structure. The bonding levels become the valence band and the antibonding levels can be named as the conduction band. In Figure 1.2 depiction of the band structure in an organic semiconductor is presented. The organic terms of Highest Occupied Molecular Orbital (HOMO) and Lowest Unoccupied Molecular Orbital (LUMO) are similar in meaning to the inorganic nomenclature of Valence Band and Conduction Band. Excitation promotes an electron from a bonding level to the antibonding level. This π → π* electron transition can be observed by UV spectroscopy. The band gap, energy difference between HOMO and LUMO, of conjugated polymers is energetically comparable to inorganic semiconductors. This band gap has energy in the range of 1.5-4 eV.

1.3 LED Structure

So far conjugated polymers found wide applications in display technology. The basic structure of the displays is Organic Light Emitting Diode (OLED). As illustrated in Figure 1.3, an OLED device consists of a sandwich containing mainly three parts, an anode, a cathode and a conducting material. As anode electrode a transparent electrode with a large work function such as Indium tin oxide (ITO) is mainly chosen. As a conducting material, a layer of OLED material, the conjugated polymer, which is less than 100 nm thick, is utilized. Lastly, for cathodic material a metallic electrode with a low work function, typically calcium is preferred.[5] The polymer in between the electrodes is electrically driven with current typically at a bias of about 5V and consequently, electrons and holes are injected at each electrode where they move into the conducting polymer under electrical bias. In conducting polymer, electrons and holes are carried through where they combine to produce light.

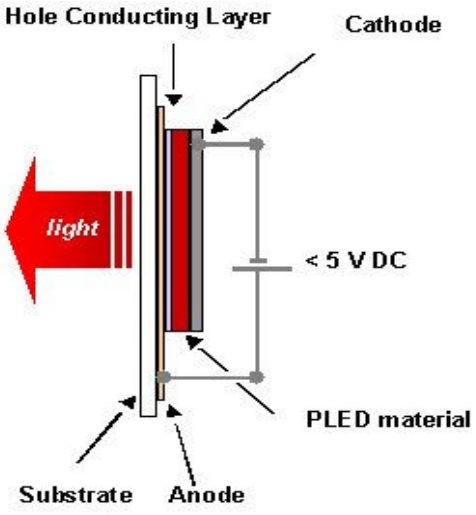

Fig. 1.3- Representation of a LED[10]

The generation of a LED device using conjugated polymers goes back to the 1990s. For the first time, it was observed at the Cambridge University that PPV emits yellow-green light when sandwiched between two electrodes.[2] As outlined in the Scheme **1** below, PPV was synthesized through two steps. Firstly the precursor polymer was prepared from α,α'-dichloro-p-xylene through polymerization of the

sulfonium salt intermediate in methanol. Dialysis with water followed by solvent removal and subsequent vacuum evaporation yielded homogeneous PPV films. The obtained polymer showed a strong photoluminescence band at 2.2 eV in the green-yellow region of the spectrum.

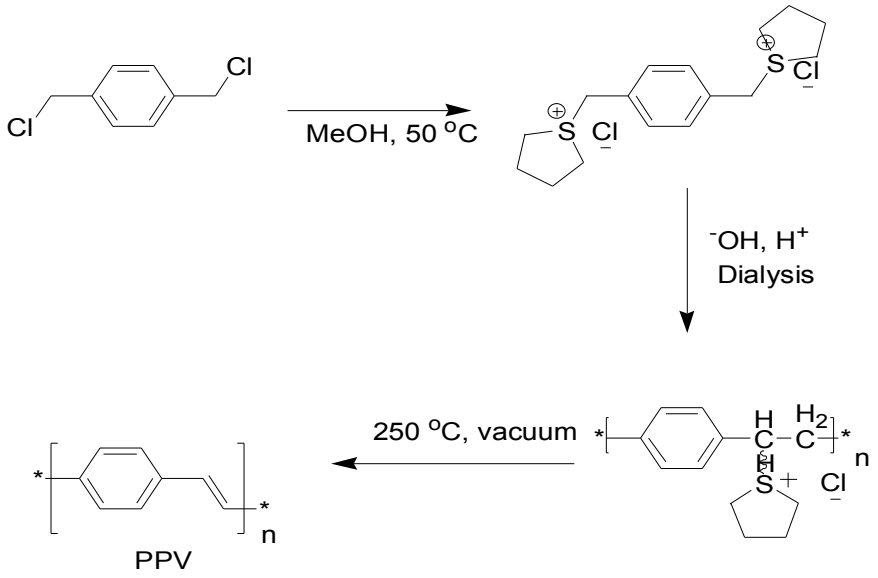

Scheme 1.1- The synthesis of PPV[2]

This discovery led to the enormous research on the preparation of various conjugated polymers that emit different colors from violet to red. Chemical modifications were made on PPV based polymers for red and green emission. However a blue light emitting polymer from PPV based polymers was not achieved as blue light required a high band gap material. Instead polyfluorene derivatives were used mostly for blue light emitting because they have high band gap. To tune the band gap, different co-monomers were used. For example, coupling a thiophene monomer with fluorene monomer generates green light in the longer wavelength of the visible spectrum. The entire visible range can be tuned by coupling fluorene monomers with narrow band gap comonomers as seen below in Figure 1.4 for generation of red, orange, and white light.

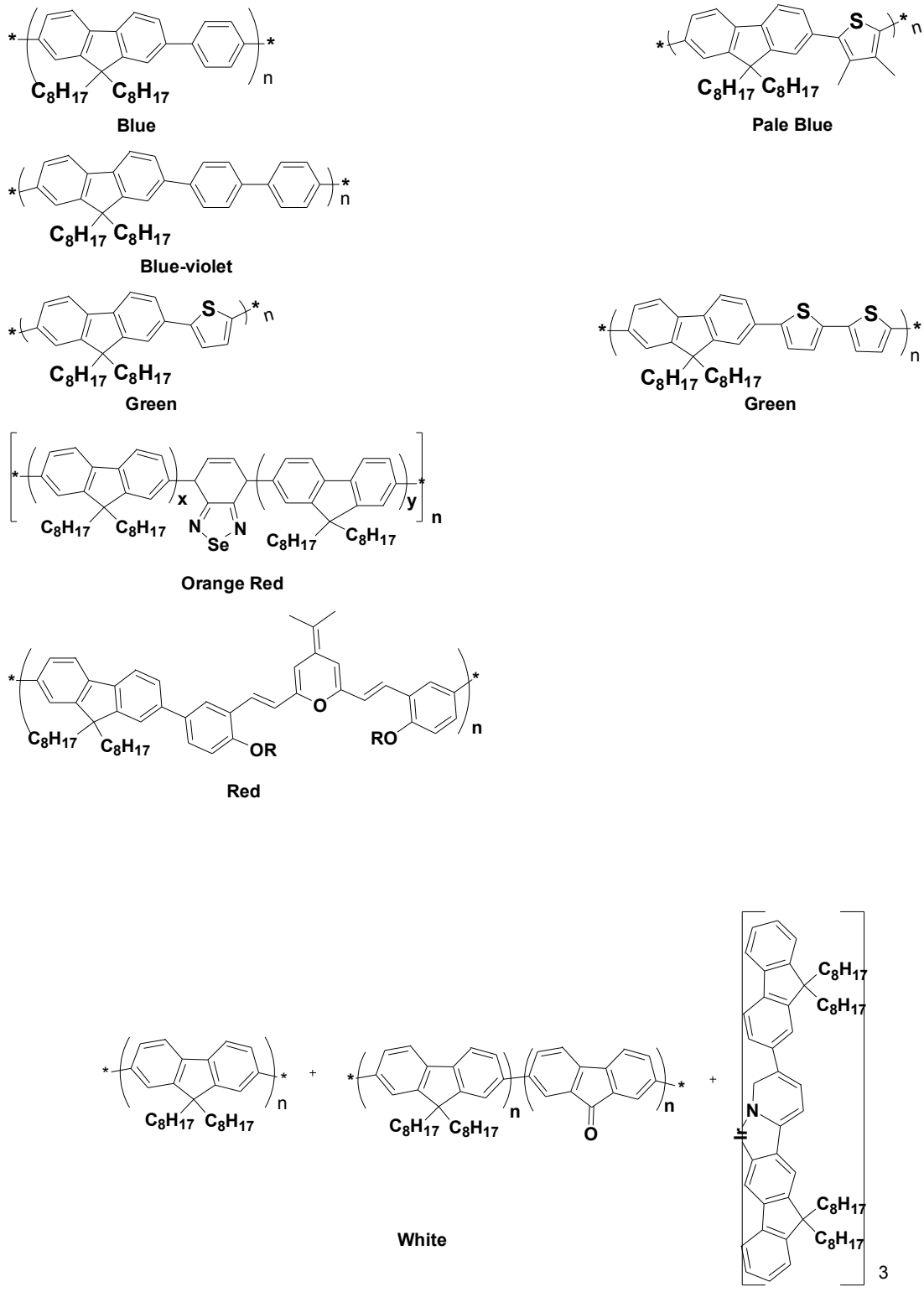

Fig. 1.4- Representations of conjugated polymers emitting specific colors

LEDs made of conjugated polymers attracted great attention as they combine the properties of metals and plastics. LEDs based on conjugated polymers have basic advantage that polymers can be easily processed from solution with spin coating or dipping techniques. Hence the preparation of a LED becomes easier and consumes less time. As polymers are processed from solution, they can be coated on large areas with any shape. Thus it will be commercially possible to fabricate flexible displays. Additionally, as polymers can be spin-coated, it will be possible to prepare ultra thin devices. Furthermore, polymers are lightweight allowing them to be used in portable devices. However, in display technology they must meet some conditions such as high luminescent efficiency and long lasting light production. Therefore, the performance is highly dependent on fluorescent quantum efficiency of polymers. For a full color display three main colors are important; red, green, and blue. So far as revealed by Cambridge Display Technology (CDT) company, green and red emitting polymers showed good efficiencies and long lasting light production to be used in a commercial electronic product. However, a stable blue LED, offers a real challenge showing low efficiencies.[10]

1.4 Polyfluorene Family

Polyfluorene and its derivatives are used as blue light emitting polymers. Polyfluorenes aided in exploding research on light emitting diodes beause they show exceptional electrooptical properties.[11] Fluorene based polymers are the most targeted molecules because they offer strong blue fluorescence, chemical and photochemical stability as well as good synthetic accessibility. Polyfluorenes are the only family of conjugated polymers that span the entire visible range with high efficiency and low operating voltage. Polyfluorenes are used in blue light emission as they posses high band gap and its band gap can be tuned by incorporating co-monomers to produce different colors. As mentioned above, a stable blue emission is still under investigation. Because, when polyfluorenes are used in LEDs, they lack stability in the solid state. They form aggregates which decreases the solubility of the polymers. And then polyfluorenes having side chains at the C9 position show some excimer emission.[11] Excimers are dimerised units in the excited state that emit at lower energies. This excimer emission affects the color of the emission and the

lifetime of the light emitting diodes. In the next section, possible causes of this excimer emission, fluorescence quenching and related subjects will be discussed in detail.

In Figure 1.5 structure of a polyfluorene based polymer is depicted. C9 is chemically very important to polyfluorene family. C9 allows for certain modifications that increase the polymers processability without disrupting the delocalization of the π bonds. Alkyl chains added at C9 makes the polymer soluble in various organic solvents. This is important for the preparation of the soluble polymers through coupling reactions like Suzuki, Heck and Stille coupling. Additionally solubilizing groups like ammonium, sulfonate, phosphonate, carboxylate can be added to this alkyl chain pendantly to dissolve the polymer in water which is friendly to the environment.

Polyfluorene homopolymer Fluorene-type copolymer

Fig. 1.5- Polyfluorene homopolymer and copolymer

1.5 Fluorescence Quenching

The problem observed with the polyfluorene family is that they are not stable during the course of functioning in the solid state. A red shift is observed, which is undesirable. In the solid state the conjugated π bonds probably interact with other π bonds as they stack over each other which is called aggregation. Hence two chains behave as a single chain and emit at the longer wavelengths By this way charge carrying pathway becomes 3-D rather nonlinear. Furthermore, fluorescence quenching can be observed in polyfluorene family. Fluorescence quenching is defined as the decrease in the intensity of fluorescence by a wide variety of processes.[12] Quenching can occur by deactivation of the excited state in contact with a quencher. The relaxation process can lead to other processes without any light

emission. The dissipated energy for excitation of the electron can be in the form of heat, rather than light. Figure 1.6 shows a non-radiative process. The quenching processes and possible causes will be discussed in a detail occurring in polyfluorene family in the following section.

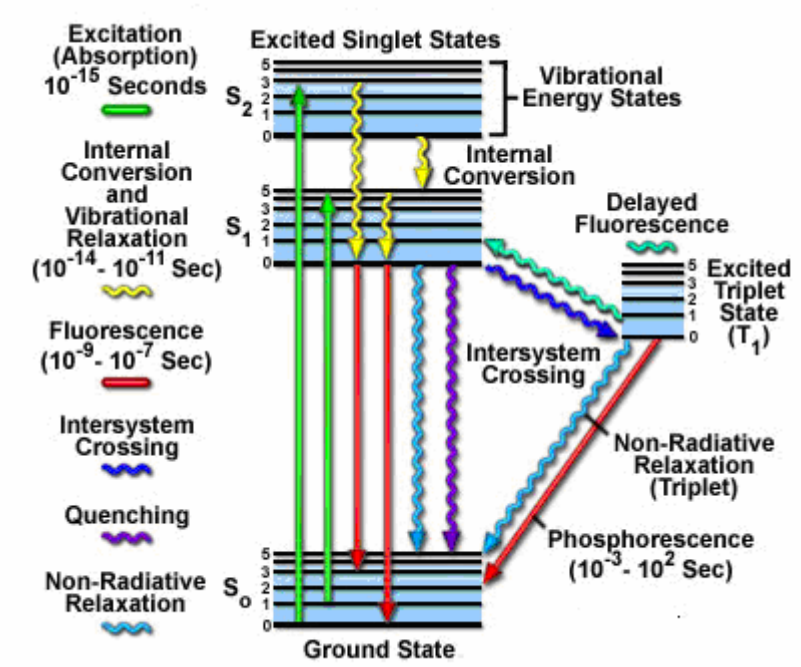

Fig. 1.6- Jablonski energy diagram[57]

1.6 Quenching mechanisms in Polyfluorenes

Aggregation of the conjugated polymers through interchain and intrachain interactions leads to fluorescence quenching. This process causes lower quantum yield and a red shift in the emission. Besides red shift in the solid state, a green emission band is observed during the course of functioning as a LED. Upon heating or UV exposure during device operation conjugated polymer chain undergoes irreversible changes where the characteristic blue emission loses both its intensity and energy. Irreversible changes can occur in the chemical structure of the polymer backbone. Some keto groups can form, in which the oxygen molecule acts as a quencher. The characteristic blue emission decreases and a green or even yellow low energy emission is observed at 535 nm.[13] The reasons for green emission have been intensely investigated over the past decade and still the reasons are controversial. However, there are some explanations such as that the green emission

may be caused from excimer formation[14], keto defect formation due to fluorenone units[13] and crosslinks[15] as shown in Figure 1.7. Keto defects act as traps where the charge carriers fall into a well. Crosslinks can distrupt the alignment of conjugation at the backbone.

1.Free Radical and Peroxy units Formation:

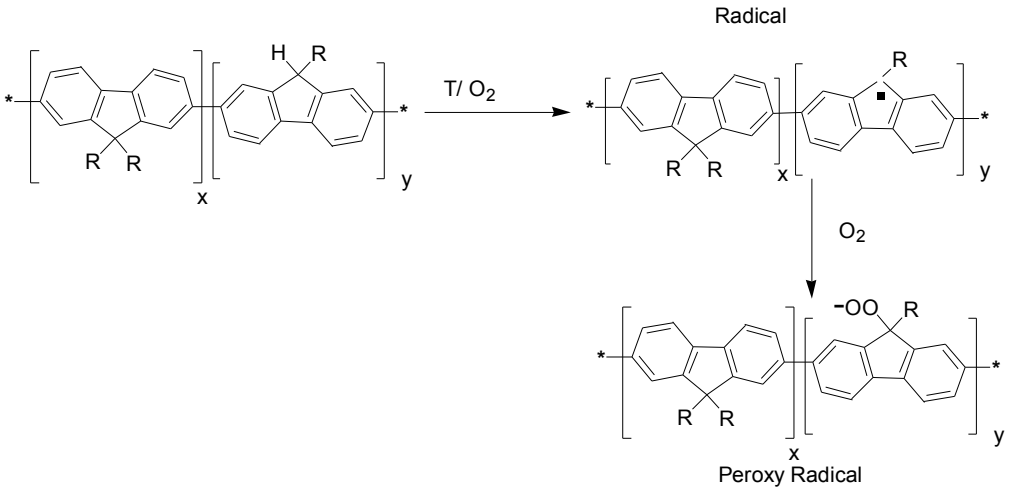

2. Ketone Formation

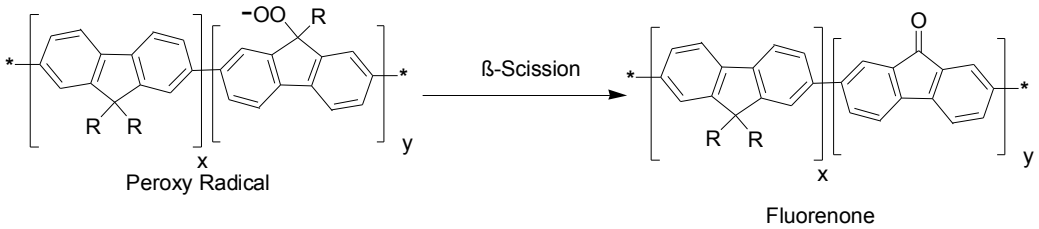

3.Crosslinking

Fig. 1.7- The possible mechanisms that cause green emission[8]

1.7 Insulated Molecular Wires

The proposed reasons in the preceeding sections for fluorescence quenching lead to research for preventing these causes. A widely studied idea was to separate the polymer chains by encapsulation to prevent interchain and intrachain interactions to make them insulated molecular wires like copper cables isolated by insulator plastic coatings.

Conducting polymer chains were tried to be isolated from each other to enhance the charge transport to occur along the individual chains. There have been different approaches and various materials were utilized. This area of research has attracted continuous attention because this approach offers some advantages. First by encapsulation, the conducting polymer can be protected from the chemical oxidation by oxygen. Atmospheric oxygen was shown to cause photoxidation of the polymers thus decreasing their stability.[16] Another point is that isolation of the conducting polymer units will allow to understand the transport mechanisms occurring along the polymer chain.

So far, conjugated polymers have been threaded into the pores of regular micro and mesoporous solids, between the planes of layered materials and pillared clays. Besides incorporation of the polymer into pores or to the pillared materials, polymers were also threaded by macrocycles. The latter approach is named as rotaxanation. Rotaxanes are interlocked molecules where an axle, the linear part, is surrounded by macrocycles forming ion-dipole interactions or van der Waals interactions. The following paragraphs will describe how insulated wires have been prepared by introducing representative examples.

1.7.1 Zeolite Hosts:

Zeolites are aluminosilicate materials and their structure is composed of XO_4^{-n} tetrahedrons. The X atom is either aluminum or silicon. Zeolites have a microporous structure as depicted in Figure 1.8 below.

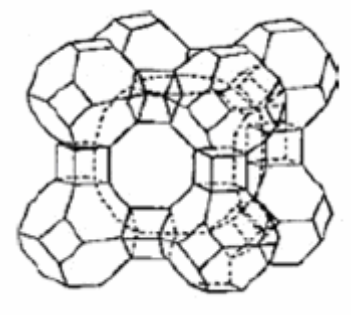

Fig. 1.8- Representation of a zeolite host.

Polyaniline was incorporated into the pores of the H-zeolites. Polyaniline was synthesized in H- zeolites in its protonated form after aniline and oxidation agent μ-peroxo-bis(trioxosulfate) (2-) was located in the pores.[17]

1.7.2 Layered Materials

Layered materials like clay offer isolation of the conducting polymer chains. Though it is not totally an encapsulation, it aids in the separation of the polymer chains. Additionally, layers serve as a protective shealth against environment. Poly[2-methoxy-5-(2'ethylhexyloxy)-p-phenylene vinylene] (MEH-PPV) was intercalated into the layers of mica type silicate.[18] Firstly clay was sonicated and stirred with a solution of polymer in 1,2-dichloro ethane. The obtained product was investigated by XRD and revealed a photoluminescence intensity increase by a factor of 9 compared to pure MEH-PPV of the same thickness.

Polyaniline (PANI) was introduced into the modified montmorillonite clay. Na^+-montmorillonite was mixed with aniline to force cation exchange and polymerization is performed by ammonium persulftate at pH 2. The product was characterized by FT-IR, UV spectroscopies and XRD. Wu et. al. reported the conductivity of the prepared nanocomposite has a relatively higher conductivity if compared to other prepared PANI/inorganic host hybrids.[19] Conductivity was enhanced as the polymer approved an extended conformation as outlined in the scheme 2.

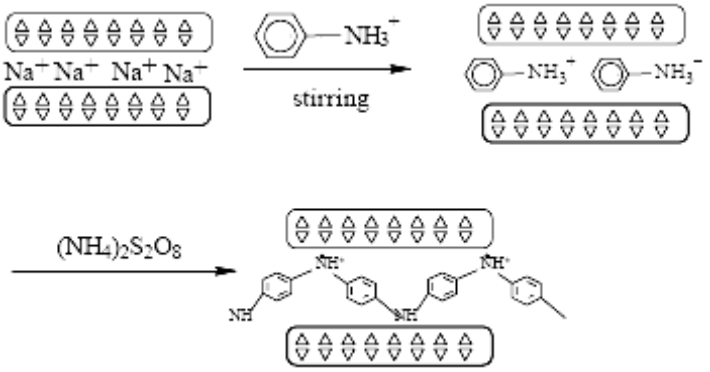

Scheme 1.2- Synthetic route for the prepared PANI-MMC nanocomposite and depiction of the extended polymer

The same experimental approach was also tried for preparation of the polypyrrole-clay nanocomposites using modified montmorillonite clay.[20,a-b] Chang et. al. reported thermal stability of the intercalated polymer as compared to pristine polypyrrole from the TGA analysis. To add that DSC measurements showed an increase in the glass transition temperature (T_g) of the nanocomposite.

1.7.3 Rotaxanes

As mentioned in the previous section rotaxanes are interlocked molecules. Rotaxanes are composed of a cyclic macrocycle threaded into a linear molecule. The nomenclature is applied for different types of prepared interlocked structures according to their composition. Pseudorotaxane corresponds to regular structures where the axle is surrounded by a cyclic unit. If the former structure is confined with bulky stopper units then it is called rotaxane. These terms can be applied to polymers where the cyclic unit and the axle form the repeating unit. If there are bulky stopper groups attached to the polymer chain ends then it is called polyrotaxane. Absence of stopper groups leads to the polypseudorotaxane. These structures are depicted in Figure 1.9.

pseudorotaxane polypseudorotaxane

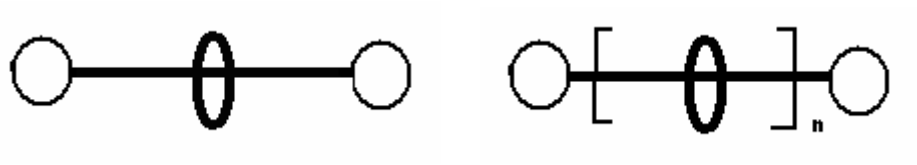

Rotaxane polyrotaxane

Fig. 1.9- Illustration of the structures for pseudorotaxane, polypseudorotaxane, rotaxane, and polyrotaxane

In the preparation of conjugated polyrotaxanes mainly cyclodextrins have been used as a macrocycle. Cyclodextrins are cyclic molecules made up of glucose units. α-, β- , γ- cyclodextrin derivatives consist of six, seven and eight glucose units respectively. The structure of a β- CD is presented in Figure 1.10. They have cavities in the range of 4.3 Å to 7.4 Å with cross sectional areas from 15 $Å^2$ to 43 $Å^2$.[54]

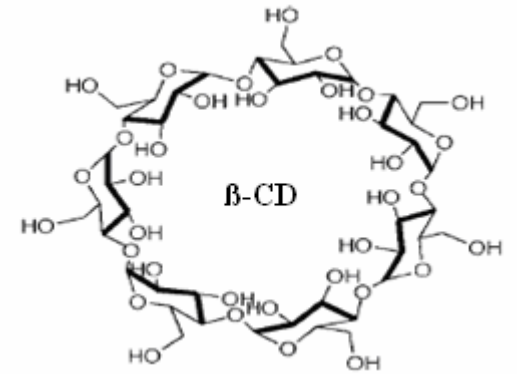

Fig. 1.10- Representation of β-cyclodextrin

This size internal cavity allows inclusion of molcules of suitable dimensions. Furthermore, its interior is hydrophobic and the exterior part is hydrophilic. The ability of cyclodextrin to form inclusion complexes comes from hydrophobic interactions with the guest molecule. Cyclodextrins can assume head to tail or head to head arrangements while packing in solid state. They are soluble in water and organic solvents like DMSO, DMF and pyridine. Its good solubility is advantageous for the preparation of inclusion complexes with conjugated polymers.

Polyaniline in its emeraldine base structure was threaded into β-cyclodextrin by Ito and coworkers as depicted in the Figure 1.11 below.[21] It was shown that encapsulation of the polymer by cyclodextrins resulted in a rod like conformation rather than coil conformation below 275 ^{o}K confirmed by scanning tunneling microscope (STM) analysis. In another study, it was also shown that prepared polypseudorotaxane was protected from the chemical oxidation by iodine.[22]

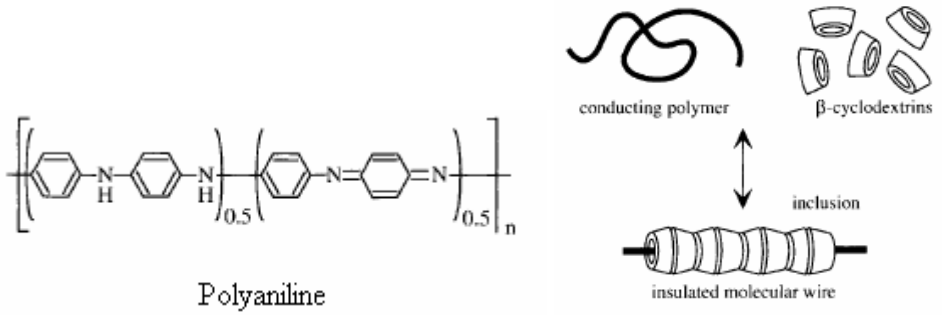

Fig. 1.11- Representation of polyaniline and prepared insulated molecular wire[21]

Encapsulated polythiophenes have been studied widely. For example, Lagrost *et al.* reported the synthesis of HP-β-CD enapsulated polythiophene from electropolymerisation of the bithiophene in aqueous solution of HP- β-CD and $LiClO_4$ as shown in Scheme 3 below. From spectroscopic analysis it was shown that polymer was threaded into CD. The polypseudorotaxane showed higher solubility in DMF (1 gL^{-1}) when compared to polythiophene of the same chain length itself.[23]

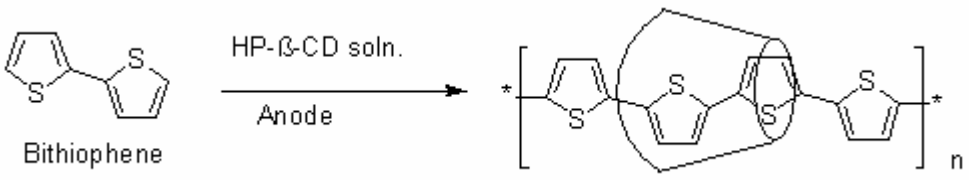

Scheme 1.3- Synthesis of polythiophene based polypseudorotaxane[23]

Harada *et al*. synthesized encapsulated polythiophene starting from bithiophene and β-CD using $FeCl_3$ as an oxidizing agent. They also managed to obtain the crystal structure of β-CD + bithiophene complex.[24]

Besides polypseudorotaxanes, polythiophene-based polyrotaxanes were also synthesized by Hadziioannou and co-workers. Bithiophene+β-cyclodextrin complex was formed in water. Hydropohic interior of the β-CD facilitated the complexation of the hydrophobic bithiophene. After preparation of the complex, polymerisation was performed with Ni-catalysed Yamamoto coupling reaction. At the end of the reaction, 9-bromoantracene was provided as stopper groups. From small-angle neutron-scattering analysis it was shown that 1.0 β-CD for each repeat unit.[25]

There are many examples to polythiophene-based polyrotaxanes. However, there are only limited numbers of examples to polypyrrole-based polyrotaxanes. For example, Ritter *et al* attempted to prepare an encapsulated polypyrrole. However after forming the inclusion complex between pyrrole and CD, upon polymerisation CD unthreads over the pyrroles and only polypyrrole is formed.[26]

Polyfluorenes have also been tried to be encapsulated by rotaxanation. The preparation of an insulated polyfluorene by CD has been tried via two different synthetic pathways. Hadziioannou and co workers utilised Ni- catalysed Yamamoto coupling for the polymerisation of the 2-7 dibromofluorene β-CD complex obtained from DMF. 9-bromoantracene was chosen as stopper groups to prevent the β-CD slip off from the polymer chains.[25]

Anderson *et al.* used Suzuki coupling to prepare insulated molecular wires.[28] Additionally, solubilizing ionic groups like -CO_2Li were added to the alkyl chains of fluorene units and –SO_3Li were added to naphthalene stopper groups, as depicted in Figure 1.12. Thus the solubility in water and DMSO was achieved. These ionic groups also aided in separation of the cyclodextrins and no interaction occurs between them. From NMR spectroscopy analysis and corresponding theoretical study, it was found that 2.2 cyclodextrins accommodated per repeat unit of the polymer. The rotaxanation of the polyfluorene backbone showed blue shifted emission and high luminescence efficiency. Aggregation tendency was reduced and reduction by impurities was prevented aiding in the chemical stability of the polymer.

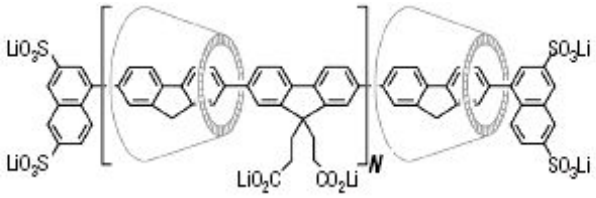

Fig. 1.12- Polyfluorene based polyrotaxane[28]

1.7.4 Dendronized Conjugated Polymers

Dendrimers are large molecules that are made up a core and regularly branched dendrons. A repeating fractal shape is characteristic with dendrimers as depicted in Figure 1.13. As they occupy a large volume, dendrimers were utilized in site isolation of conjugated polymer chains. Dendrimers are attached chemically to the backbone of the conjugated polymer. As dendrimers occupy large volume they cause separation of the polymer chains due to steric reasons. These kinds of molecules are also named as insulated molecular wires because dendrimers are wrapping the conjugated polymer chain.

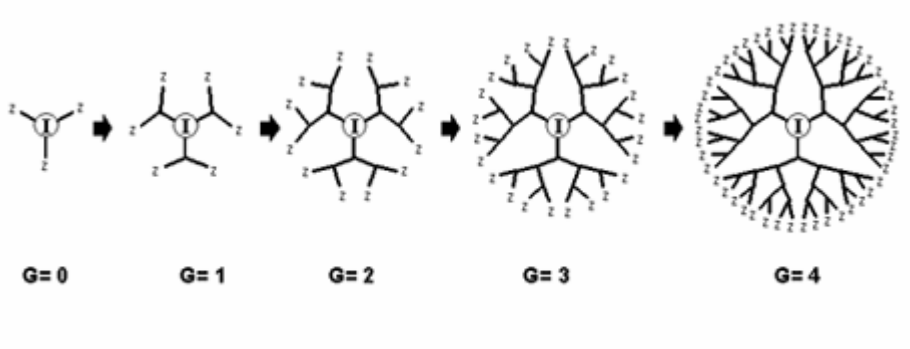

Fig. 1.13- Representation of dendrimer structure growth after 4 generations

Dendrimers were added to various conjugated polymers. Two methods were tracked. First method was, forming the polymer backbone from monomers and then addition of the dendron after a chemical reaction. Steric reasons retard the addition of the bulky dendrimers thus lowering the dendron coverage in the polymer. The second method involved dendronized monomers coupled with other monomers to form the polymer. For a representative study, polyfluorenes possessing the 1st,2nd and 3rd generations of Frechet type dendrimers were obtained by Carter et. al. Monomers containing the Frechet type dendron as seen in Schem 4, were prepared. These

dendronised monomers were coupled with dialkyl containing fluorene monomers through Yamamoto and Suzuki coupling to form homopolymers and copolymers. Especially 2nd-generation containing copolymers exhibited aggregation free solid state spectra.[29]

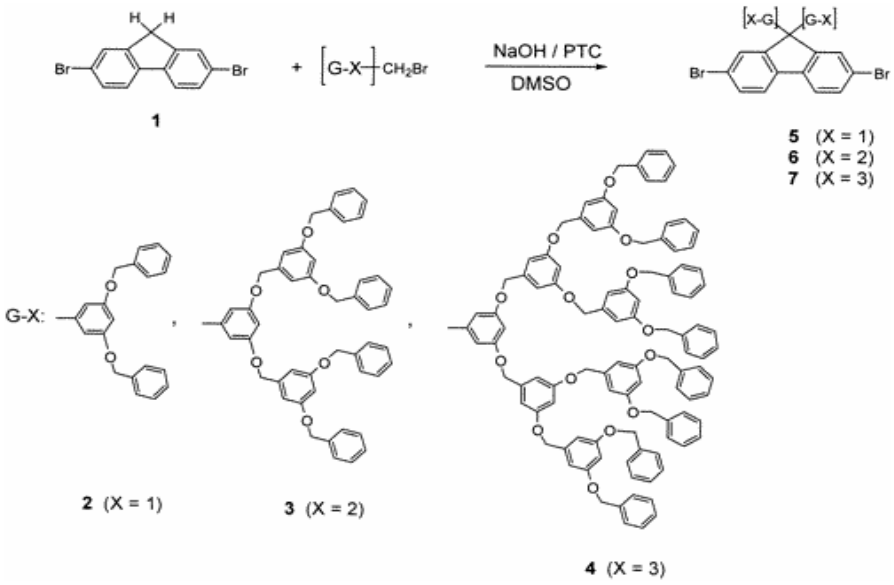

Scheme 1.4-Synthesis of dendronised fluorene monomer[29]

Frechet type dendrons are flexible, however dendrimers prepared by Müllen exhibits rigid structure. These dendrons are made up of polyphenylene dendrons as depicted below in Figure 1.14. The dendrons form more stable linkages and cause shape persistency.[45] Polyfluorenes containing Müllen-type dendrons showed good solubilities because of the dendrons formed from polyphenylene groups. Furthermore, these dendrons permitted spatial control of the polymer chain and hindered aggregation.[31]

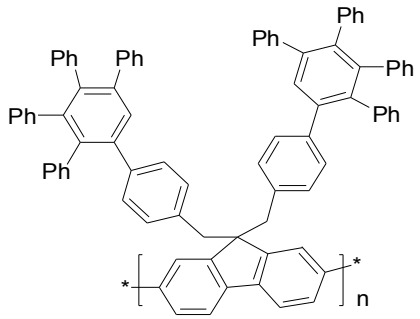

Fig. 1.14- Polyfluorene with Mullen type dendrons[31]

1.8 Objective of the study

Our work is aimed to synthesize a series of polyfluorene based polymers for applications in LEDs and photovoltaics. In this work, it is intended to use supramolecular chemistry to achieve control at the molecular level to prepare insulated molecular wires by rotaxanation or encapsulation of polymer backbone by a macrocycle. Rotaxanation of these polymers is aimed to be done in two ways to control the molecular structure. First is the encapsulation of the polymer backbone with macrocyles, e.g., cucurbit[6]uril, which will be discussed in detail in the next section. The second approach is to attach CB(6) to the modified alkyl chains added to the C9 of the polyfluorenes. By introducing bulky CB(6) it will be probable to distrupt the π-π stacking causing the interchain interactions. As a result, it is aimed to prevent quenching and to increase electroluminescence efficiency.

In Figure 1.15 the rotaxanation of the conjugated polymers by CB(6) is illustrated in comparison with the π-π stacking between the polyfluorene chains. In a, π-π stacking is shown which causes the aggregation. In b, sepearation of the polyfluorene chains by CB(6) macrocycles by forming polyrotaxanes.

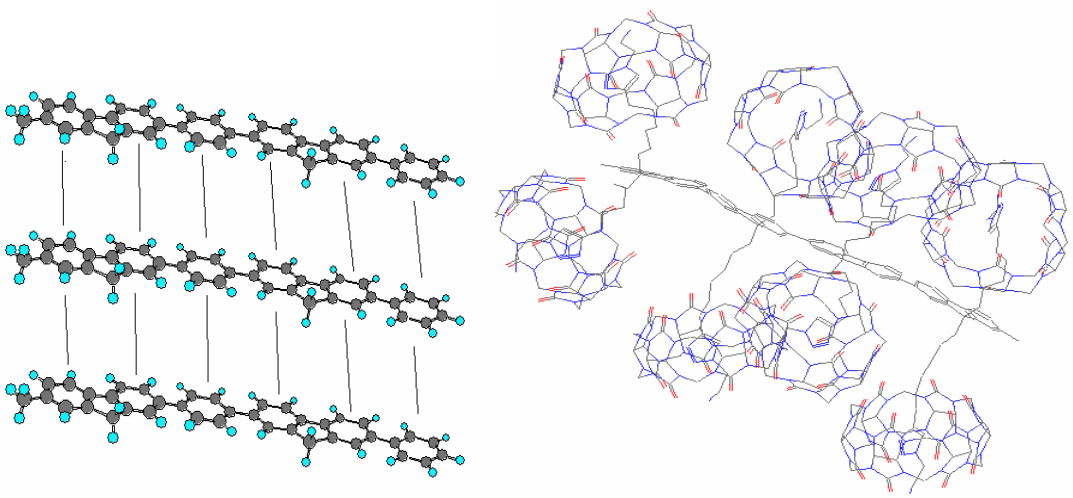

Fig. 1.15- Representation of π-π stacking between polymer chains (a) and CB[6] based polyfluorene rotaxanes (b)

1.9 Cucurbit[6]uril

The "bead" used in our work is cucurbit[6]uril which is first introduced by Behrend *et al*.[32] Cucurbit[6]uril is chosen as a bead for rotaxanation because of its easy synthesis and rigid structure with a hollow core. Cucurbit[6]uril is a hexameric symmetrical macropolycyclic compound and it is self-assembled from an acid-catalyzed condensation reaction of formaldehyde and glycoluril.

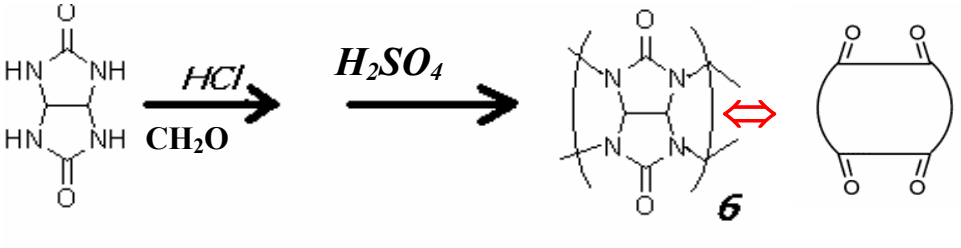

Figure 1.16- Synthesis of cucurbit[6]uril

It has a cavity diameter of ~5.7 A^0 with the occuli of diameter of ~4 A^0. CB(6) has a hydrophobic interior so hydrocarbon molecules can be easily included and the polar carbonyl groups at the occuli forms a hydrophilic environment which aids its solubility in aqueous medium. CB(6) can bind ions and molecules through charge-dipole and hydrogen bonding interaction through its polar carbonyl groups. Another remarkable feature is that it can serve readily as a catalyst. CB(6) can catalyze 1,3-dipolar cycloaddition between azide and alkyne groups inside the cavity as depicted in Scheme 5.

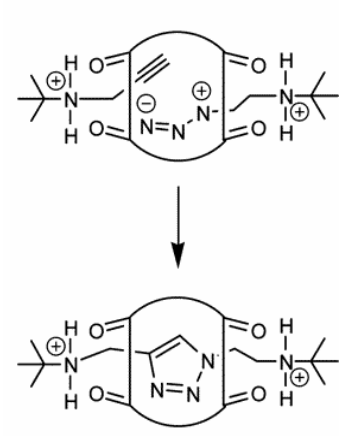

Scheme 1.5- 1,3-dipolar cycloaddition between azide and alkyne groups inside CB(6)

Additionally, an important feature of the cucurbit[6]uril is that, it can host diammonium salts very well. In 1990, Mock reported a pseudorotaxane that consist of CB(6) as a bead and linear triamine unit, $PhNH(CH_2)_6NH(CH_2)_4NH_2$.[37] At low pH all nitrogen atoms in the thread protonated so CB [6] bead stays at the diprotanated diaminohexane site because they form more stable complex than with diprotanated diaminobutane. At high pH, bead moves to diprotanated diaminobutane site because diaminohexane group has only one protonated amino unit.

1.10 White Light Generation using Polymers

In recent years white polymer light emitting diodes (WLEDs) attracted intense research as they offer applications in displays and lighting as lighting by incandescent sources uses up % 40 per cent of the electricity in the domestic buildings.[33] The incandescent sources are inefficient, WLEDs provide basic advantages like low-cost solution processing and easy manufacture. Especially conjugated polymers used in WLEDs offer good processability, low operating voltage, fast response times and facile color tunability over the full visible range.[34]

For the production of white light different strategies were undertaken. One of the approaches is to design a multilayer device possessing two or more active layers where each layer emits a primary color. In 2006, Forrest et. al. reported the highest external quantum efficiency 18.7% and power efficiency of 500 cd m^{-2} using phosphorescent triplet exitons for the high wavelengths and an organic polymer acting as a singlet exciton emitter.[33] This approach has obtained the highest results for WLEDs. However, the preparation of such WLEDs is difficult as solution processing of one layer may result in the dissolution of the other previous layers.[35]

Another widely studied approach is to blend two or three fluorescent polymers into a blue emitting polymer host as a single layer. However, these types of WLEDs suffer from phase separation during long term device operation and spectral changes over the applied voltage resulting in unstable devices.[36]

The recent approach is to use a single polymer, compromising the three Red, Green, Blue (RGB) emitting chromophore groups in itself. This method, though it is tedious about the synthesis part, advantages over the other strategies yielding no phase segregation or dissolution of other layers. The results from this approach yield lower efficiency values if compared to other methods but easy fabrication creates a reason of investigation. A very recent study by Luo et. al. prepared a fully conjugated copolymer consisting of poly(9,9-dioctylfluorene) (PFO), 2,1,3-benzothiadiazole(BT) and 4,7-bis(2-thienyl)-2,1,3-benzothiadiazole (DBT) as blue, green and red emitting parts, respectively.[35] They obtained external quantum efficiency of 3.84% and luminescence efficiency 6.20 cdA^{-1} with CIE coordinates of (0.35, 0.34). However, the synthesis is up to an optimum mixing of the green and red units. To get a best balance between the red-green-blue emissions, the amounts of each unit must be controlled. Thus the emission efficiency is highly dependent on the unit composition. In addition, there is also a problem caused by the dopant content which is less than 0.05% mol. It is almost impossible to determine an actual composition of the copolymers. Earlier, Liu et. al. benefited the same approach using polyfluorene backbone as a blue emitting host, 4-diphenylamino-1,8-naphtalimide (DPAN) as a green dopant and 4,7-bis(5-(4-(N-phenyl-N-(4-methylphenyl)amino)phenyl)-thienyl-2-)-2,1,3-benzathiadiazole (TPATBT) as a red dopant. These additive red and green dopants are in low concentration to allow incomplete energy transfer from the blue host to the green and red emitters. If the dopants were used at stoichiometric proportions a complete energy transfer between the blue host and the other emitters would occur and the last emitter will give the only color instead of the whole color system, *i.e.* white. They obtained a white luminescence with CIE coordinates (0.31, 0.34), a luminescence efficiency of 1.59 cdA^{-1}. Lee et. al. in 2005 were the first to report their results using the blue-green-red emitting copolymers on the single backbone. The device exhibited a maximum brightness of 820 cdm^{-2} under 11 V with CIE coordinates of (0.33, 0.35). In the same year Wang et. al. reported a single polymer by attaching a small amount of a green emissive component to the pendant chain and incorporating a small amount of a red emissive component into the main chain of the blue emissive polyfluorene.

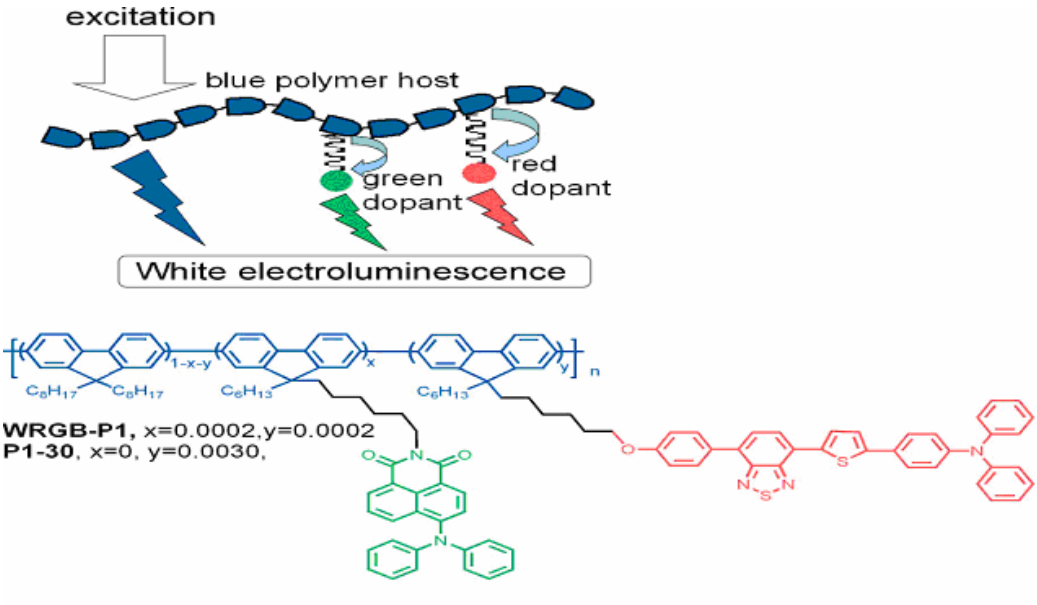

Figure 1.17- White luminescence from single polymer[38]

By using a slghtly different strategy Liu et. al. realizing the same approach followed a bit different design, rather than adding the green and red dopants into the backbone directly, they introduced the green and red emitting dopants directly to the side chain of the blue emitting polyfluorene backbone as seen above.[38] (Figure 2.1). It is reported that this approach has the advantage of forming an intramolecular dopant/host system without affecting the electronic properties of the polymer backbone. The incomplete energy transfer acts for realization the white light emission with CIE coordinates of (0.31, 0.32). The single polymer device generates a luminescence efficiency up to 7.3 cdA^{-1} and power efficiency.

Rather than using a single polymer layer, hybrid systems emerged. The hybrid devices will be covered in detail in the following chapter.

CHAPTER 2

RESULTS AND DISCUSSION

This chapter consists of three main sections. In the first section, synthesis and characterization of monomers and polymers are discussed. As mentioned in the introduction, it is intended to prepare conjugated polymers for applications in LEDs and photovoltaics. Furthermore these polymers were intended to be encapsulated by cucurbit[6]uril by rotaxanation. Rotaxanation was aimed through two paths. First was the encapsulation of the polymer backbone with cucurbit[6]uril. The second path was to attach CB(6) to the modified alkyl chains added to the C9 of the polyfluorenes. In the second section, the features of the prepared hybrid WLED will be covered with an investigation of the stability and thermal degradation behaviour. In the last section rotaxanation through the conjugated polymer backbone will be discussed. This section compromises the results from the polypyrrole based polypseudorotaxanes.

2.1 Synthesis and characterization of monomers and polymers

In this section attempts to prepare a polypsedurotaxane with fluorene based conjugated polymer will be discussed. Here, the aim was to modify conductive light emitting polymers through supramolecular chemistry to obtain polymers with interesting and different properties than the parent polymers. For example, it is possible to functionalise the C9 of blue light emitting polyfluorene through rotaxanation using cucurbit[6]uril as a macrocycle. This will result a decrease in the inter chain interactions and in turn, an increase in the luminescent efficiency.

For this purpose, we have tried two approaches as shown in the Scheme 2.1. First approach involves the preparation of a series of appropriate copolymers whose side chains allow us to carry out rotaxanation.

In the second approach, first a fluorene monomer is functionalized with a suitable alkyne monomer. Then, by addition of azido monomer and CB(6), rotaxane is formed via CB(6)-catalysed 1,3 dipolar cycloaddition. This rotaxane is polymerized using Suzuki coupling conditions.

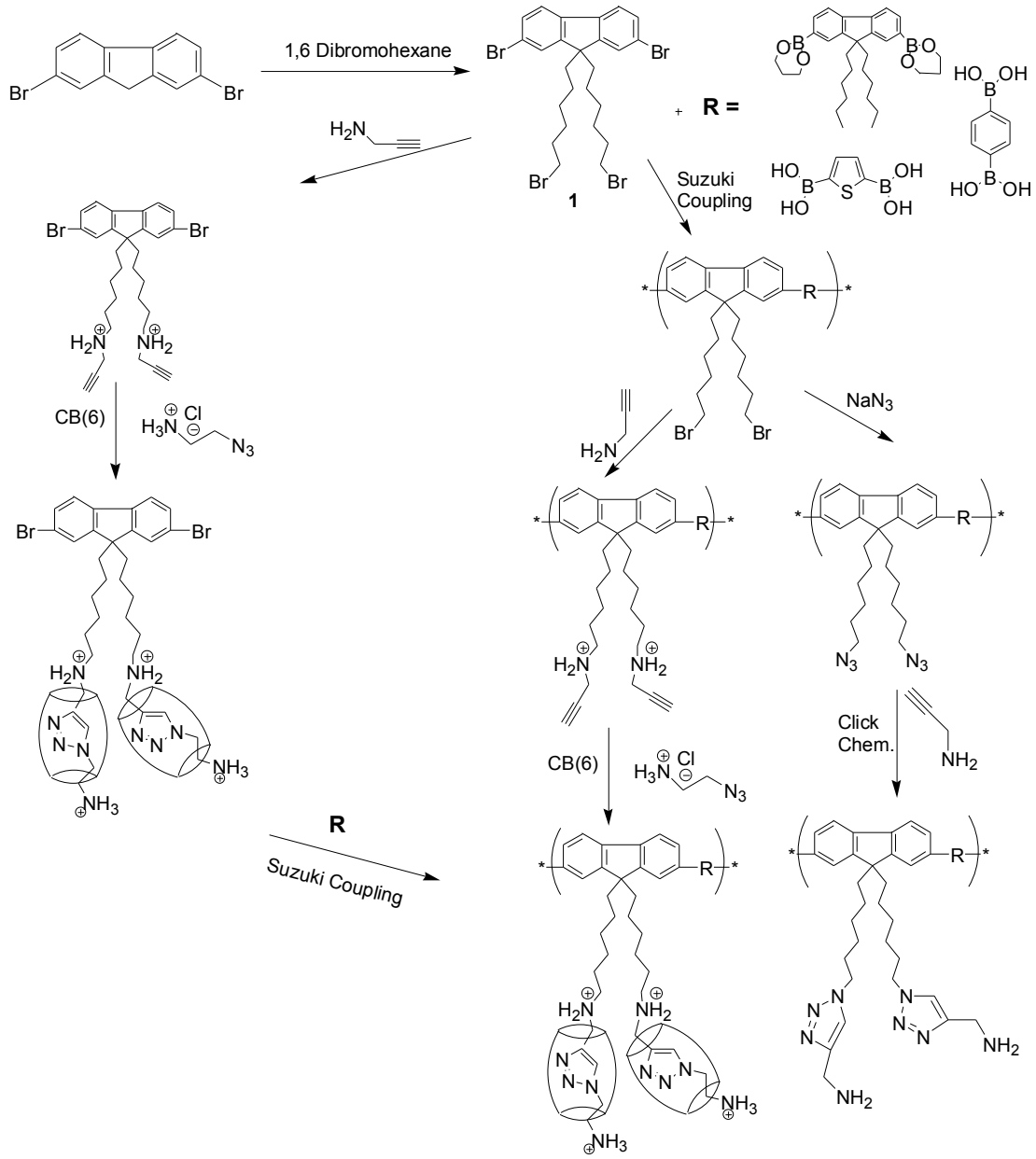

Scheme 2.1- General reaction schemes for the rotaxanation of polyfluorene's side chains.

2.1.1 Synthesis and Characterization of 2,7-dibromo-9,9-bis-(6-bromo-hexyl)-9H-fluorene (1)

Commercially available 2-7 Dibromofluorene was treated with highly basic NaOH solution (% 50) in DMSO in the presence of the phase transfer catalyst, tetrabutylammonium bromide. Highly basic NaOH was used for the abstraction of the protons at the C9 of the fluorene precursor. A nucleophilic substitution reaction was perfomed to this C9 with 1,6 dibromohexane with a 40 % yield at room temperature. Without supplying any inert atmosphere, side reactions were observed. The reaction scheme is outlined below in Scheme 2.1

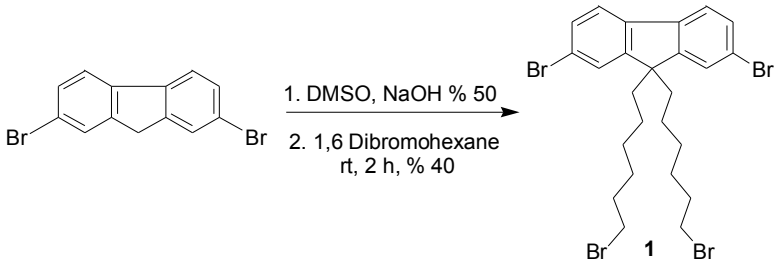

Scheme 2.2- The synthesis of **1**

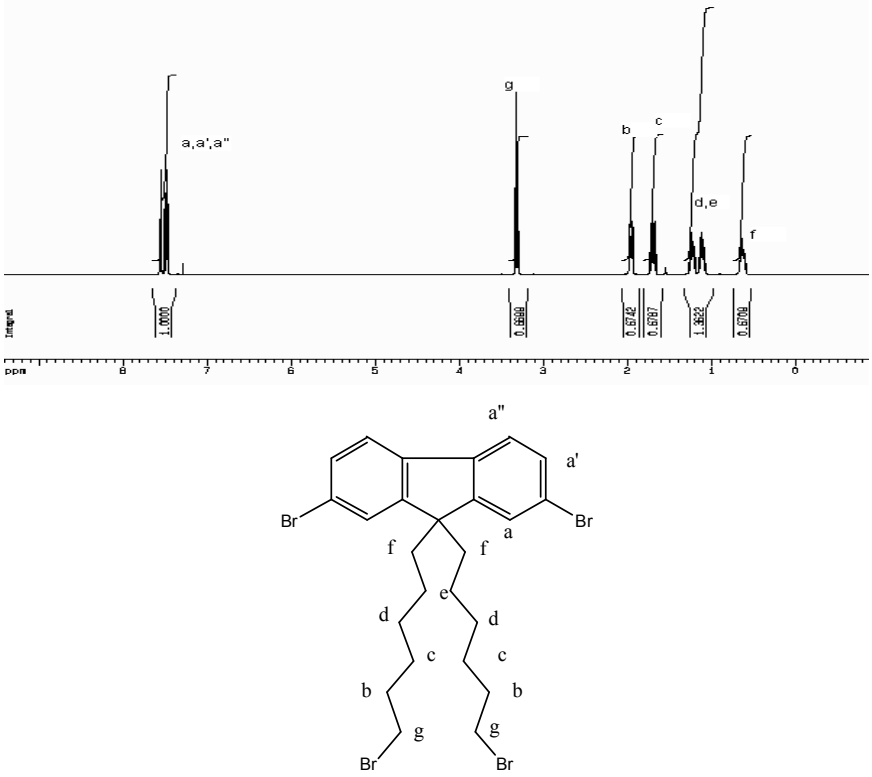

Fig. 2.1- ^{1}H-NMR Spectrum of **1** (400 MHz, $CDCl_3$, 25 ^{o}C)

2,7-dibromo-9,9-bis-(6-bromo-hexyl)-9H-fluorene was characterized by ^{1}H-NMR,^{13}C-NMR, FT-IR spectroscopy. ^{1}H-NMR spectrum showed multiplet at 7.2 and 7.35 ppm due to the aromatic protons. Signal at 3.34 ppm appeared as a triplet for $-CH_2$ protons close to bromine were deshielded because of the electronegative bromine atom. Also multiplets at 1.95, 1.7, 1.20 and 0.65 ppm were observed for the rest of alkyl protons.

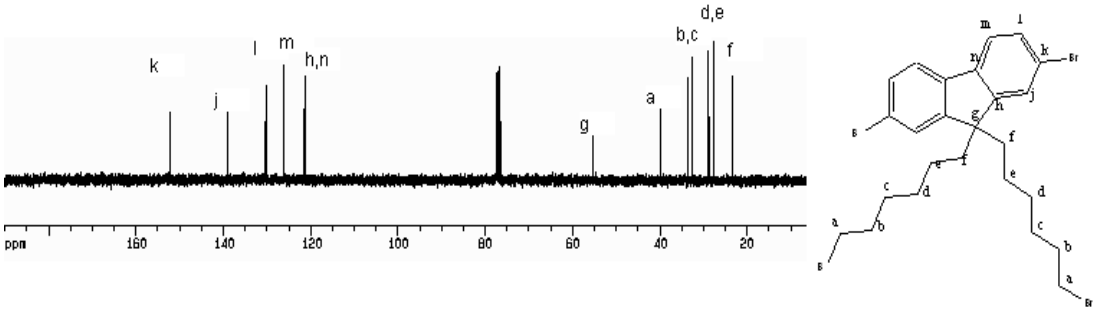

Fig. 2.2- ^{13}C-NMR of **1** (100 MHz, $CDCl_3$, 25 ^{o}C)

^{13}C-NMR showed 6 non equivalent aromatic carbon atoms at 121.9, 122.3, 126.9, 131.1, 139.9, 153.1 ppm. The carbon bonded to bromine was deshielded and appeared at 153.1 ppm. Also, quaternary carbon at the 9th position was observed at 55.9 ppm because of the quaternary effect. The alkyl carbons appear at 23.6, 27.9, 29.1, 32.8, 33.9, 40.2 ppm because of the 6 different carbon atoms.

In the FT-IR spectrum of **1**, aromatic carbon hydrogen stretching at 3025 cm^{-1} and aliphatic carbon hydrogen stretchings at 2922 cm^{-1} are observed. The aromatic carbon double bonds appear as a weak peak at 1598 cm^{-1}.

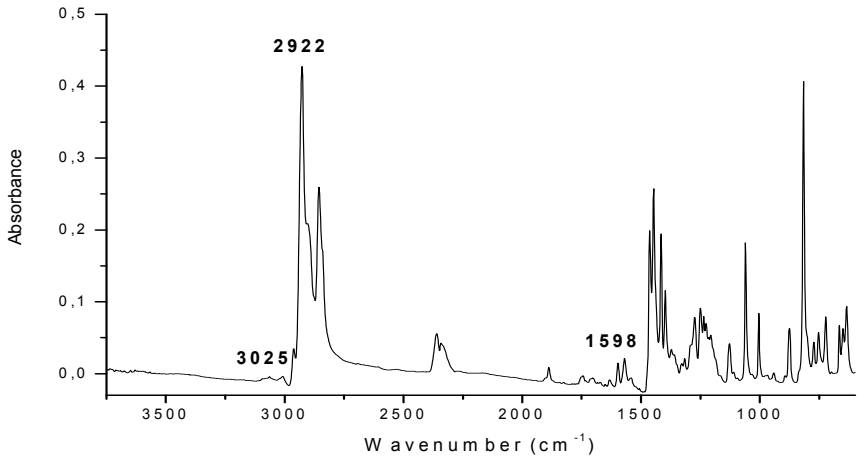

Fig. 2.3- FT-IR spectrum of **1**

2.1.2 Synthesis and Characterization of 2,7-Dibromo-9,9-bis-(3-bromo-propyl)-9H-fluorene (2)

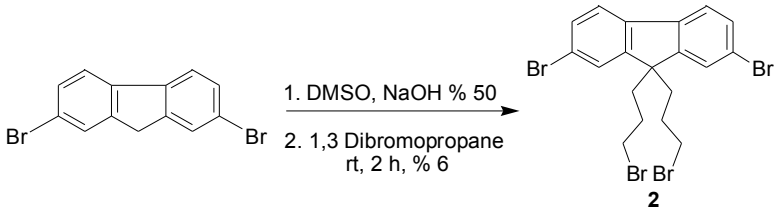

Scheme 2.3- The synthesis of **2**

The previous synthetic route (Scheme 2.1) was applied to the preparation of the monomer **2**. 1,3- dibromopropane was used for the nucleophilic substitution reaction with a % 6 yield. (Scheme 2.2) Low yield was caused by the formation of side products which were separated by column chromatography. The product was characterized by ^{1}H-NMR, ^{13}C NMR, FT- IR spectroscopy techniques

Figure 2.4 shows the FT-IR spectrum of **2**. Aromatic carbon hydrogen bond stretchings are observed as a weak band at 3048 $cm^{-1}$and the aliphatic carbon hydrogen stretchings are seen at 2927 cm^{-1}. The aromatic carbon double bonds at around 1605 cm^{-1} are present.

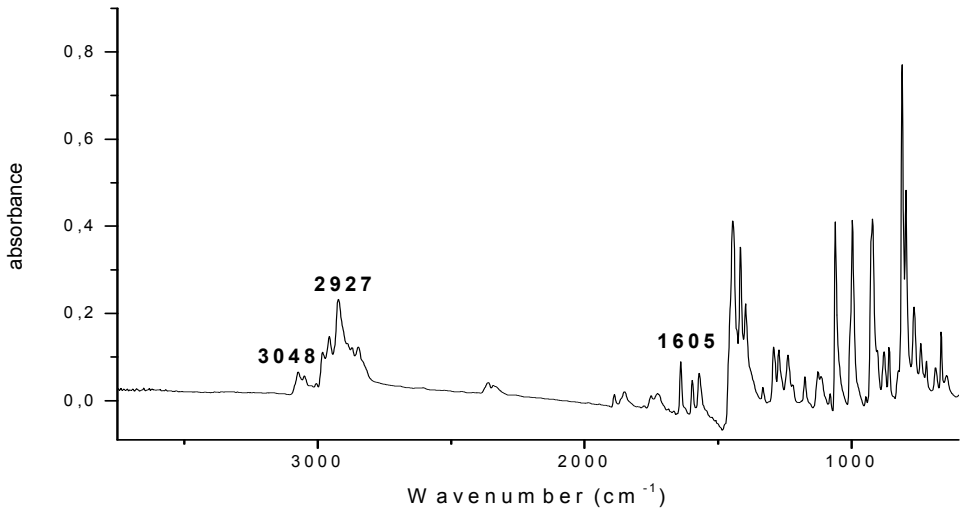

Fig. 2.4- FT-IR spectrum of **2**

^{1}H-NMR spectrum showed 6 aromatic protons as a multiplet between 7.2-7.45 ppm. The triplet at 3.05 ppm was due to the methylenic protons next to the bromine atom. Signals at 2.06 ppm and 1.08 ppm. were seen for other alkyl protons.

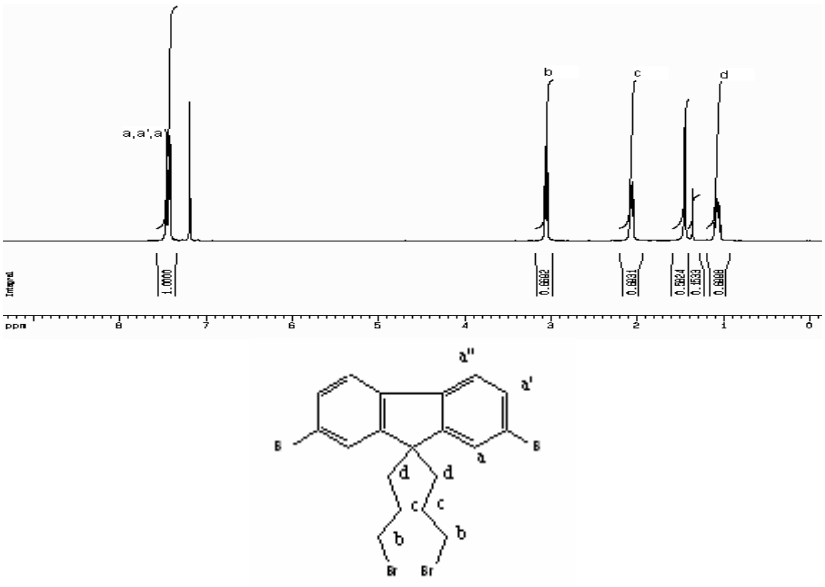

Fig. 2.5- ^{1}H-NMR Spectrum of **2** (400 MHz, $CDCl_3$, 25 ^{o}C)

In the **^{13}C-NMR** spectrum 10 signals were observed, 6 of non equivalent aromatic carbon atoms at δ_C :122.2, 122.7, 127.0, 131.7, 139.8, 151.6 and 4 signals for the carbon atoms at δ_C : 27.1, 33.7, 38.7, 54.8 ppm. The quaternary carbon atom is observed at 54.8 ppm.

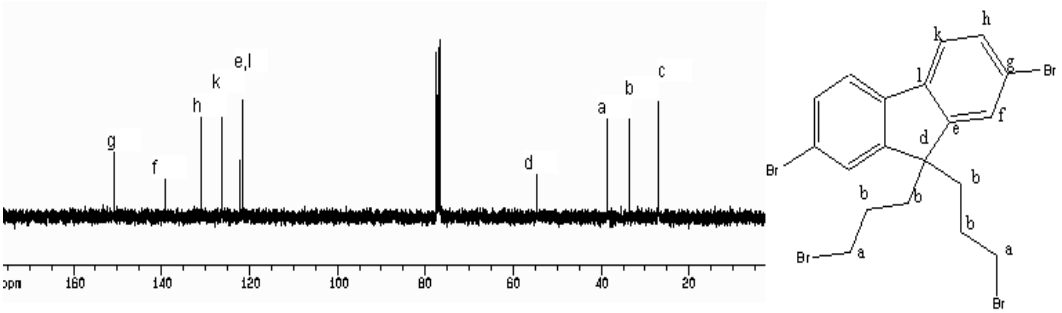

Fig. 2.6- ^{13}C-NMR of **2** (100 MHz, $CDCl_3$, 25 ^{o}C)

2.1.3 Synthesis of Azidoethylamine[43]

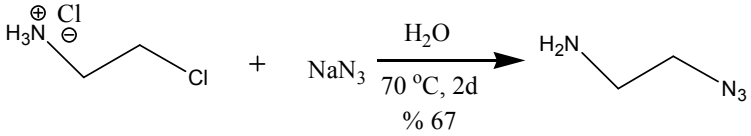

Scheme 2.4- The synthesis of azidoethylamine

2-chloroethylamine hydrochloride was subjected nucleophilic substitution reaction with sodium azide in water. Product was obtained with a % 67 yield after work-up. The product was treated with NaOH to abstract the acidic protons and product became soluble in organic solvents.

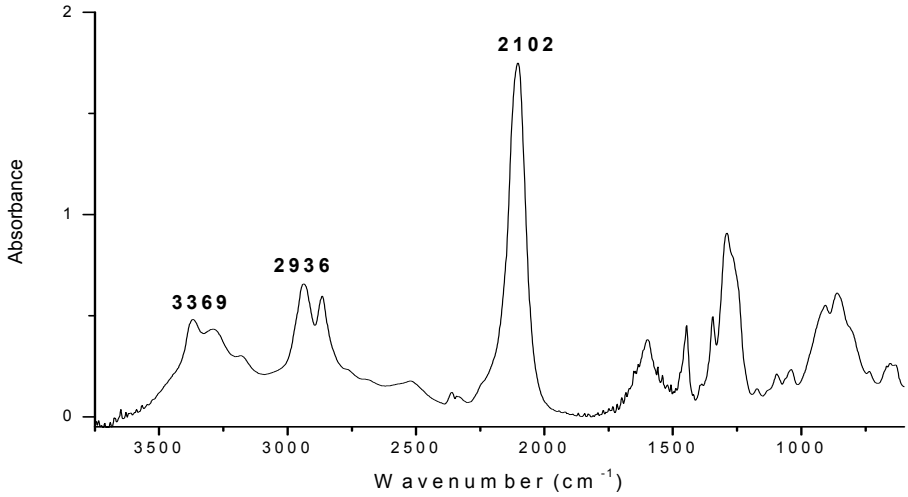

Fig. 2.7- FT-IR spectrum of azidoethylamine

The characterization of azidoethylamine was carried out by FT-IR spectroscopy. In the FT-IR spectrum, carbon azide stretching peak at 2102 cm $^{-1}$ and aliphatic carbon-hydrogen stretching at 2936 cm $^{-1}$ were present. The primary amine was observed as a band with a maximum at 3369 cm $^{-1}$.

After preparation of the monomers, our intention was to prepare poly[2,7-Dibromo-9,9-bis-(6-bromo-hexyl)-9H-fluorene]. We intended to do rotaxanation at the homopolymer. For the preparation of the homopolymer corresponding boronic ester of the monomer **1** was to be prepared. We tried various experimental methods. As an example, bis(pinacolato)diborane addition to the monomer via Suzuki coupling will be discussed.

2.1.4 Towards the synthesis of boronic ester derivatives

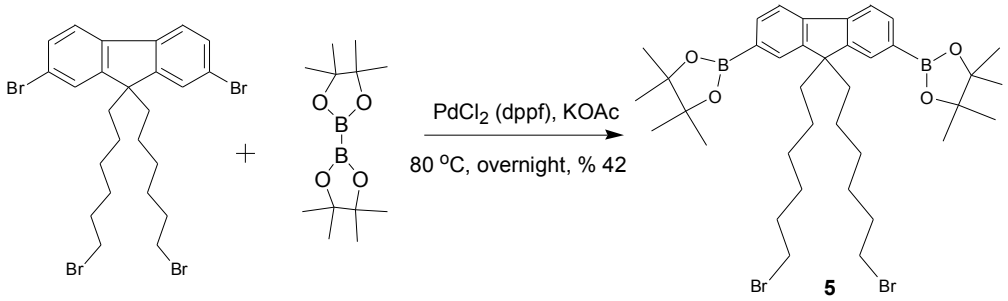

Scheme 2.5- The synthesis of **5**

Suzuki coupling conditions were applied for the addition of bis(pinacolato)diborane to 2,7-dibromo-9,9-bis-(6-bromo-hexyl)-9H-fluorene using potassium acetate and Pd(II) catalyst at a catalytic amount at 80 ^{o}C. After purification by column chromatography using cyclohexane:ethyl acetate (10:1) as an eluent the product was obtained with a % 42 yield after recrystallisation from cyclohexane.

We applied Suzuki coupling conditions for this reaction. Suzuki coupling is widely used to form aryl-aryl bonds.[43] The precursors of the reaction are, aryl halide and boronic acid dervative of an aryl compound in a weakly basic medium with Pd catalysts. Pd catalyst can be used either as Pd(II) and Pd(0). Suzuki coupling can be performed at moderate temperatures and in aqueous medium. The reaction is highly tolerant to other groups. To increase the reactivity of boron atom a slightly basic medium is supplied. The mechanism of the reaction involves the usage of palladium catalyst. Firstly, aryl halide is added to the palladium catalyst via oxidative addition. Then basic medium activates this intermediate for the reaction with aryl-boronate compound. The last step is the releasing of the precursor palladium catalyst by formation of the desired aryl-aryl compound via reductive elimination.

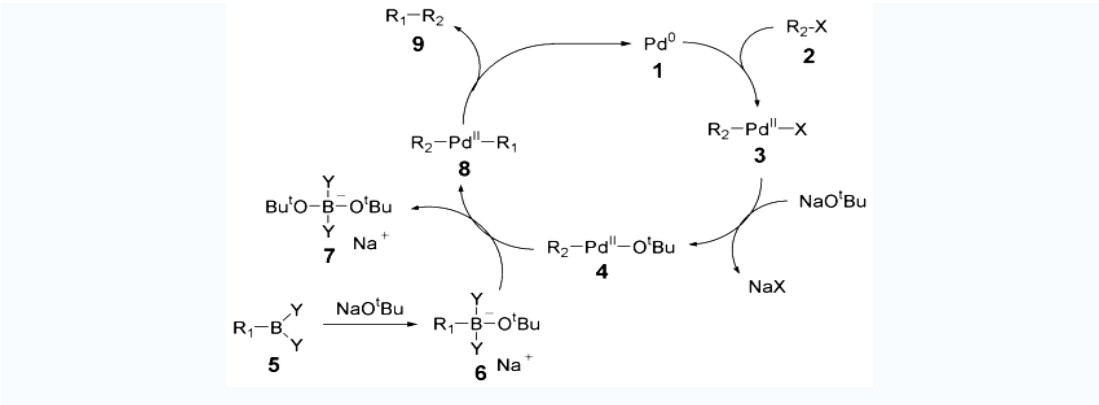

Scheme 2.6- Mechanism for Suzuki reaction.

5 was investigated through FT-IR and ^{1}H NMR spectroscopy. In the FT-IR spectrum boron-oxygen bond stretching was observed at 1380 cm $^{-1}$. Also the medium peaks for carbon-bromide bond stretching at 753 and 650 cm $^{-1}$ were present. However, a peak at 1738 cm^{-1} for carbonyl stretching was observed.

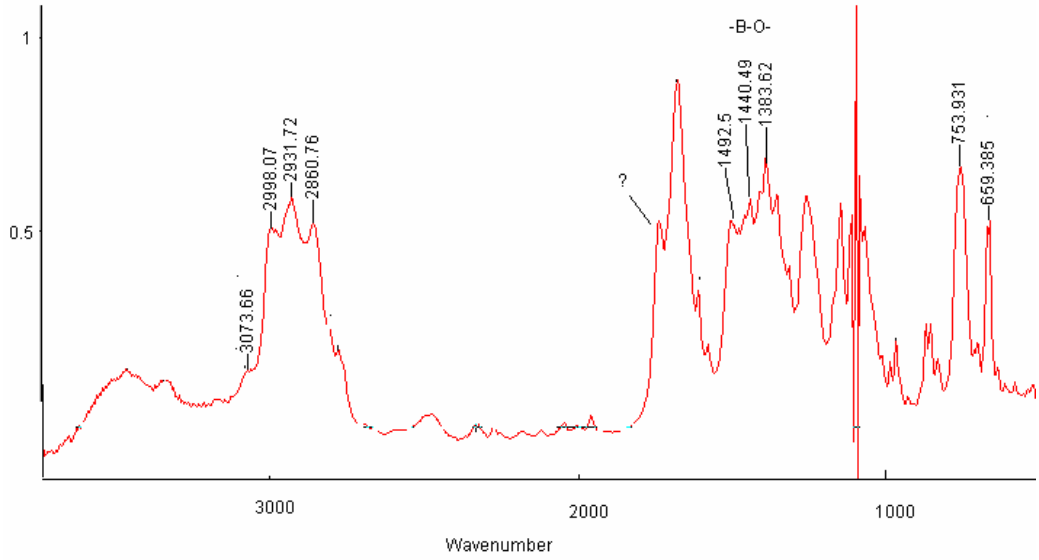

Fig. 2.8- FT-IR spectrum of **5**

The peak at 1738 cm^{-1} for carbonyl stretching was thought to be from potassium acetate or ethyl acetate residues, however the peak didn't disappear after recrystallisation from cyclohexane as shown in Figure 2.9.

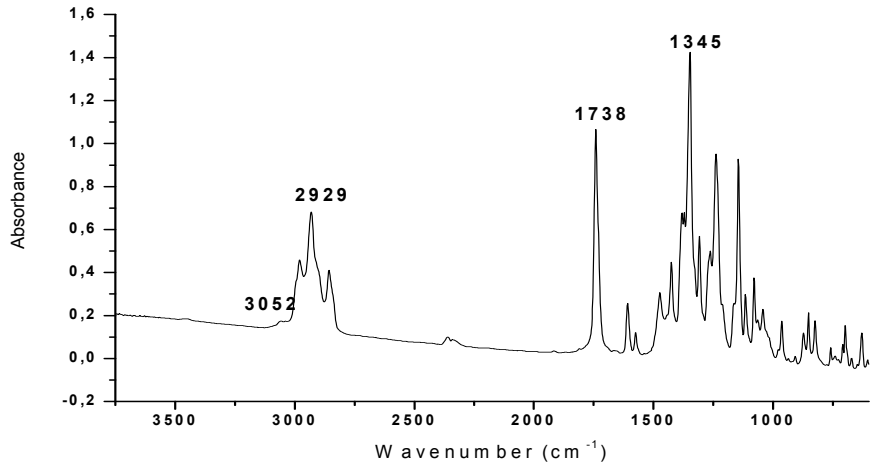

Fig. 2.9- FT-IR spectrum of **5** after recrystallization

^{1}H NMR spectroscopy was used to characterize the formation of the product. ^{1}H NMR spectrum (Figure 2.10) shows methyl protons at 1.31 ppm. The aromatic protons were observed between 7.7 ppm and 7.3 ppm. The –CH_2 protons next to bromine atom were seen at 3.9 ppm as a triplet. Deshielding of these protons was higher compared to the monomer **1**.

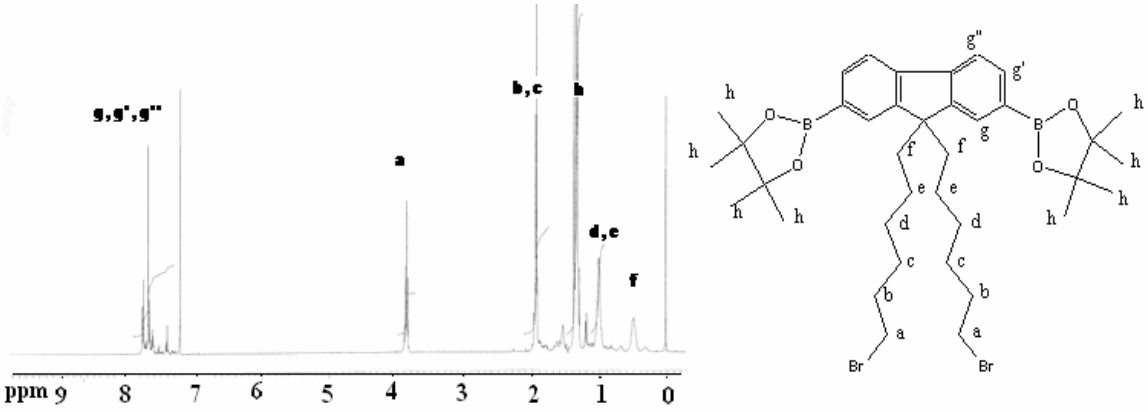

Fig. 2.10- ^{1}H-NMR Spectrum of **5** (400 MHz, $CDCl_3$, 25 ^oC)

The spectroscopic investigations showed some abnormalities like the carbonyl bond and a very downfield triplet due to –CH_2 group close to bromine atom. These might have a sign of an oxidation in some part of the molecule. We knew that the Suzuki coupling conditions are tolerant other functional groups. Monomer might have oxidized at some position that we don't know completely. So unreliability of the

formation of boronic ester derivative of the monomer we did not continue to syhnthesize the homopolymer. Instead we prepared a copolymer made up of fluorene backbone. The copolymer was composed of monomer **1** and its unfuctionalised hexyl chains.

2.1.5 Synthesis and Characterization of of poly[(9,9-Dihexyl-9H-fluorene)-co-alt-(9,9-bis-(6-bromo-hexyl)-9H-fluorene)] (P1)

Monomer **1** was subjected to Suzuki coupling reaction with 9,9-dihexylfluorene-2,7-bis(trimethyleneborate) to produce a novel copolymer with a % 64 yield. The reaction was carried out at the water/THF mixture in a weak base medium supplied by potassium carbonate and using Pd (0) metal as a catalyst at 80 ^{o}C. Purification of the polymer was done by precipitation into methanol three times.

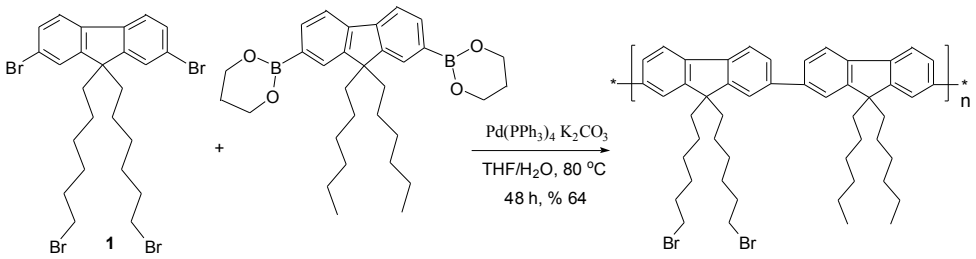

Scheme 2.7- The synthesis of **P1**

Poly[(9,9-Dihexyl-9H-fluorene)-co-alt-(9,9-bis-(6-bromo-hexyl)-9H-fluorene)] **P1** is characterized by ^{1}H-NMR spectroscopy. The ^{1}H-NMR spectrum (Figure 2.11) of **P1** shows 12 aromatic protons as a multiplet at 7.85 ppm. Signal at 3.32 ppm is for the methylene protons next to bromine atom. Signals between 3.32 ppm and 0.85 ppm are due to hexyl chains of both monomers. Methylene protons are seen at 3.32 ppm bcause of the electron withdrawing bromine atom.

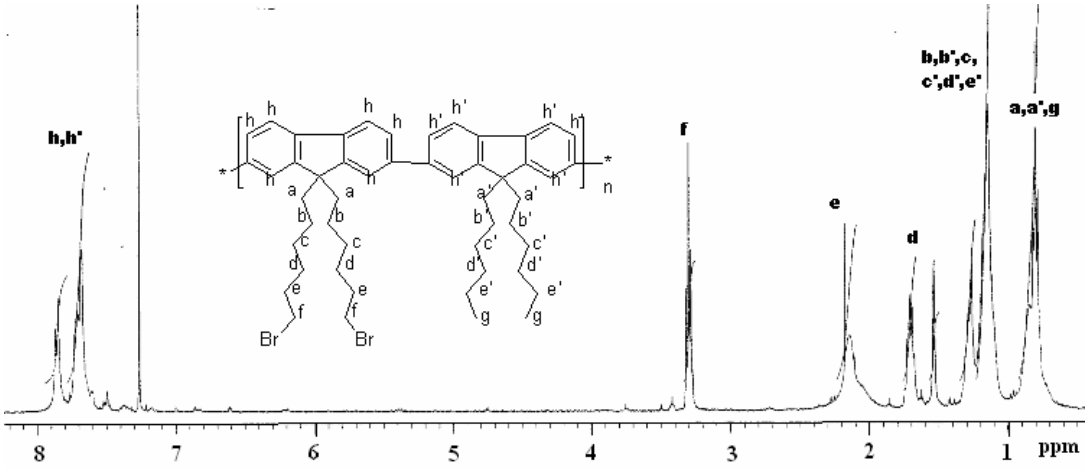

Fig. 2.11- ^{1}H-NMR spectrum of **P1** (400 MHz, $CDCl_3$, 25 ^{o}C)

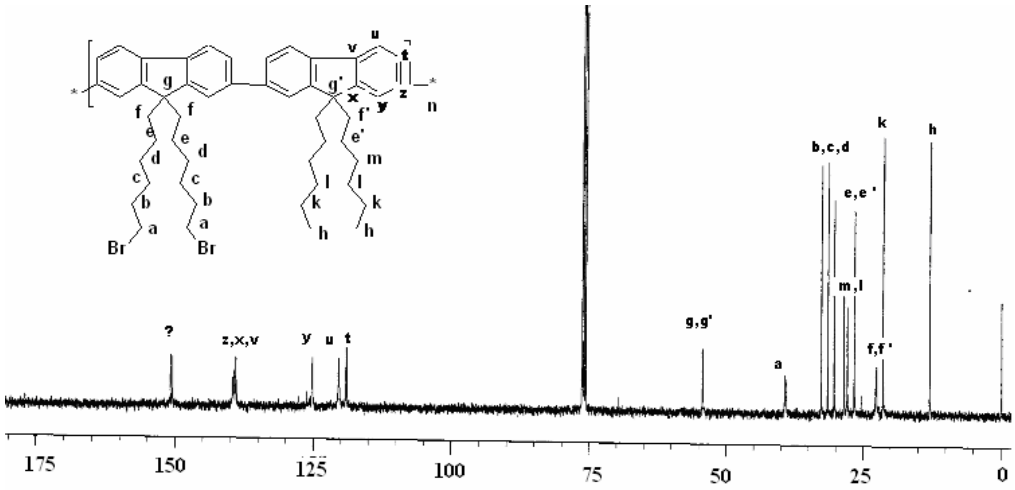

Fig. 2.12- ^{13}C-NMR Spectrum of **P1** (100 MHz, $CDCl_3$, 25 ^{o}C)

In the ^{13}C NMR spectrum aromatic carbons were observed between119 ppm and 141 ppm. The aromatic quaternary carbons were seen at 140.5ppm, 140.2 ppm, and 139 ppm. Signal at 54.7 ppm was due to C9 quaternary carbon atom. The hexyl alkyl carbons were seen at δc: 39.6, 32.9, 31.8, 30.6, 28.8, 28.2, 26.9, 23.0, 21.6, 13.1 ppm. The peak at 39.6 ppm was due to the carbon bonded to bromine atom.

Absorption and emission spectra for P1 were measured in chloroform at room temperature. Figure 2.13 shows the UV-VIS and PL spectra for this polymer. Poly[(9,9-Dihexyl-9H-fluorene)-co-alt-(9,9-bis-(6-bromo-hexyl)-9H-fluorene)], **P1** shows an absorption band peaking at 378 nm due to the π-π* transition with an absorption coefficient 72,750. Optical excitation at 378 nm gives a strong violet

fluorescence in the range of 400-550 nm with a maximum at 417 nm. In the solid state strong blue fluorescence is observed at 449 nm with 32 nm red shift for **P1**. The solid film was obtained by spin coating of the dissolved polymer (20 mg) in chloroform (2 mL) at 800 rpm for 1.5 min.

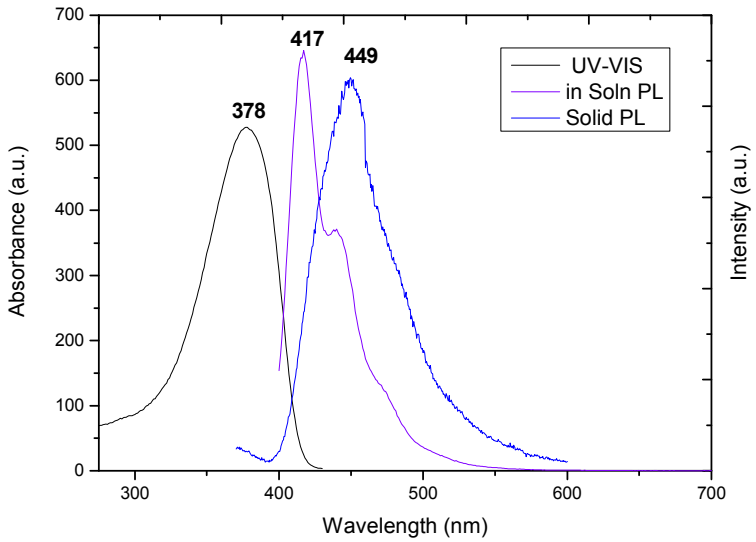

Fig. 2.13- UV-VIS and PL spectrum of **P1** in $CHCl_3$

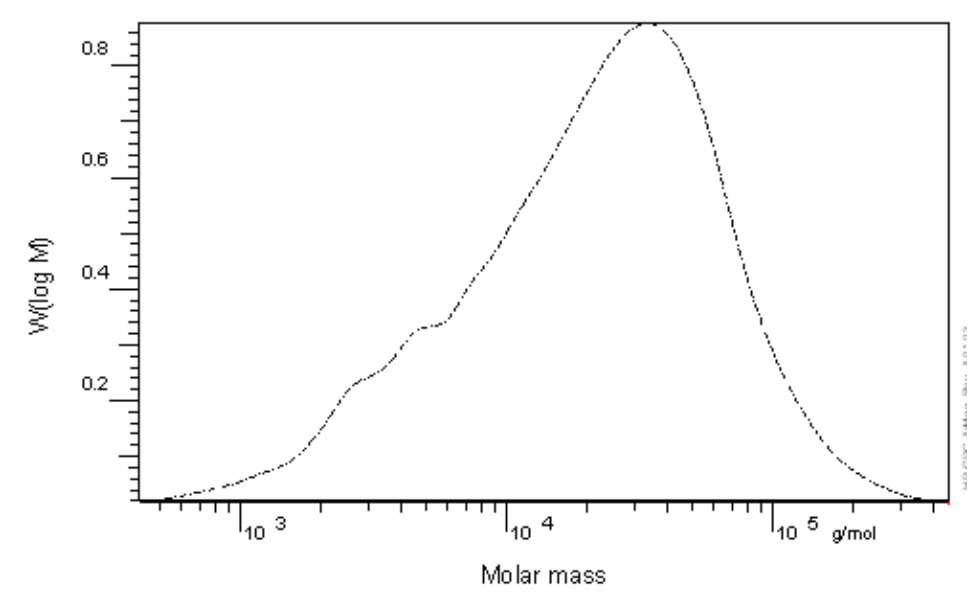

Fig. 2.14- GPC analysis of **P1** (Polystyrene as standard)

GPC analysis with THF as an eluent and polystyrene as a standard provides number average molecular weight of (M_n) 8,900 gr/mol. This result points out to degree of polymerization of 10. However the analysis also yields weight average molecular weight (M_w) of 35,900 gr/mol.

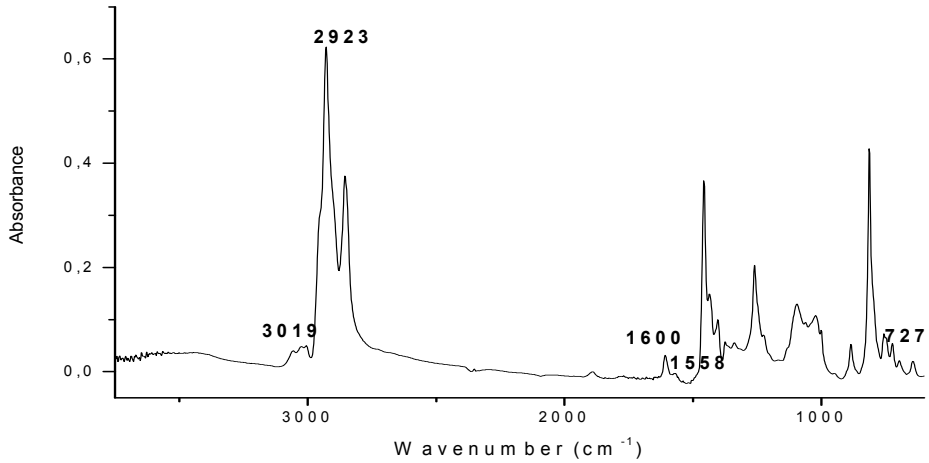

Fig. 2.15- The FT-IR spectrum of **P1**

In FT-IR spectrum of **P1**, aromatic carbon hydrogen bond stretching at 3019 cm^{-1} and aliphatic carbon hydrogen bond stretching at 2923 cm^{-1} are observed. The aromatic carbon double bonds appear at 1600 cm^{-1} and 1558 cm^{-1}.

2.1.6 Synthesis and Characterization of poly[(9,9-Dihexyl-9H-fluorene)-co-alt-(9,9-bis-(6-azido-hexyl)-9H-fluorene)] (P2)

As seen in Scheme 2.8, **P1** was subjected to a nucleophilic substitution reaction with NaN_3 in DMF at 60 ^oC to prepare the poly[(9,9-Dihexyl-9H-fluorene)-co-alt-(9,9-bis-(6-azido-hexyl)-9H-fluorene)] **P2**. It was purified by precipitation into methanol three times. The product was obtained as a yellow fine powder.

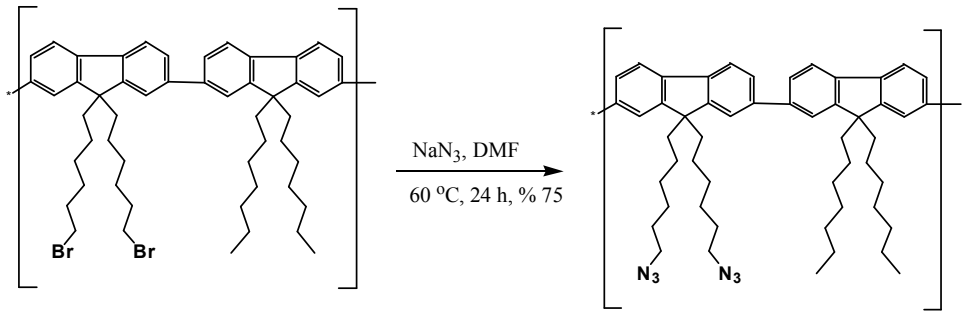

Scheme 2.8- The synthesis of **P2**

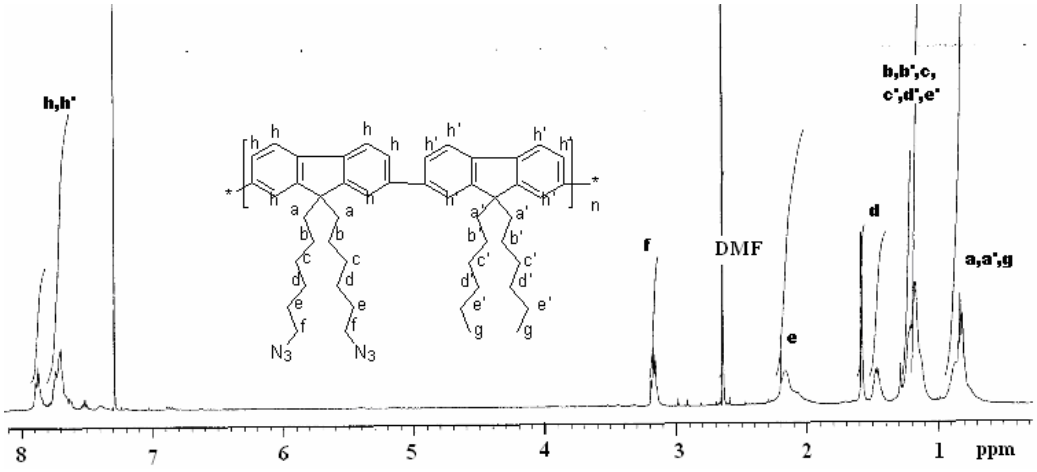

Fig. 2.16- ^{1}H-NMR spectrum of **P2** (400 MHz, $CDCl_3$, 25 ^{o}C)

The characterization of **P2** was carried out by ^{1}H NMR, UV-VIS, Fluorescence and FT-IR spectroscopy. The ^{1}H NMR spectrum shows 12 aromatic protons at 7.75 ppm as a multiplet. The hexyl protons are seen between 3.16 ppm and 0.82 ppm The characteristic **f** protons next to the electronegative nitrogen atom are observed at 3.16 ppm.. The methylene protons next to nitrogen atoms are less deshielded compared to precursor **P1**.

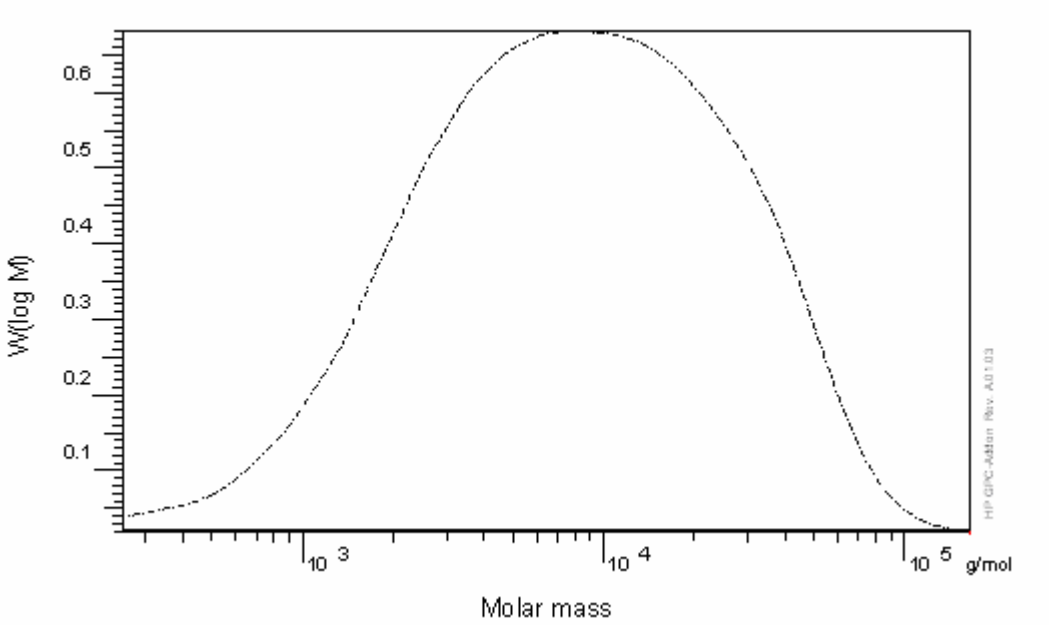

Fig. 2.17- GPC analysis of **P2** (Polystyrene as standard)

GPC analysis was done using THF as an eluent and polystyrene as a standard providing number average molecular weight of (M_n) 3,680 gr/mol. The degree of polymerization was found to be around 5. The weight average molecular weight (M_w) was determined as 14,700 gr/mol.

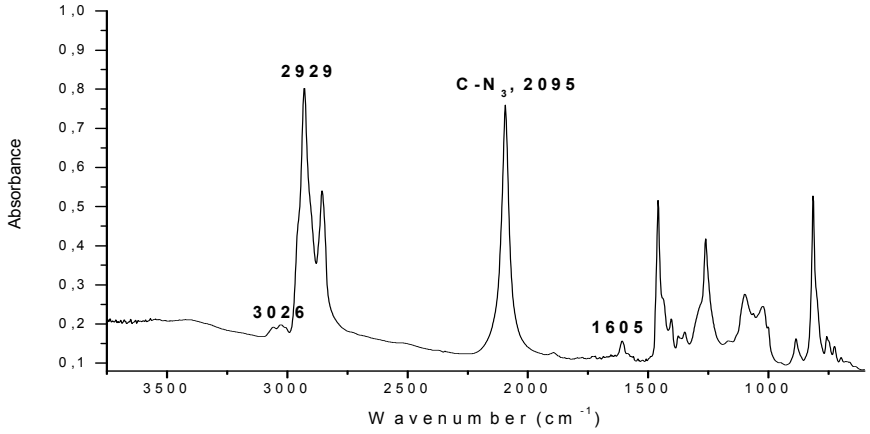

Fig. 2.18- FT-IR spectrum of **P2**

In the FT-IR spectrum of **P2** carbon azide stretching peak at 2095 cm $^{-1}$ confirmed the product formation. The aromatic carbon-hydrogen stretching at 3026 cm^{-1} and aliphatic carbon-hydrogen stretching peak at 2929 cm^{-1} were present. The aromatic carbon double bonds were observed at 1605 cm^{-1}.

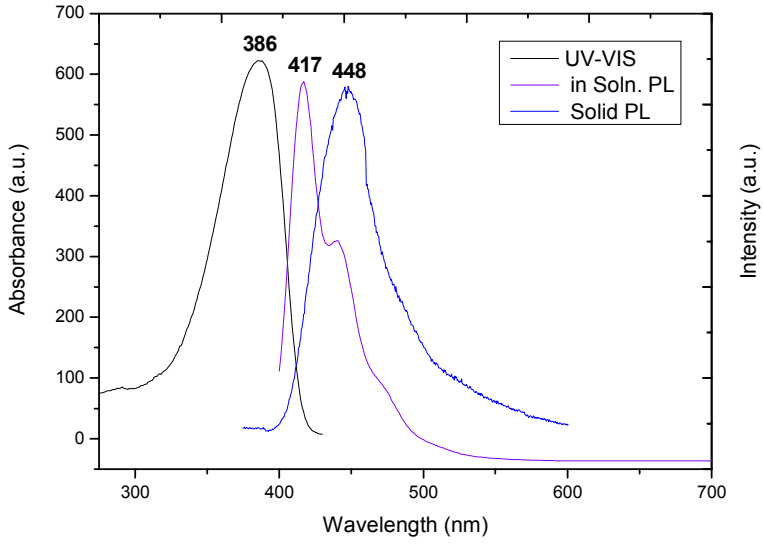

Fig. 2.19- UV-VIS and PL spectrum of **P2** in $CHCl_3$

Absorption and emission spectra for **P2** were recorded in chloroform at room temperature. Figure 2.19 shows absorption band peaking at 386 nm due to the π-π* transition with an absorption coefficient of 25,680. Optical excitation at 386 nm gives a strong violet fluorescence in the range of 400-550 nm with a maximum at 417 nm. In the solid state strong blue fluorescence is observed at 448 nm with 31 nm

red shift for **P2**. The solid film wa obtained by spin coating of the dissolved polymer (20 mg) in chloroform (2 mL) at 800 rpm for 1.5 min.

2.1.7 Towards functionalization of the P1 and P2

Formation of **P1** and **P2** was confirmed by spectroscopic techniques. Then we attempted click chemistry reaction between **P2** and propargylamine. Click chemistry reaction is a useful reaction in formation of triazoles from coupling of azido and alkyne monomers catalysed by Cu (II). The reaction can run in water through reduction of Cu(II) to Cu(I). In our synthetic route **P2** having a azide group was reacted with propargylamine in THF/H_20 solvent in rt as outlined in Scheme 2.9.

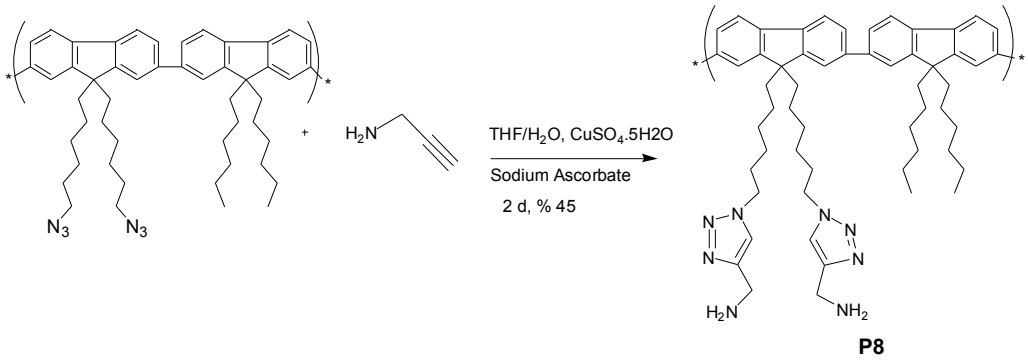

Scheme 2.9- The synthesis of **P8**

The product obtained was insoluble in both organic solvents and water. So its total characterization was not possible. However, FT-IR spectrum showed the absence of carbon-azide peak at 2092 cm^{-1}. A band with a maximum at 3431 cm^{-1} was seen due to amine groups. Also the aromatic and aliphatic carbon hydrogen bond stretchin were seen at 3026 cm^{-1} and 2929 cm^{-1}.

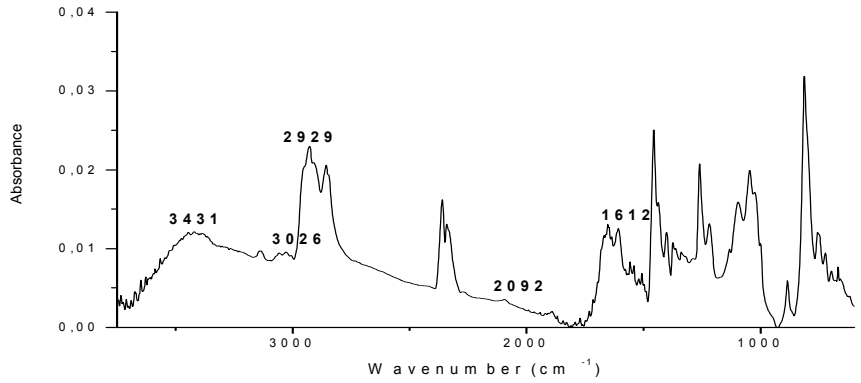

Fig. 2.20- FT-IR spectrum of **P8**

FT-IR spectroscopy confirms the formation of the product. However, the obtained product is insoluble in both organic and aqueous solvents. Insolubility of the product can be explained by the formation of network like structure because of hydrophobic interactions; hydrogen bonding interactions and π-π interactions between the triazole rings.[30]

Insolubility of the product prevented us to continue threading the polymer with triazole ring into CB(6). So, we tried next the azidoethylamine addition to poly[(9,9-Dihexyl-9H-fluorene)-co-alt-(9,9-bis-(6-bromo-hexyl)-9H-fluorene)], **P1**. This reaction's product was important for 1,3 dipolar addition reaction catalyzed by CB(6). Because CB(6) can form stable complexes with the amine groups.

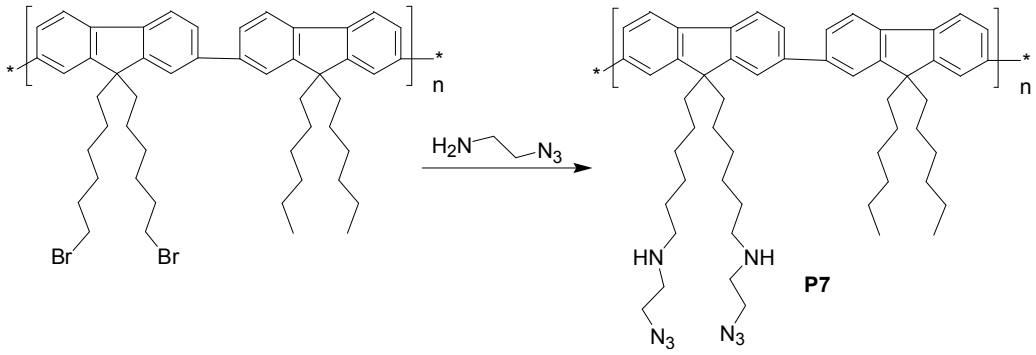

Scheme 2.10- The synthesis of **P7**

P7 was synthesized by the reaction of **P1** with excess azidoethylamine in THF with % 94 yield. The reaction is a nucleophilic substitution reaction in which bromine

atoms are substituted by amine groups. Excess azidoethylamine was used as a solvent to prevent over alkylation. The reaction scheme of **P7** is shown in Scheme 2.10 above.

P7 was investigated by FT-IR spectroscopy. In the FT-IR spectrum the carbon azide stretching is seen at 2099 cm^{-1} confirming the addition reaction. At 3327 cm^{-1} the amine stretching is observed. The carbon-hydrogen stretching for aromatic 3053 cm^{-1} and for aliphatic at 2929 cm^{-1} are present.

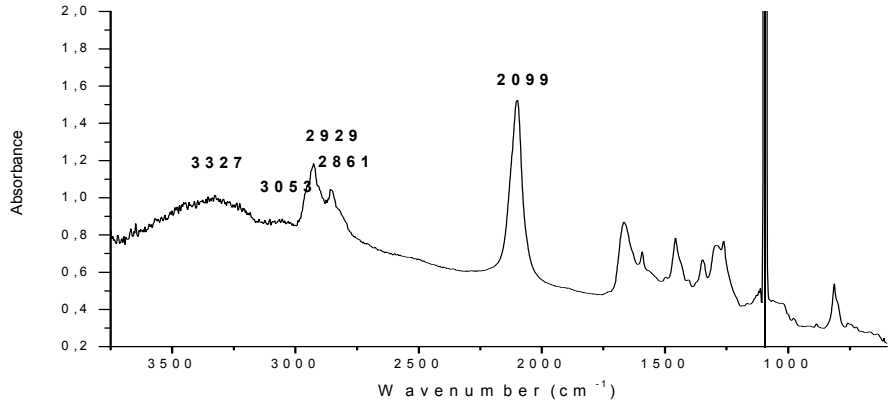

Fig. 2.21- FT-IR spectrum of **P7**

We attempted to treat **P7** with acid to make it water soluble. To obtain water soluble product was difficult. After extraction of the aqueous layer and evaporation of the solvent very little amount of yellow solid was obtained. This product was investigated by FT-IR spectroscopy. In Figure 2.22, FT-IR spectrum is shown. The amine stretching band peaking at 3410 cm^{-1} is observed. The azide peak is present at 2113 cm^{-1}.

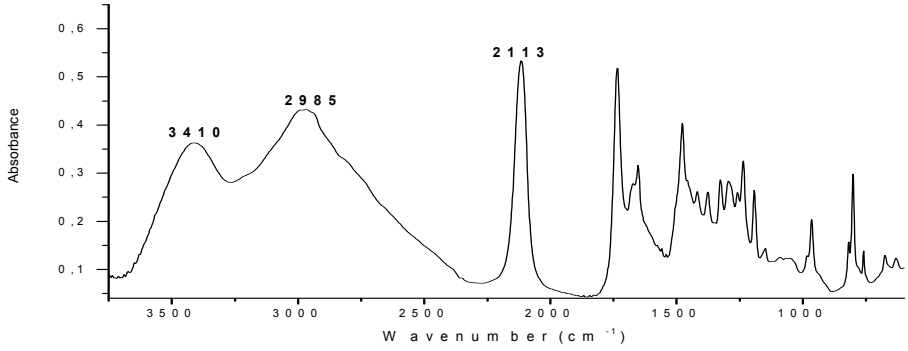

Fig. 2.22- FT-IR spectrum of **P7** after acid treatment

The insolubility of the product in acidic medium prevented us to continue 1,3 dipolar addition catalysed by CB(6). Because 1,3 dipolar addition reaction runs in acidic medium.

2.1.8 Synthesis and Characterization of poly[9,9-bis-(6-bromo-hexyl)-9H-fluorene-co-1,4-phenylene] (P3)

Insolubility of the polyfluorene copolymers did not allow us to continue to prepare the desired pseudopolyrotaxane as discussed in the preceeding section. Then we tried the preparation of fluorene-phenylene copolymers. Phenylene monomer is less apolar because it contains no alkyl chains and less aromatic groups if compared to former fluorene monomer with hexyl chains. We thought that in further steps solubility in aqueous medium can be supplied with less apolar groups. 2,7-dibromo-9,9-bis-(6-bromo-hexyl)-9H-fluorene was subjected to Suzuki coupling reaction with 1-4, phenylene-diboronic acid using Pd(II) catalyst in THF/H_2O as solvent. As shown in Scheme 2.11 the reaction was carried out at 80 ^oC for three days to obtain **P3** in 94 % yield.

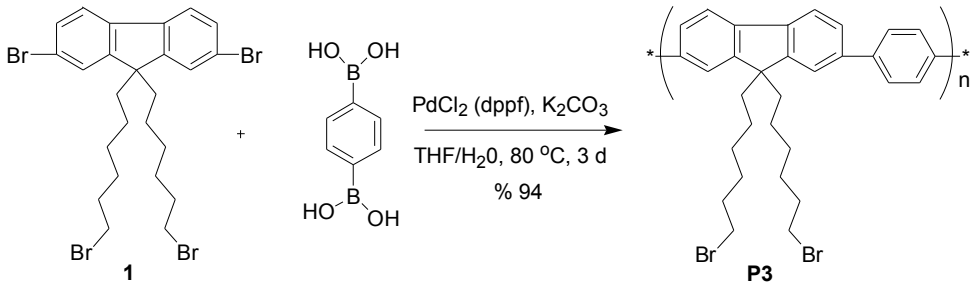

Scheme 2.11- The synthesis of **P3**

^1H NMR spectroscopy of **P3** showed broad peaks at about 7.65 ppm for aromatic protons. The signals between 3.32 ppm and 0.80 ppm are due to alkyl protons. The signal at 3.32 ppm is for the methylene protons next to bromine atom.

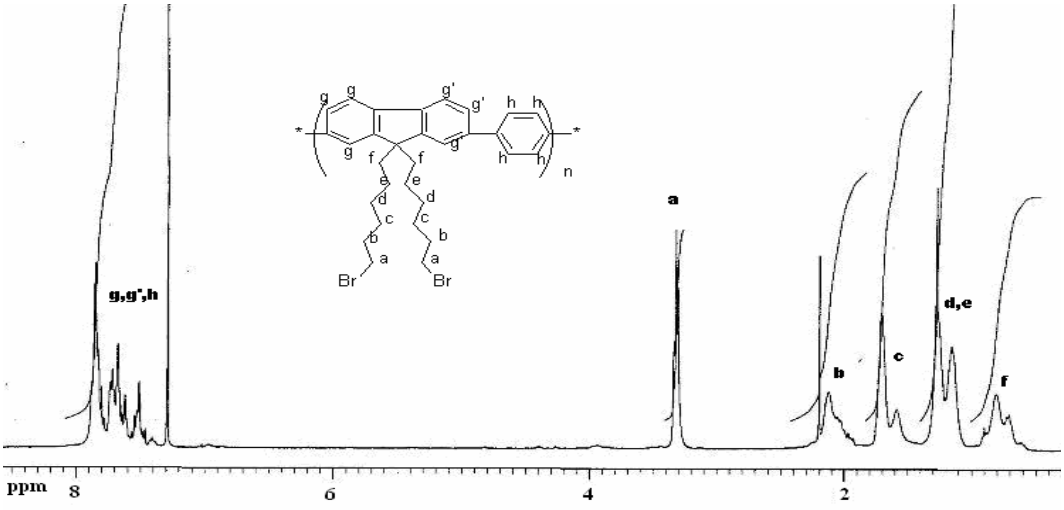

Fig. 2.23- H-NMR spectrum for **P3** (400 MHz, $CDCl_3$, 25 ^oC)

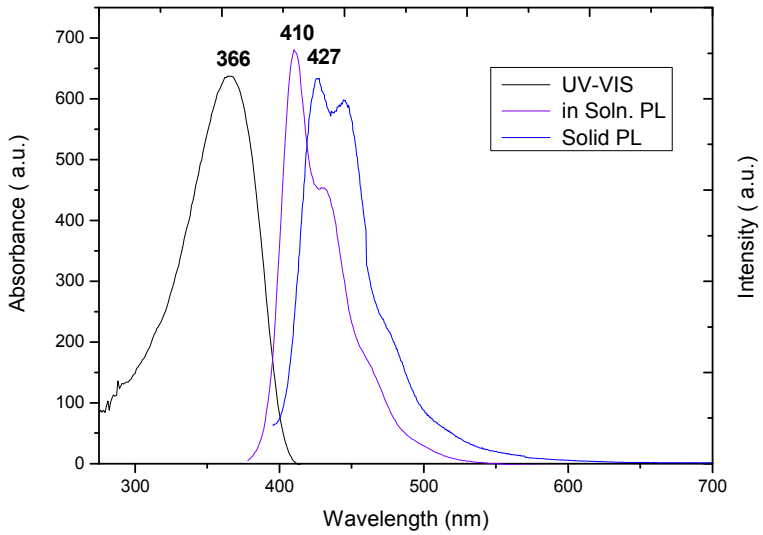

Fig. 2.24- UV-VIS and PL spectrum of **P3** in THF

Figure 2.23 shows the absorption and emission spectra for **P3**. In THF solution **P3** display an absorption band peaking at 366 nm. due to the π-π* transition with an absorption coefficient of 28,450. **P3** absorbs in lower wavelength than polyfluorene copolymer as it has less double bonds. Optical excitation of **P3** at 366 results a strong violet emission at 410 nm. **P3** shows strong blue fluorescence at 427 nm in the solid state with a 17 nm red shift. The solid film was obtained by spin coating of the dissolved polymer (20 mg) in THF (2 mL) at 800 rpm for 1.5 min.

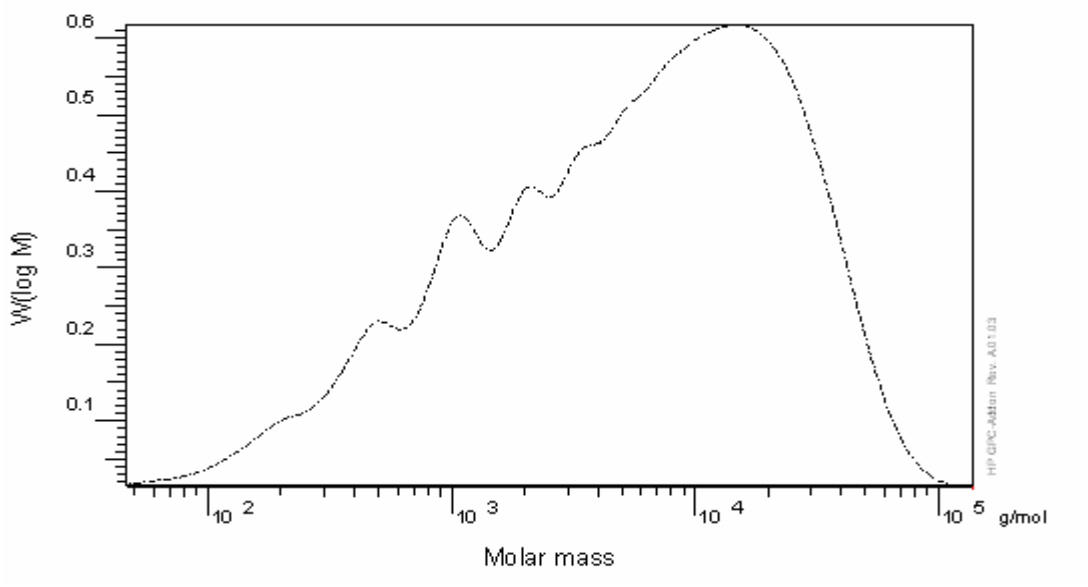

Fig. 2.25- GPC analysis of **P3** (Polystyrene as standard)

GPC analysis with THF as an eluent and polystyrene as a standard provides number average molecular weight of (Mn) 1,370 gr/mol. This result points out to degree of polymerization of around 3. However, the analysis provides a weight average molecular weight (Mw) of 11,900 gr/mol.

Figure 2.24 shows the FT-IR spectrum of **P3**. In the FT-IR spectrum aromatic carbon hydrogen at 3024 $cm^{-1}$and aliphatic carbon hydrogen stretchings at 2929 cm^{-1} are present. The aromatic carbon double bonds are observed at 1606 cm^{-1}.

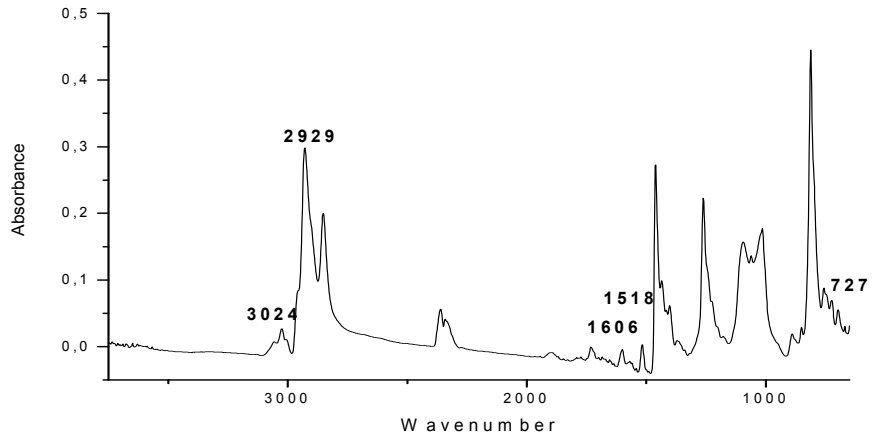

Fig. 2.26- FT-IR spectrum of **P3**

2.1.9 Synthesis and Characterization of poly[9,9-bis-(6-azido-hexyl)-9H-fluorene-co-1,4-phenylene] (P4)

P3 was subjected to nucleophilic substitution reaction with sodium azide in aprotic solvent, DMF, at 60 ^{o}C. The reaction time was two days as outlined in Scheme 2.12 below. Extraction and precipitation into methanol yielded the product in 62 % yield.

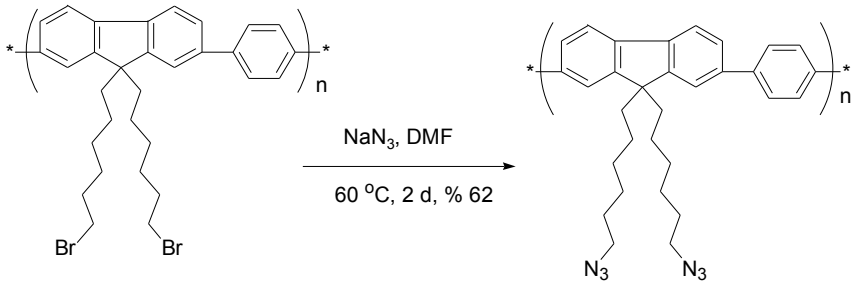

Scheme 2.12- The synthesis of **P4**

The product was characterized by ^{1}H-NMR,UV-VIS, Fluorescence and FT- IR spectroscopy techniques. In Figure 2.27, ^{1}H-NMR spectrum of **P4** is seen. In the ^{1}H-NMR spectrum 10 aromatic protons are observed at 7.35 ppm. The other methylenic protons are seen between 3.25 ppm and 0.75 ppm. The appearance of two triplets at 3.25 ppm and 3.32 ppm shows that bromine atoms are not substituted with the azide groups completely.

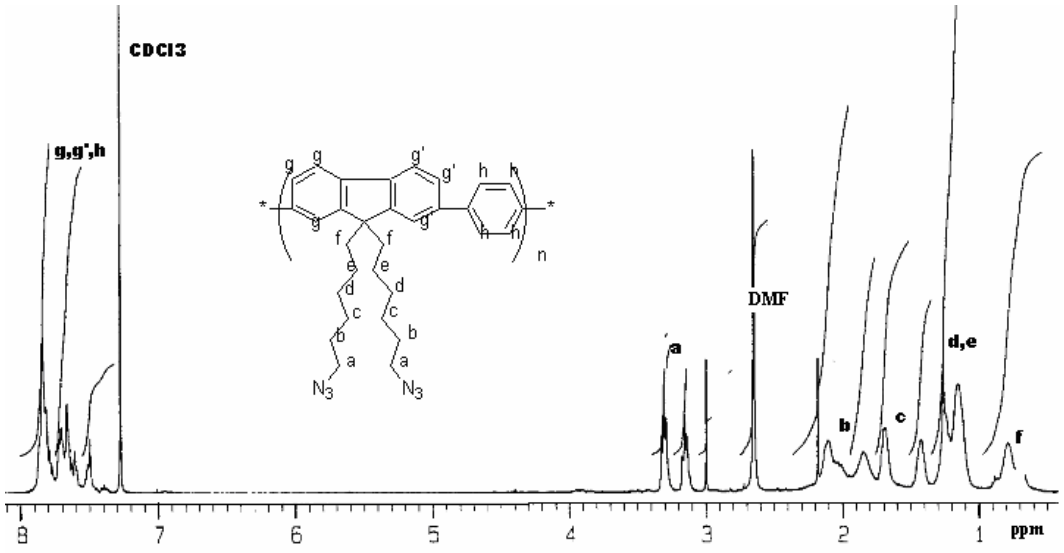

Fig. 2.27- FT-IR spectrum of **P4** (400 MHz, $CDCl_3$, 25 ^{o}C)

The UV-VIS and Fluorescence spectra of poly[9,9-bis-(6-azido-hexyl)-9H-fluorene-co-1,4-phenylene] show an absorption maximum at 366 nm with an absorption coefficient of 21,650 and an emission maximum at 410 nm by excitation at 366 nm in chloroform solution. In the solid state, **P4** shows strong blue fluorescence at 427 and 446 nm with a red shift. The solid film were obtained by spin coating of the dissolved polymer (20 mg) in $CHCl_3$ (2 mL) at 800 rpm for 1.5 min.

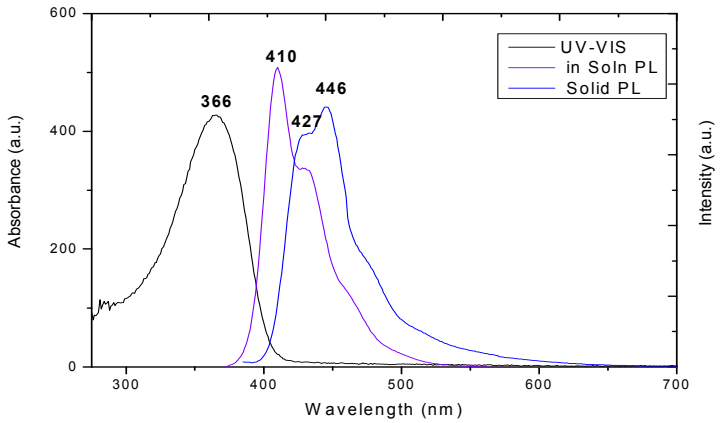

Fig. 2.28- UV-VIS and PL emission spectra of **P4** in $CHCl_3$

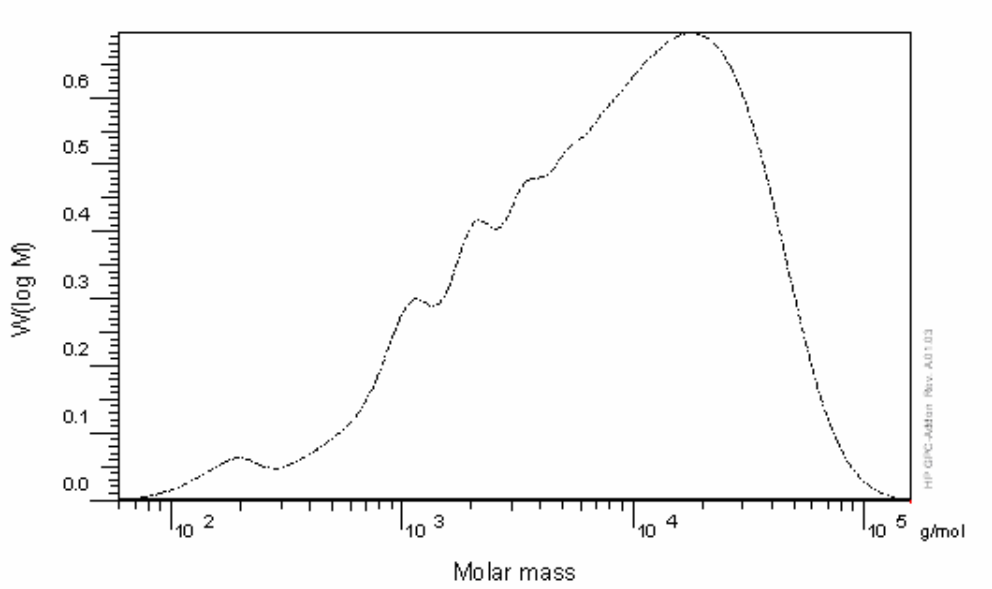

Fig. 2.29- GPC analysis of **P4** (Polystyrene as standard)

GPC analysis of **P4** was done with THF as an eluent and polystyrene as a standard providing a number average molecular weight of (M_n) 2,410 gr/mol corresponding

to a degree of polymerization of 5. The weight average molecular weight (M_w) was obtained 14,600 gr/mol.

In the FT-IR spectrum, carbon azide stretching peak at around 2093 cm^{-1}, carbon hydrogen stretchings for aromatic at 3026 $cm^{-1}$and for aliphatic at 2925 cm^{-1} are present. The aromatic carbon double bonds are observed at 1596 cm^{-1}.

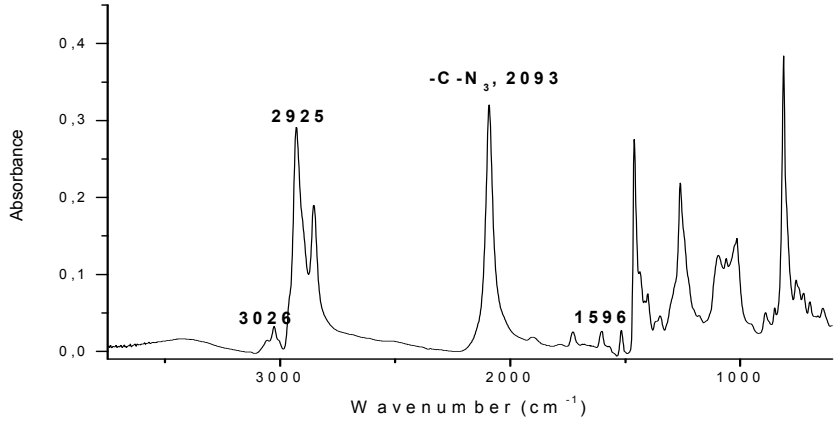

Fig. 2.30- FT-IR spectrum of **P4**

Formation of **P3** and **P4** was confirmed by spectroscopic techniques. **P4**, having a azido group was tried to undergo click hemistry reaction as in Scheme 2.12. **P9** was synthesized by click chemistry reaction between **P4** and propargylamine in THF/H_2O solvent mixture by the catalysis of Cu(II) at rt. After work-up brown product was obtained in % 92 yield.

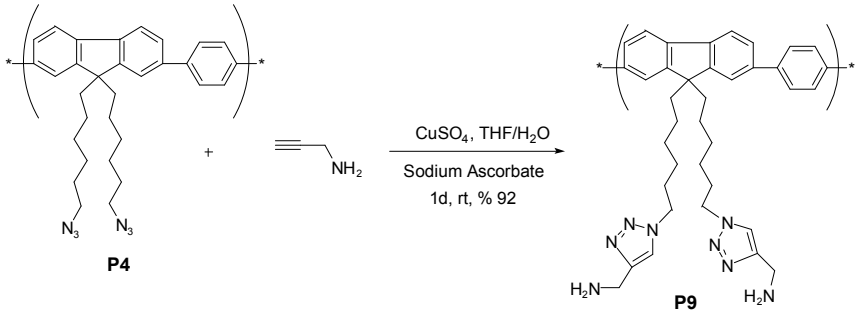

Scheme 2.13- The synthesis of **P9**

The obtained was tried to dissolve in both organic and aqueous solvents. However, the product was insoluble. So full characterization of the product was not possible. The product was characterised only by FT-IR spectroscopy. Its FT-IR spectrum

showed the presence of amine group due to the band with a maximum at 3431 cm^{-1}. The aromatic and aliphatic carbon hydrogen bon stretchings were present at 3037 cm^{-1} and 2930 cm^{-1}. The carbon azide peak at 2093 cm^{-1} disappeared.

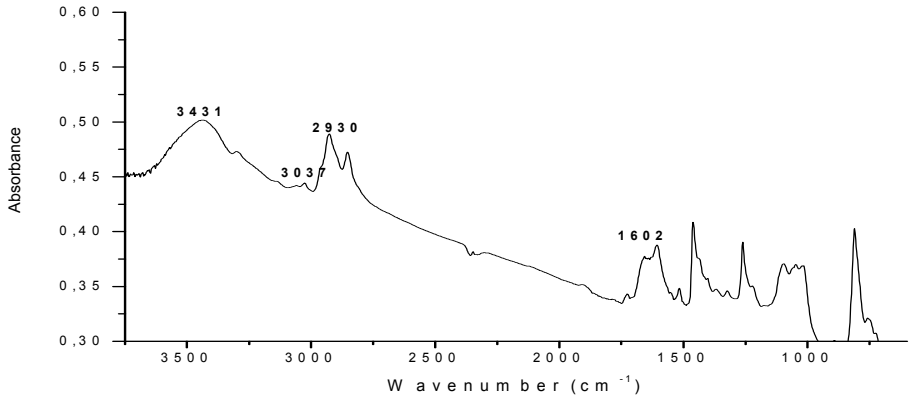

Fig. 2.31- FT-IR spectrum of **P9**

Insolubility can be explained by formation of network like structure because of hydrophobic interactions; hydrogen bonding interactions and π-π interactions from the triazole rings as explained above.[30] Insolubility of the product disabled us to attach CB(6) for the preparation of polypseurotaxane.

2.1.10 Synthesis and Characterization of poly[9,9-bis-(6-bromo-hexyl)-9H-fluorene-co-2,5-thienylene] (P5)

We tried to synthesize pseudopolyrotaxane with a different band-gap copolymer. We tried to synthesize fluorene-thienylene copolymer as shown in Scheme 2.12 below. Poly[9,9-bis-(6-bromo-hexyl)-9H-fluorene-co-2,5-thienylene] **P5** was synthesized by Suzuki coupling reaction of 2,7-dibromo-9,9-bis-(6-bromo-hexyl)-9H-fluorene with thiophene-2,5-diboronic acid using Pd(II) catalyst with phase transfer catalyst, tetrabutlyammoniumbromide in THF/H_2O solvent. We added phase transfer catalyst to increase the yield. Extraction and precipitation into methanol yielded 62 % of poly[9,9-bis-(6-bromo-hexyl)-9H-fluorene-co-2,5-thienylene].

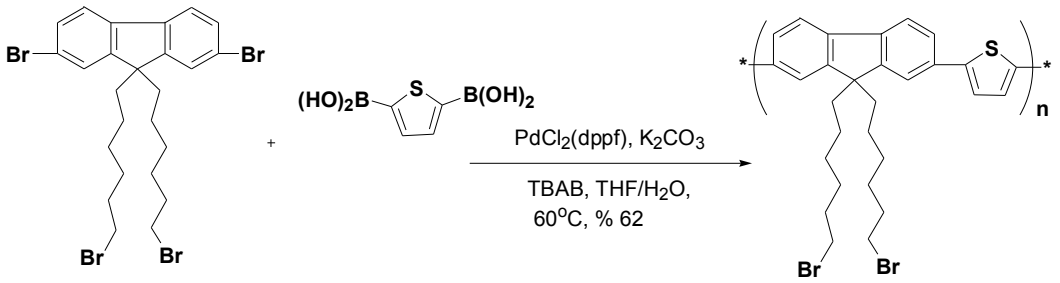

Scheme 2.14- The synthesis of **P5**

The product was investigated by FT-IR, UV-VIS, Fluorescence and ^{1}H-NMR spectroscopy. In Figure 2.32, ^{1}H-NMR is shown. ^{1}H-NMR spectrum shows broad multiplet at 7.35 ppm for aromatic fluorene protons and thienylene protons. The alkyl protons are observed between 3.20 ppm and 0.60 ppm. The signal at 3.20 ppm is due to methylene protons close to bromine atom.

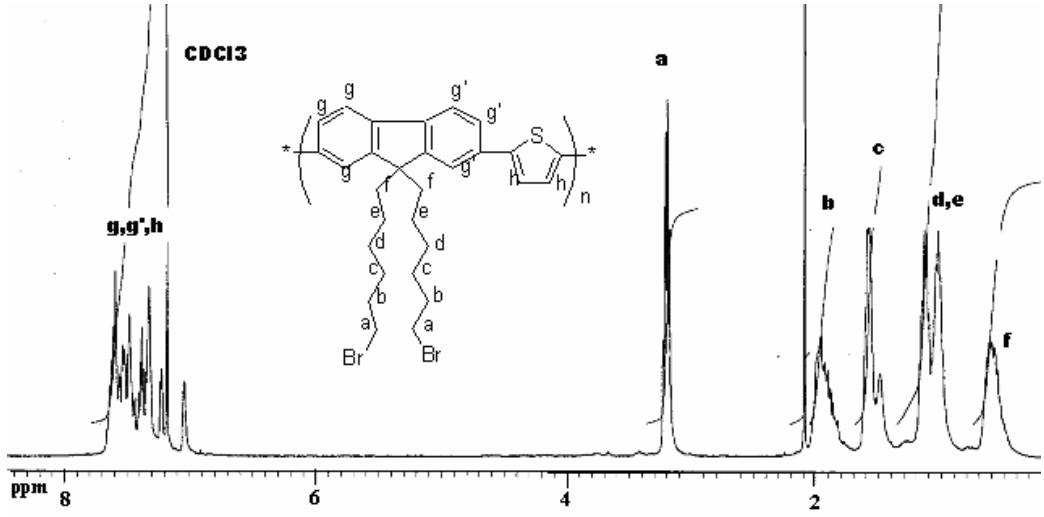

Fig. 2.32- ^{1}H-NMR spectrum of P5 (400 MHz, $CDCl_3$, 25 ^{o}C)

UV-VIS and Fluorescence spectra of **P5** shows an absorption band with a maximum at 400nm with an absorption coefficient of 12,675 and an emission maximum at 464 nm in chloroform solution. At the solid state copolymer shows strong green fluorescence at 506 nm with a 42 nm red shift. The solid film were obtained by spin coating of the dissolved polymer (20 mg) in $CHCl_3$ (2 mL) at 800 rpm for 1.5 min.

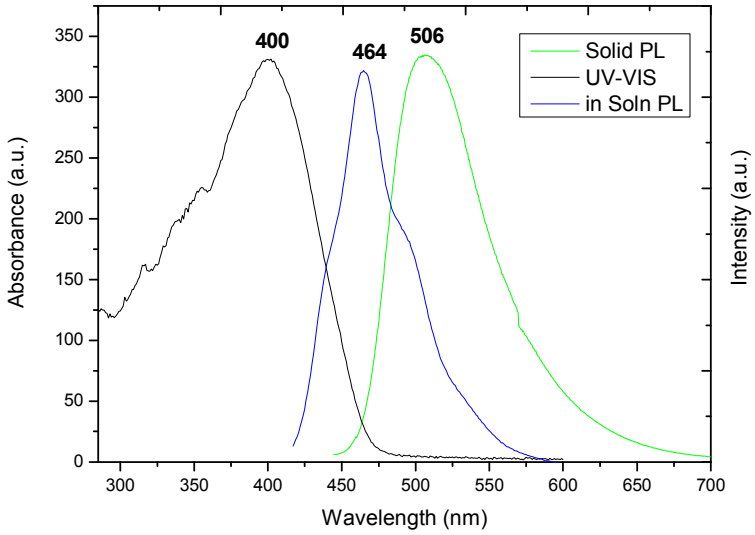

Fig. 2.33- UV-VIS and PL emission spectra of **P5** in $CHCl_3$

GPC analysis of **P5** with THF as an eluent and polystyrene as a standard showed a number average molecular weight of (M_n) 698 gr/mol corresponding to a very low degree of polymerization. The analysis showed a weight average molecular weight (M_w) of 1,970 gr/mol

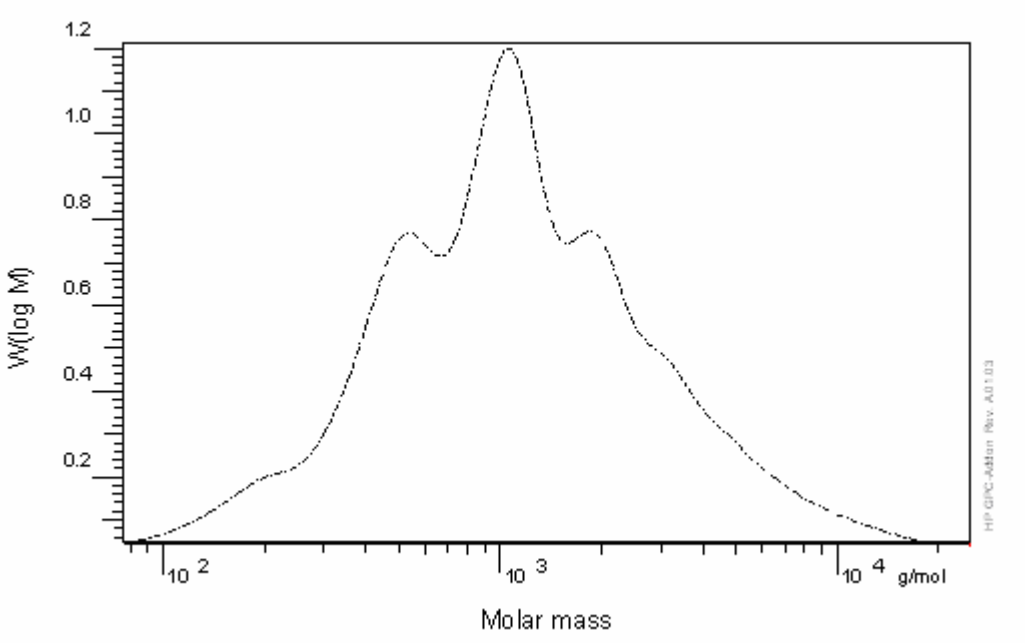

Fig. 2.34- GPC analysis of **P5** (Polystyrene as standard)

In the FT-IR spectrum of **P5** carbon-hydrogen stretchings for aromatic at 3034 cm^{-1} and aliphatic at 2926 cm^{-1} are present. The aromatic carbon double bonds are seen at 1604 and 1568 cm^{-1} as weak peaks.

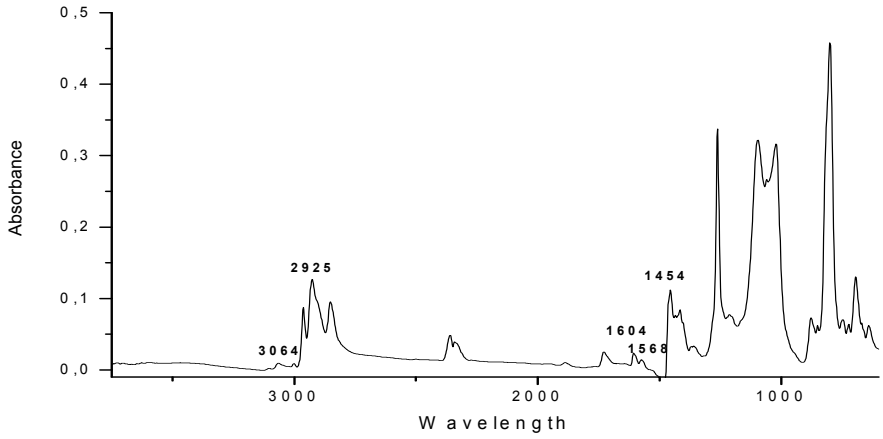

Fig. 2.35- FT-IR spectrum of **P5**

We could not continue further modifications on **P5** because of the time restriction.

2.1.11 Synthesis and Characterization of 9, 9-Bis-(6-azido-hexyl)-2,7-dibromo-9H-fluorene (3)

The second method was forming rotaxane at the monomer level and then trying the polymerization. We tried to functionalize fluorene monomer with a suitable azido or alkyne monomer. Then, by addition of azido monomer and CB(6), rotaxane would be formed via CB(6)-catalysed 1,3 dipolar cycloaddition or by click creaction with propargylamine by Cu(II) catalysis was attempted.

2,7-dibromo-9,9-bis-(6-bromo-hexyl)-9H-fluorene was subjected to a nucleophilic substitution reaction with NaN_3 in DMSO solvent at 70 ^oC. DMSO was chosen as an aprotic solvent favoring the SN_2 reaction. The reaction was carried out for one day as shown in Scheme 2.13. Extraction yielded 9, 9-Bis-(6-azido-hexyl)-2,7-dibromo-9H-fluorene in a % 82 yield as a yellow oil.

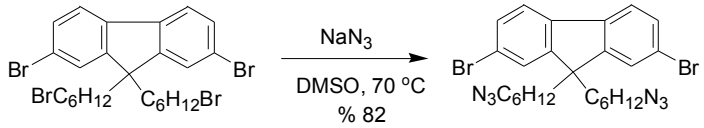

Scheme 2.15- The Synthesis route of **3**

The product was investigated through FT-IR spectroscopy. The presence of a strong peak at 2091 cm $^{-1}$ confirms the carbon azide stretching. Carbon hydrogen stretchings for aromatic at 3042 cm^{-1} and for aliphatic at 2927 cm^{-1} are present.

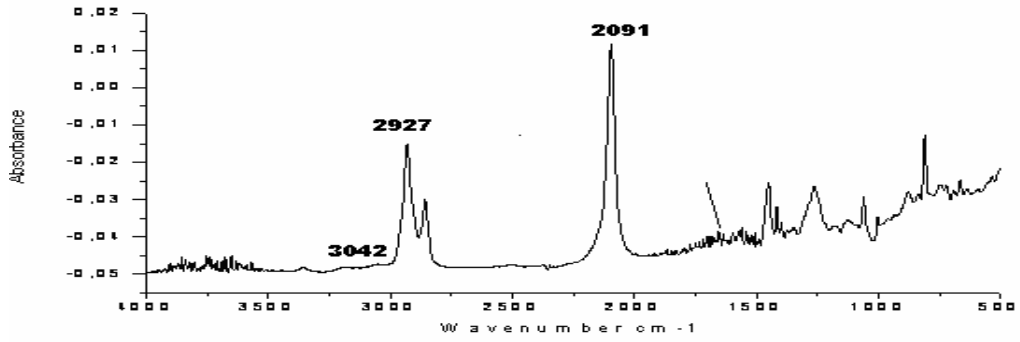

Fig. 2.36- FT-IR spectrum of **3**

Then, **3** was subjected to click chemistry reaction with propargylamine using Cu(II) as a catalyst as outlined in Scheme 2.14

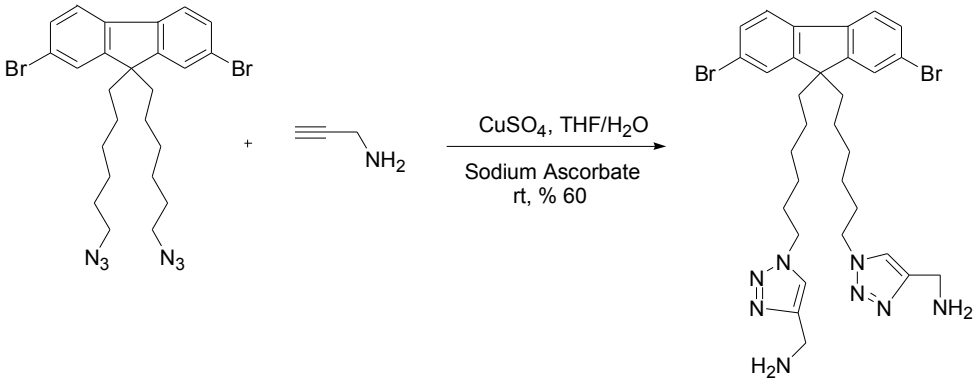

Scheme 2.16- Click chemistry reaction between **3** and propargylamine

The reaction was done at rt to obtain brown gel in 60 % yield. The product was insoluble in both organic and aqueous solvents. So its full characterization was not possible. It was investigated by FT-IR spectroscopy. Its FT-IR spectrum showed the presence of amine group due to a band with a maximum at 3410 cm^{-1}. The strong carbon azide bond stretching has disappeared. Also aliphatic carbon hydrogen stretching was seen at 2936 cm^{-1}.

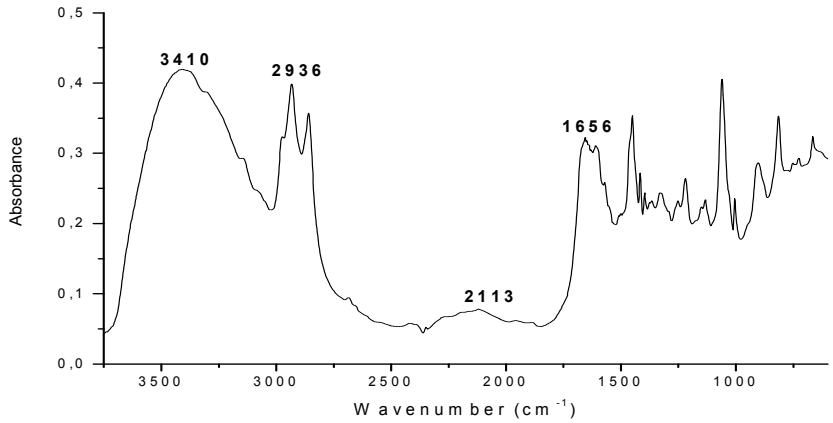

Figure 2.37- FT-IR spectrum of click chemistry reaction product

2.1.12 Synthesis of {6-[2,7-Dibromo-9-(6-prop-2-ynylamino-hexyl)-9H-fluoren-9-yl]-hexyl}-prop-2-ynyl-amine 4

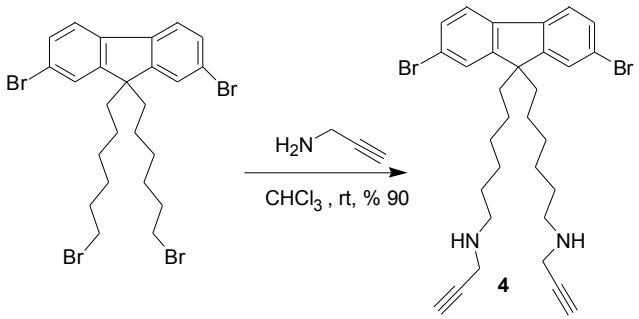

Scheme 2.17- The Synthesis of **4**

{6-[2,7-Dibromo-9-(6-prop-2-ynylamino-hexyl)-9H-fluoren-9-yl]-hexyl}-prop-2-ynyl-amine **4** was synthesized by the reaction of 2,7-dibromo-9,9-bis-(6-bromo-hexyl)-9H-fluorene with excess propargylamine in chloroform in % 90 yield. The reaction was a nucleophilic substitution reaction in which bromine atoms are substituted by propargylic amine groups. Excess propargylamine was used as a solvent to prevent over alkylation. The reaction scheme of **4** is shown in Scheme 2.17 above.

The product was investigated by FT-IR spectroscopy. The terminal alkyne is seen as a strong peak at 3300 cm^{-1}.The amine stretching at 3362 cm^{-1} is present. The aliphatic carbon-hydrogen stretching is observed at 2936 cm^{-1}

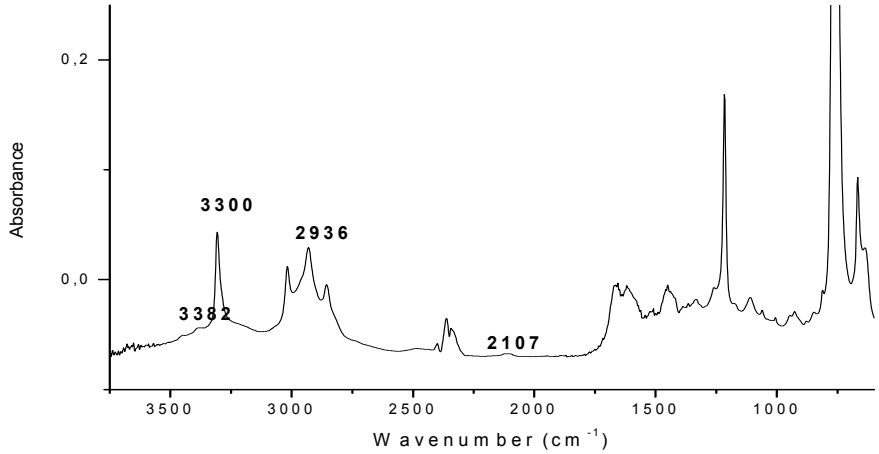

Fig. 2.38- FT-IR spectrum of **4**

After treatment with dilute NaOH and extraction the product was tried to be acidified to make it water soluble. However, the product was insoluble in water. The insolubility can be explained by the formation of the crosslinking between the terminal alkyne groups. So, strong crosslinking between the chains might have formed an impenetrable molecule. The insolubility prevented us to continue 1,3 dipolar addition with an azido monomer catalysed by CB(6).

2.1.13 Formation of Rotaxane

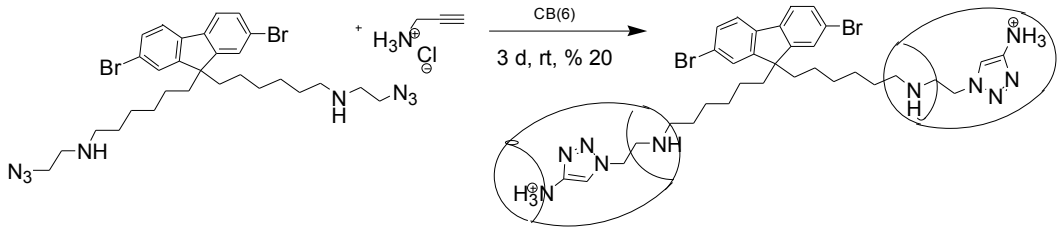

Scheme 2.18- The synthesis of rotaxane

Monomer functionalized with azidoethylamine was subjected to 1,3-dipolar cycloaddition catalysed by cucurbit[6]uril with propargylammonium salt. The reaction was carried out at water as a solvent. Precipitation into acteone yielded the rotaxane in % 20 yield. The product was characterized by FT-IR and ^{1}H-NMR spectroscopy.

In Figure 2.39 FT-IR spectrum shows the carbonyl stretching at 1730 cm^{-1} due to CB(6). Amine stretching is seen as a band with a maximum at 3431 cm^{-1}. Aliphatic carbon-hydrogen sretching at 2929 cm^{-1} is present.

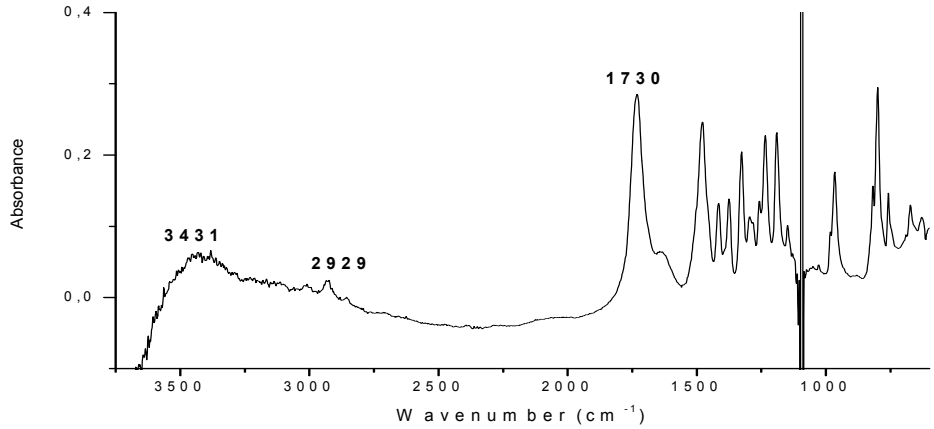

Fig. 2.39- FT-IR spectrum of rotaxane

The ^{1}H-NMR shows the presence of shielded triazole proton at 6.5 ppm. The aromatic protons are observed as a multiplet between 7.8 ppm and 7.5 ppm. The spectrum also shows alkyl protons between 4.0 ppm and 0.6 ppm.

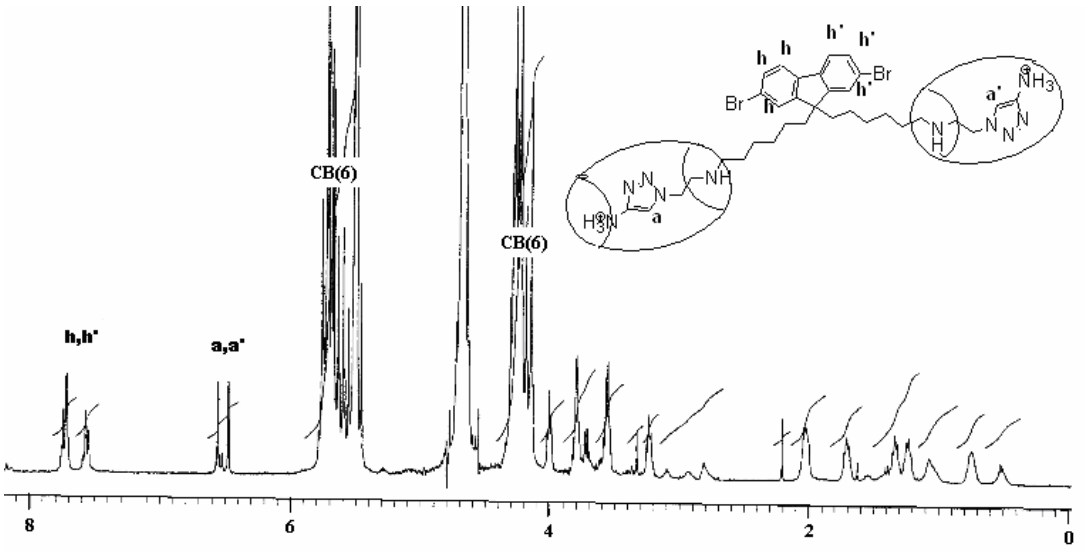

Fig. 2.40- ^{1}H-NMR spectrum of Rotaxane. (400 MHz, D_2O, 25 ^{o}C)

We could not prepare pseudopolyrotaxane by Suzuki coupling reaction between the rotaxane and the corresponding monomer boronic ester because of the time restriction.

2.1.14 Synthesis and Characterization of poly[9,9-Dihexyl-9H-fluorene] (P6)

An unfunctionalised polyfluorene homopolymer was synthesized. This homopolymer without any functional groups at the alkyl chains will be used in LEDs.

2,7-Dibromo-9,9-dihexyl-9H-fluorene was subjected to a Suzuki Coupling reaction with 9,9-dihexylfluorene-2,7-bis(trimethyleneborate) using Pd(0) catalyst and tetrammoniumbromide as a phase transfer catalyst in toluene as solvent. The reaction was carried out at 80 ^{o}C as shown in Scheme 2.16. Extraction and precipitation into methanol yielded poly[9,9-Dihexyl-9H-fluorene] **P6** in 64 % yield.

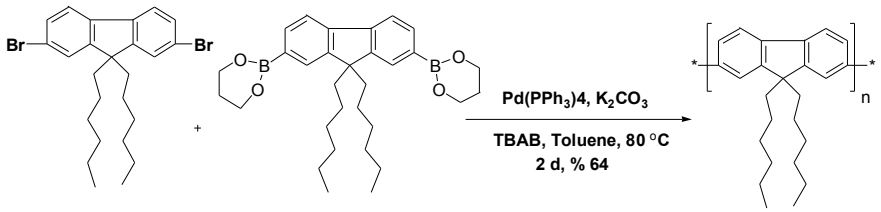

Scheme 2.19- The synthesis of **P6**

The product was characterized by FT-IR, UV-VIS and Fluoresecence spectroscopy. In Figure 2.41 absorption and emission spectra are shown. **P6** shows an absorption band with a maximum at 373 nm with an absorption coefficient of 49,595. Optical excitation at 373 nm results a strong violet fluorescence emission at 418 nm in dichloromethane solution. In the solid state **P6** shows strong blue emission at 446 nm with a 28 nm red shift. The solid films were obtained by spin coating of the dissolved polymer (20 mg) in dichloromethane (2 mL) at 800 rpm for 1.5 min.

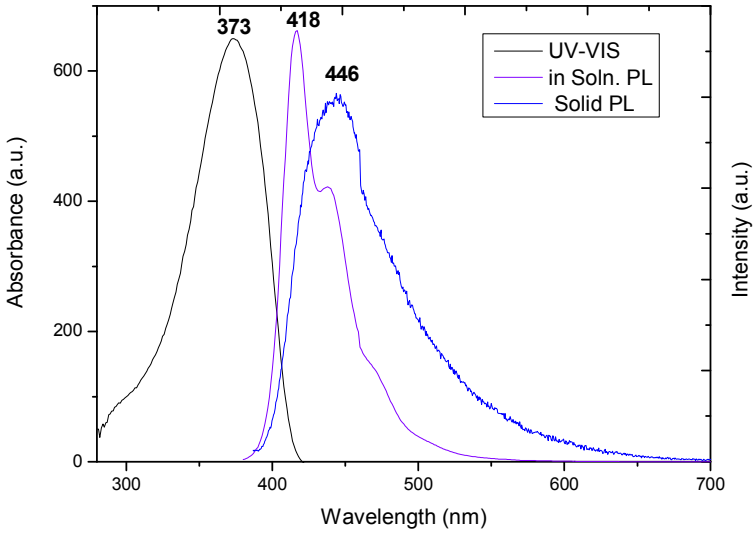

Fig. 2.41- UV-VIS and PL emission spectra of **P6** in Dichloromethane

The FT-IR spectrum shows carbon-hydrogen bond stretchings for aromatic at 3031 $cm^{-1}$and for aliphatic at 2929 cm^{-1}. The aromatic carbon double bonds are observed at 1606 cm^{-1}.

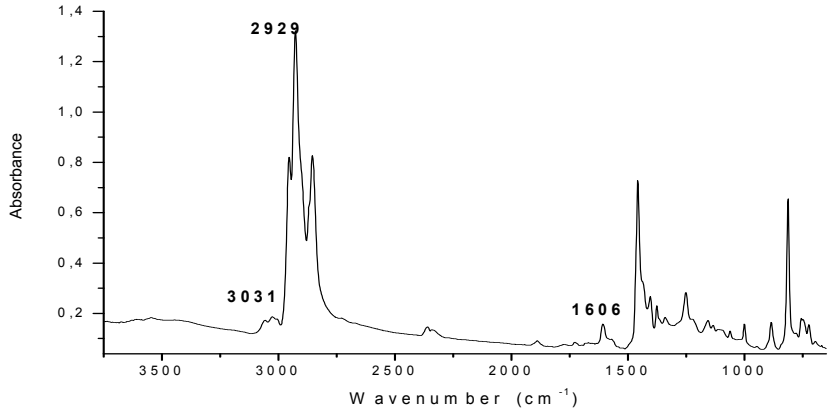

Fig. 2.42- FT-IR spectrum of **P6**

2.2 White light generation by a hybrid polymer-inorganic device[55]

In this section we introduce our results for white light generation exploiting a recent approach; a small polymer excited with near UV light sourced by GaN. GaN acts as a near UV LED to excite our polymer, and the only layer of the polymer emits white light. This hybrid organic/inorganic LED approach was frstly introduced by Hide et. al.[39] InGaN LED emitted blue UV light to pump the red emitting MEH-PPV and green emitting BuEH-PPV polymers. There was reported a produced white light with CIE coordinates of (0.34, 0.29). Almost at the same time Guha et. al. reported hybrid inorganic/organic based LEDs using coumarin derivatives for production of different emissive LEDs.[40] Recently, Heliotis et. al. reported a hybrid LED pumped by InGaN UV LED at 370 nm. and a blended mixture of blue-emitting poly-9,9-dioctylfluorene-*co*-9,9-di-4-methoxy phenylfluorene, the green-emitting poly-9,9-dioctyl fluorene-*co*-benzothiadiazole, and the Dow proprietary red emission copolymer Dow Red F.[41] The blend composition was adjusted between the blue and the green and red emitters so that an incomplete energy transfer occurs to produce white light with CIE coordinates of (0.30, 0.34).

Our WLED device relies on the use of a single, simple conjugated polymer namely poly[(9,9-dihexylfluorene)-co-alt-(9,9-bis-(6-azidohexyl)fluorene)] **P2** intentionally cross-linked on top of the integrating near-ultraviolet (n-UV) LED platform. In this approach, pumped by the near-UV InGaN/GaN LED at 378 nm, the P2 emitters that are hybridized and cross-linked into the form of a thin film generates a down-converting broad photoluminescence (PL) at longer wavelengths across the entire of the visible spectrum, yielding a very high color rendering index above 90.

2.2.1 Device Fabrication

InGaN/GaN, based n-UV LED is epitaxially grown in a GaN dedicated metal organic chemical vapor deposition (MOCVD) reactor at Bilkent University Nanotechnology Research Center (NANOTAM). After the growth of a 25 nm thick nucleation layer, a 200 nm thick GaN buffer layer is deposited, which is followed by the Si doped, GaN n layer. Subsequently, 5 quantum wells and barriers with thickness of approximately 2-3 nm, respectively, are grown as the active region to

emit in the n-UV. A thin AlGaN hole blocking layer and finally a Mg doped p layer is deposited on top of the active layer. Mg dopants are activated at 750 ^{o}C for 15 minutes. LEDs are then fabricated using standard semiconductor fabrication procedure at Bilkent University Advanced Research Laboratory. P type ohmic contacts are metallized with Ni (10 nm)/Au (100 nm) and annealed at 825 ^{o}C for 1 minute in a flowing N_2 atmosphere. Also, Ti (10 nm)/Al (300 nm) are used for the n-type ohmic contacts annealed at 625^{o}C for 1 minute in a flowing N_2 atmosphere. Fig. 2.43 shows electroluminescence (EL) of our n-UV LED with its EL peak at 392 nm and a full width at half maximum of 12 nm, along with its micrograph in the inset.

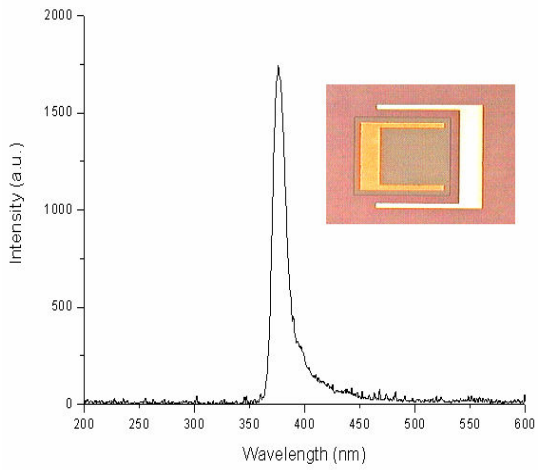

Fig. 2.43- Electroluminescence (EL) of our fully fabricated n-UV LED with its EL along with its micrograph in the inset.

For hybridization, **P2** is dissolved in THF at a concentration of 8.33 mg/mL and spun at 600 rpm for 10 seconds and 2000 rpm for 30 seconds on the sapphire side of the LED. The film thickness is measured to be 1.5 μm. Here the n-UV LED platform that is intimately integrated with the **P2** thin film serves as an efficient pump source for the excitation of **P2** to generate a wide optical spectrum across the visible. The emission spectrum of the **P2** film is observed to be broader than that of the **P2** in solution.

In Table 1, the CIE chromaticity diagram (1931) for the (x, y) tristimulus coordinates of **P2** integrated hybrid LEDs with their corresponding color temperatures and color rendering indices are listed with Samples 1, 2, and 3. In

addition, Sample 4 demonstrates the coordinates of P1 as the control group. The three filled circles on the CIE diagram in Fig. 2.44 schematically represent the pairs of (x, y) chromaticity coordinates of the **P2**-hybridized device listed in Table 1.

	X	**Y**	**T_c (K)**	**CRI**
1	0.2434	0.2723	19634	86
2	0.2913	0.2770	9416	87
3	0.2554	0.2426	32371	91
4	0.1932	0.1408	34367	64

Table 1- Chromaticity coordinates, color temperature, and color rendering index results

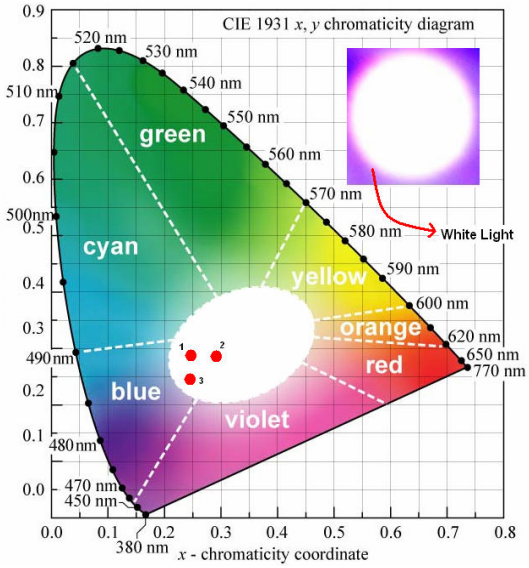

Fig. 2.44- P2 hybridized on n-UV LED in the white region on CIE chromaticity diagram (inset: a photograph of its white light emission).[55]

We intentionally used polyfluorene whose side chains can be substituted with a group facilitating the cross-linking. For example, bromide groups can be converted to azide groups to allow thermal or photochemical crosslinking.[44] Thus, it is known that by heating or UV-irradiation the azide group ($-N_3$) decomposes to a highly reactive nitrene (-N:) with the loss of nitrogen and the resulting nitrene can subsequently insert into side chains or the polymer backbone leading to the formation of crosslinks. This, in turn, causes a change in the polymer chain conformations and in optical properties of the polymer.

While the spectral broadening that stems from cross-linking is not desired in polymers for display applications, which are preferably aimed to be operated at specific wavelengths, this is an advantageous feature for white light generation applications. The ability of azide functionalized polyfluorene (**P2**) to feature the broadest spectrum across the visible is caused by uncontrollable cross-linkable reacting species, which damage or eventually lengthen the conjugation chain by random ruptures and linkages of bonds. The randomness of the cross-link mechanism of **P2** is specifically verified after an investigation of two independent film of **P2** after heat exposure. Next, the heat exposure on the polymers will be discussed methodologically.

2.2.2 Thermal Stability and Degradation Behaviour of the Polymers

Firstly, decomposition of the carbon azide bond and formation of the fluorenone species in azide functionalized copolymer were investigated via in-situ FT-IR spectroscopy. The azide functionalized copolymer was heated gradually from rt. to 237 ^{o}C. Temperatures at rt, 50 ^{o}C, 80 ^{o}C, 100 ^{o}C, 120 ^{o}C, 150 ^{o}C, 170 ^{o}C, 195 ^{o}C, 220 ^{o}C, 230 ^{o}C, 233 ^{o}C, 237 ^{o}C were recorded as shown in Figure 2.45. The investigation was dependent upon the disappearance of the $-C-N_3$ peak at 2094 cm $^{-1}$ and the formation of carbonyl peak at 1720 cm $^{-1}$ coming from fluorenone species. At 195 ^{o}C the carbon azide peak began to decrease while no substantial occurrence of fluorenone species was observed. It seemed that some azide groups are decomposed to reactive nitrene species. This enhanced the crosslinking of the polymer began earlier than keto formation. At 220 ^{o}C the formation of the fluorenone species were observed because of the peak at1720 cm^{-1}. Above 220 ^{o}C

the carbon azide peak disappeared completely, and the carbonyl peak became evident in an additional 17 ^{o}C.

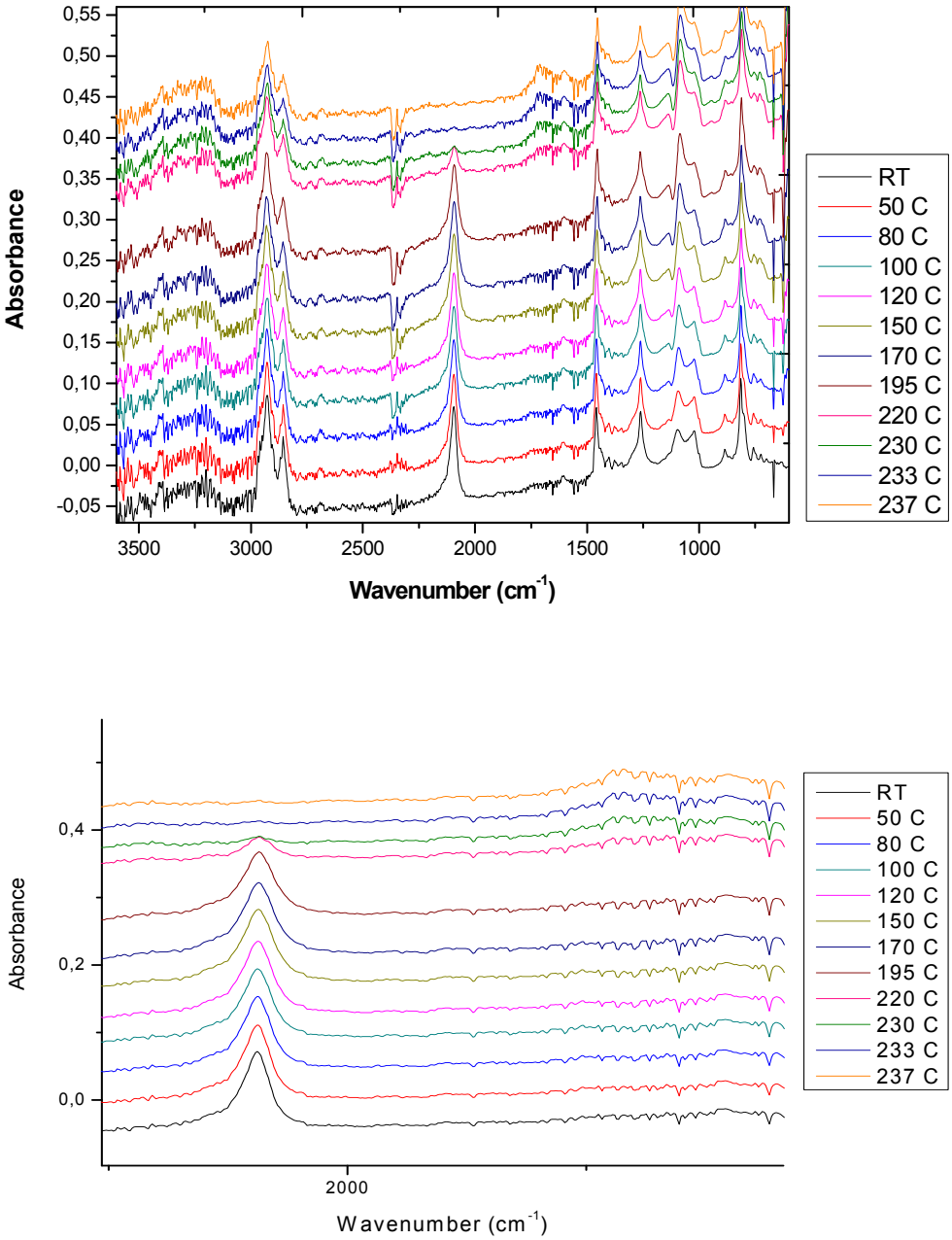

Fig. 2.45- (a)In-situ FT-IR measurement of P2 under heat exposure, (b)Inset between 2300 cm $^{-1}$ and 1500 cm $^{-1}$

The crosslinking and degradation beaviour of **P2** were also investigated by in-situ Fluorescence spectroscopy. The azide functionalized copolymer was heated gradually from rt. to 235 ^{o}C. Temperatures at rt., 50 ^{o}C, 100 ^{o}C, 150 ^{o}C, 200 ^{o}C, 235

°C were recorded as shown in Figure 2.46. Furthermore, to investigate whether the changes in the polymer reversible or not the polymer was cooled down to rt from the heated temperature. When heated above rt., we observed a decrease in the the intensity of the PL without forming a new band or changing the emission spectrum band. However, after cooling the polymer to rt. the polymer relieved the intensity decrease but never achieved the former intensity. Heating above 150 °C a new band occured at about 540 nm spanning the green region. Hence it seemed that, in this occasion, crosslinking causes the formation of the green emission band. And further heating caused the increase of this band while the keto sites increase as shown by FT-IR spectrum above.

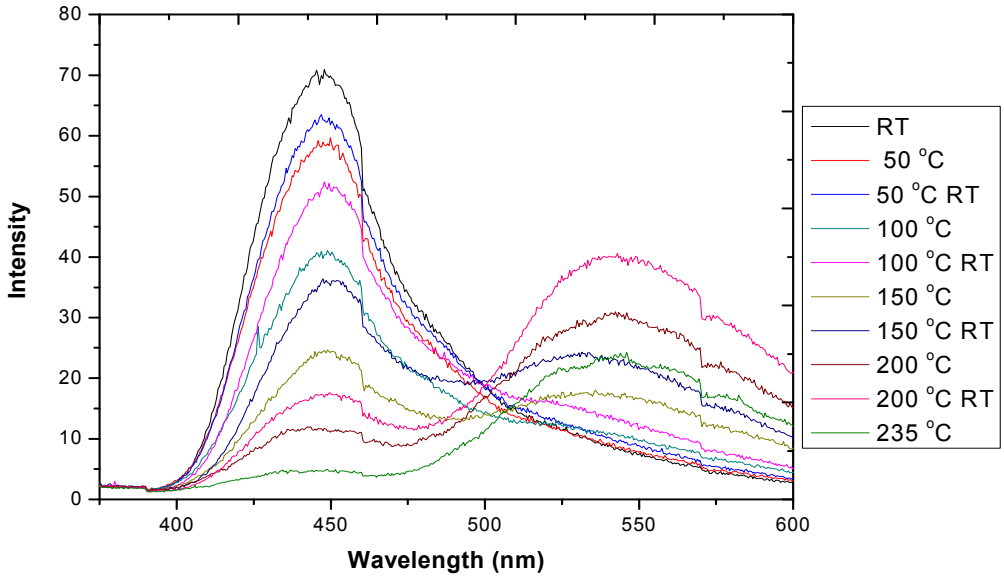

Fig. 2.46- In-situ PL measurement of **P2** under heat exposure

In-situ UV-VIS spectroscopy was also used for investigation of the thermal stability of **P2**. Absorption behaviour during heat exposure was investigated. Absorptions at rt, 50 °C, 100 °C, 150 °C, 200 °C and 235 °C were recorded as shown in Figure 2.47. The azide functionalized copolymer absorbs at about 385 nm because of the π-π* transition in the solid state at room temperature. In general picture, during gradual heat exposure the polymer kept its band shape. We only observed a brief shift in λmax value. We expected no lowering in the absorption spectra as in the emission spectra because the absorbing species stayed always the same, the polyfluorene

backbone. The absorbing species in the molecule did not change but the pathways they relaxed changed.

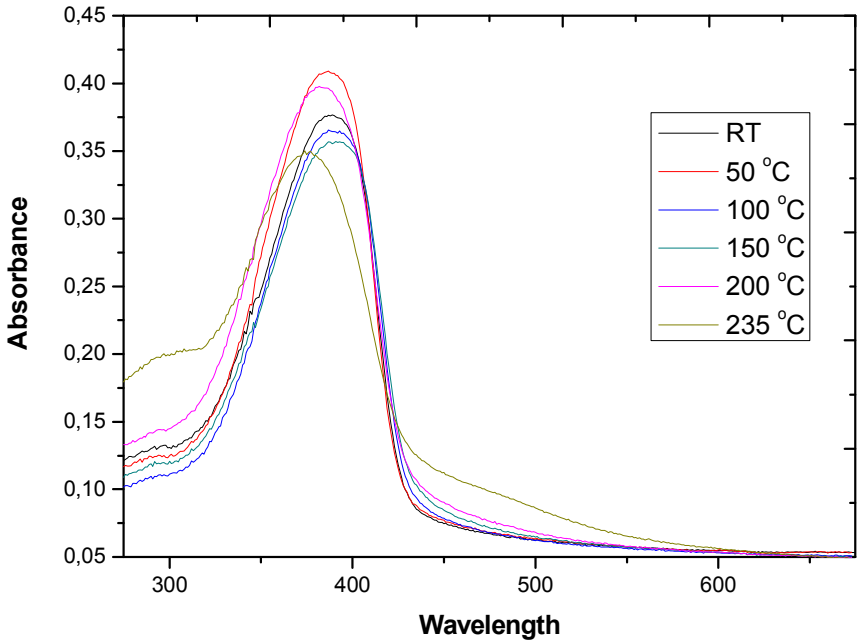

Fig. 2.47- In-situ UV-VIS measurement of **P2** under heat exposure

To compare the thermal stability behaviour of **P2** and to investigate what azide functionalisation adds to **P2**, thermal stability experiments were done for bromo-fuctionalised copolymer (**P1**) and the unfunctionalised homopolmer (**P6**) via in situ Fluorescence Spectroscopy. In Figure 2.48 the emission spectra of the bromide functionalized copolymer is shown for rt, 50 ^{o}C, 100 ^{o}C, 150 ^{o}C, 200 ^{o}C and 235 ^{o}C. Also rt emission was recorded after cooling to rt from the heated temperature. At the first sight, increasing temperature decreased the intensity of the emission and subsequent cooling to rt relieved this decrease but the emission never reached to the former rt emission. Also, it was observed that band shape did not change until 200 ^{o}C. The green emission band was observable at 200 ^{o}C. However, in the azide fuctionalised copolymer the new band appeared at 150 ^{o}C. From this, we can comment that crosslinking of the **P2** began earlier than the formation of keto defects.

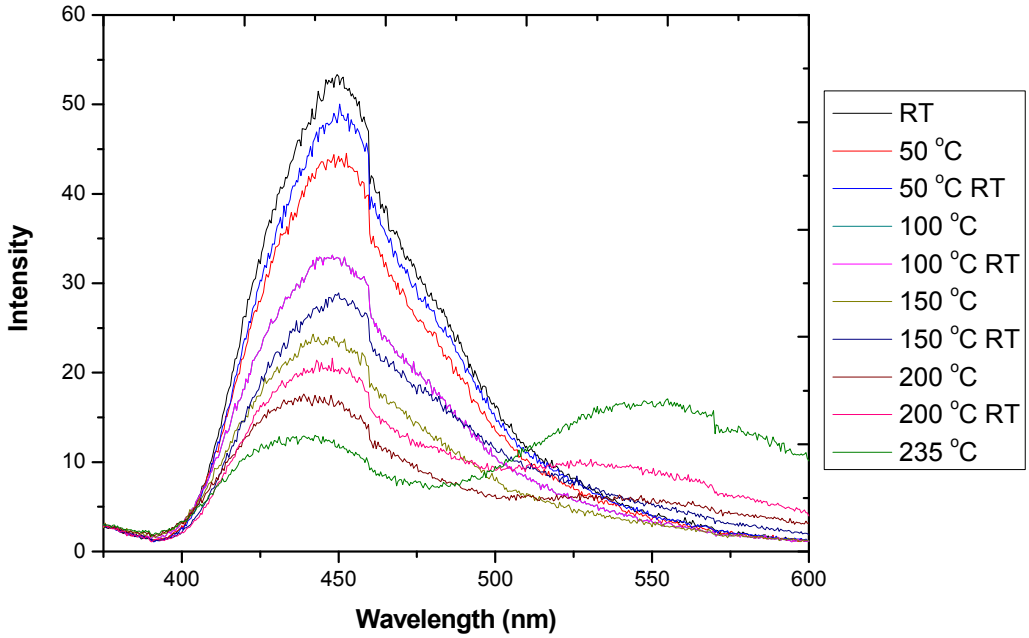

Fig. 2.48- In-situ PL measurement of **P1** under heat exposure

The above analysis conditions are applied to homopolymer (**P6**) to investigate thermal stability and degradation behaviour. In Figure 2.49 the emission spectra of the unfunctionalised homopolymer is illustrated for rt, 50 ^{o}C, 100 ^{o}C, 150 ^{o}C, 200 ^{o}C, 235 ^{o}C. Also rt emission was recorded for after each cooling from the heated temperature. The homopolymer showed the same trend as bromo- functionalised polymer **P1**. Subsequent cooling to rt relieved the decrease of the intensity at higher temperatures but the emission never reached the former rt emission. The appearance of the green emission band was observed at 200 ^{o}C. This result supported that the formation of crosslinking began earlier than formation of keto defects in **P2**.

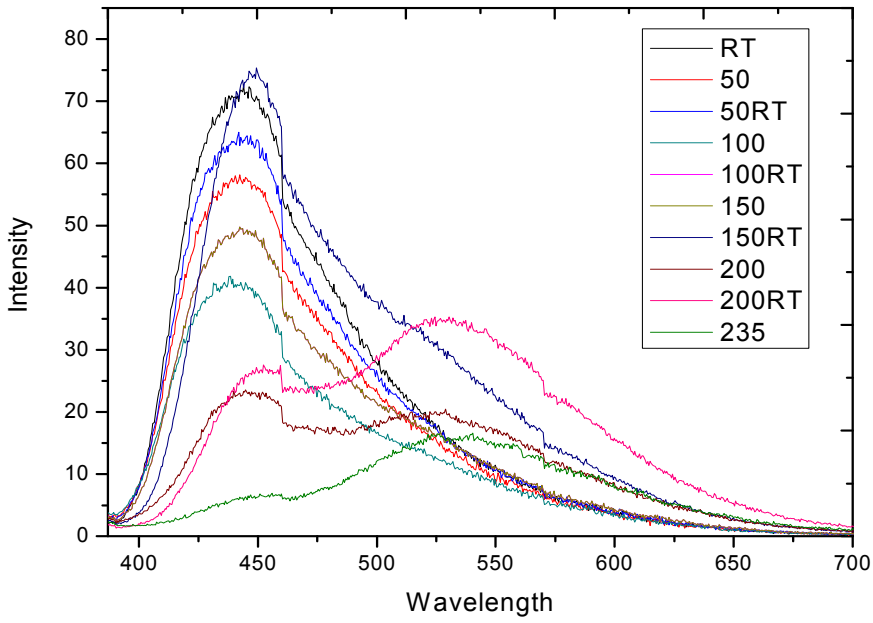

Fig. 2.49- In-situ PL measurement of **P6** under heat exposure

2.3 Synthesis and characterization of cucubit[6]uril encapsulated polypyrrole pseudopolyrotaxane[56]

Polypyrrole (PPy) was first introduced by D.E. Weiss *et al.*[46] They were able to synthesize polypyrrole from pyrolysis of tetraiodopyrrole. Since then polypyrrole was widely studied because it has metallic electrical conductivity, environmental stability and relative easy synthesis.[47] These advantages led to the utilisation of the material in various applications in electrochromic devices, sensors and electronic devices etc.[47] For example, a rechargeable battery prepared by Palmore *et al.* recently.[48] However, a soluble polypyrrole was not able to be synthesized because of strong intra and inter-chain interactions except adding some surfactants and counterions.[49] This latter approach creates a drawback for processability of the polymer.

Rotaxanation was suggested to separate the polymer chains. Thus, solubility can be enhanced by breaking intra and inter-chain interactions. Encapsulation of the polypyrrole main chain into macrocycles can help in controlling chain packing. Achieving encapsulation of PPy into macrocyles have not been reported thoroughly yet. Pyrrole monomers were successfully complexed with cyclodextrin units.[26] However, the polymer unthreads from the macrocycle in the course of oxidation.

Our objective was to explore methods of synthesising CB(6)-encapsulated polypyrrole. Our synthetic strategy involved first the preparation of an inclusion complex between CB6 and pyrrole (Py) in NaCl solution and the subsequent polymerisation of this complex with an oxidising agent to form pseudopolyrotaxanes. Polypyrrole formation failed using $FeCl_3$ as an oxidising agent in a NaCl solution, but replacing NaCl solution by an acid solution produced polypyrrole. Spectroscopic methods including FT-IR, UV-VIS and fluorescence clearly indicated the formation of CB6-encapsulated polypyrrole. This is one of the first reported examples of the photoluminescence (PL) of non substituted polypyrrole and the synthesis of CB-encapsulated conjugated polymers.

In order to prepare poly-pyrrole-pseudorotaxane, we first prepared an inclusion complex between CB6 and pyrrole in 0.1M NaCl solution as outlined in Scheme

2.20. We used a NaCl solution, because CB6 dissolves in an aqueous solution of alkaline metal salts. One equivalent of CB6 was dissolved in 0.1M NaCl solution and one equivalent of pyrrole was added at rt. The addition produced a clear solution which became cloudy and viscous after about 15 min. This mixture was stirred overnight at rt and in air. White precipitates were collected by centrifugation and dried under vacuum overnight.

The mechanism of the CB6-Py inclusion complex formation is similar to complex formation between CB6 and THF in NaCl solution.[50] However, pyrrole has a more rigid structure than THF and consequently, when it enters the cavity of CB6, it probably pushes away the Na^+ ions and thus, pseudorotaxane precipitates out.

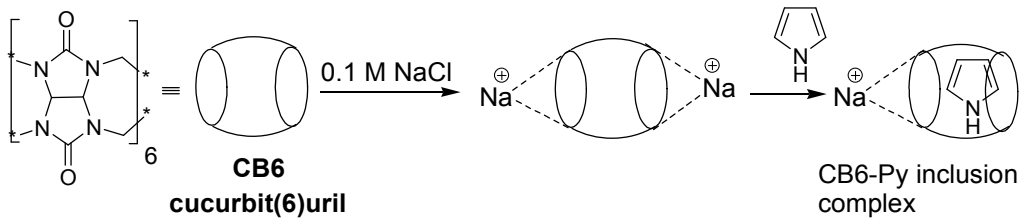

Scheme 2.20- Synthesis of the inclusion complex between CB6 and pyrrole in 0.1M NaCl solution.

When this inclusion complex was left in air for weeks, no colour change caused by oxidation of pyrrole was observed. It seems that, by encapsulation pyrrole becomes chemically more stable. Pseudorotaxane is sparingly soluble in water and completely soluble in acidic water, but it is insoluble in any organic solvents. The solubility of pseudorotaxane in D_2O is insufficient to obtain a ^{1}H-NMR spectrum but it is relatively more soluble in a NaCl solution, so that the ^{1}H-NMR spectrum was recorded in this solution. In Figure 2.50, the ^{1}H-NMR spectrum shows four sets of distinct chemical shifts which correlate well with the proposed structure in Scheme 2.3.1. There are two well-resolved triplets with coupling constants of about 2 Hz at 5.92 and 5.25 ppm due to protons labelled as c and b; there are also two broad peaks at 6.79 and 6.13 due to protons d and a respectively (Scheme 2.21, labelled structure). Chemical shifts due to CB6 protons appear to split further, confirming the asymmetrical nature of the inclusion complex.

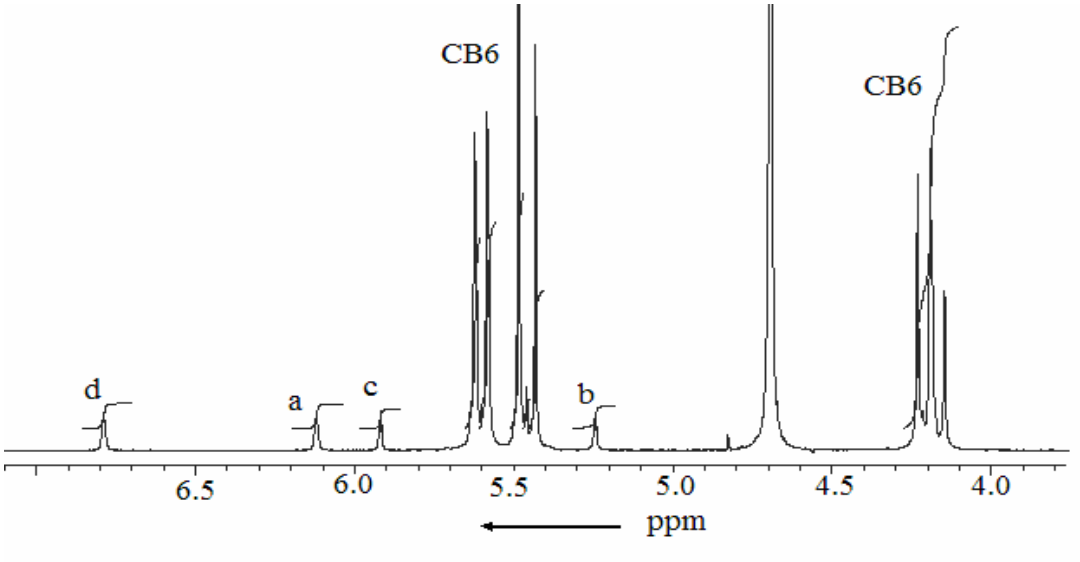

Fig. 2.50 - ^{1}H-NMR spectrum (400 MHz, 0.2 M NaCl in D_2O, 25 ^{o}C) of CB6-pyrrole inclusion complex.

After characterizing the inclusion complex by ^{1}H-NMR, we set out to investigate the formation of polypyrrole-pseudorotaxane. Various methods were tried. In the first, one equivalent of CB6-Py complex was dissolved in 0.2M NaCl solution and subsequenty one equivalent of aqueous $FeCl_3$ solution was added. The solution became yellow and remained yellow through 24 h of stirring at rt. No colour change associated with the reduction of iron to form polypyrrole was seen. The UV-VIS spectrum of this solution was recorded but there was no band from polypyrrole formation around the visible region. The reaction mixture was heated at 60 °C overnight and the UV-VIS spectrum was recorded, however, the spectrum was similar to the previous one. We therefore, concluded that $FeCl_3$ could not oxidize pyrrole to polypyrrole because it probably coordinates with carbonyl of the CBs portals and could not reach the pyrrole. Another possibility is that the sodium ions act as a gate-keeper preventing the $FeCl_3$ from getting close to the pyrrole molecules.

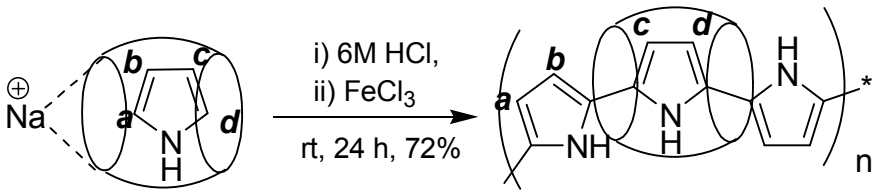

Scheme 2.51- The synthesis of CB6-encapsulated polypyrrole.

To eliminate the effect of sodium ions on polymerisation, we decided to dissolve the complex in HCl solution instead of NaCl solution. Accordingly the complex was dissolved in 6M HCl solution; a yellowish clear solution was obtained. We divided this solution in two parts. The aqueous solution of $FeCl_3$ was added to one part leaving the other part of the mixture $FeCl_3$-free; both reactions were stirred at rt following the progress of the reactions by UV-VIS spectroscopy (Scheme 2.21). Within a few hours, in UV-VIS spectra of both reaction mixtures, a broad band in the region of 450-480 nm appeared and over time it became sharper and shifted to 485 nm; its intensity also increased. This result indicates that when CB6-Py inclusion complex is dissolved in HCl solution, regardless of the presence of oxidant, polypyrrole forms confirming that the polymerisation is mainly initiated by HCl.

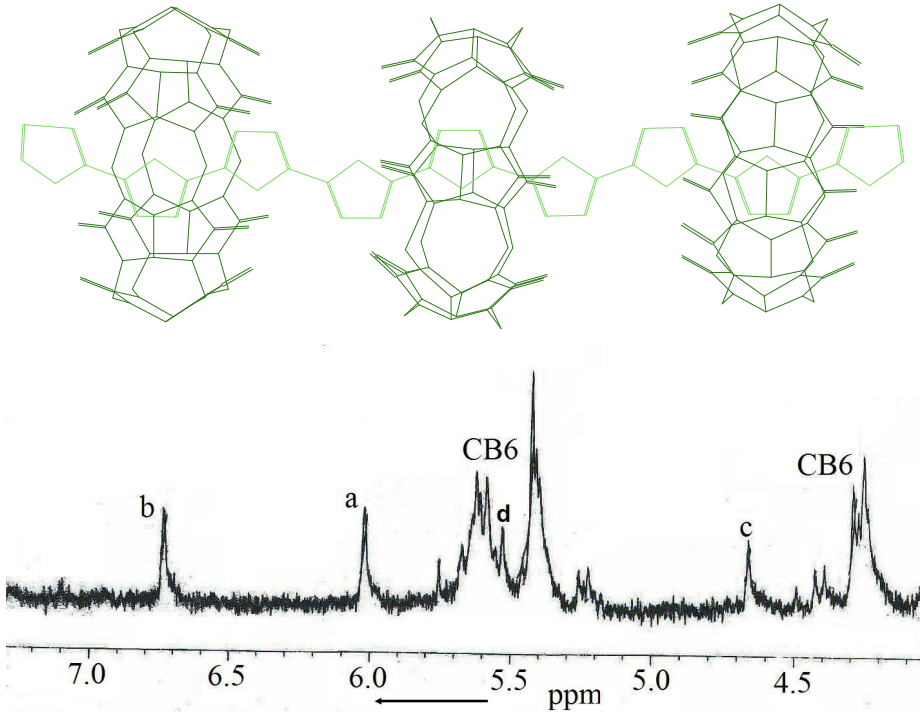

Fig. 2.51- Ball-and-stick model of CB6-encapsulated polypyrrole and its ^{1}H-NMR spectrum (400 MHz, DMSO/D_2O, 25 ^oC).

The solution was poured into a large excess of acetone and the salmon coloured precipitate (Figure 2.55b) was collected by centrifugation and dried overnight in a vacuum. Pseudopolyrotaxanes is slightly soluble in acidic water, in DMSO and in

DMF. However, at high concentrations an aggregate forms due to dissociation. We were able to obtain a ^{1}H-NMR spectrum of CB6-psudopolyrotaxanes in the mixture of DMSO/D_2O. The main interactions between CB and polypyrrole are hydrophobic effect, hydrogen bonding between the –NH and carbonyl groups and the interaction between carbonyl oxygen and the pyrrole rings protons. Because of these interactions, probably the best ratio CB to pyrrole would be 1:3. Probably one pyrrole unit is located inside the cavity and the other two are close to the carbonyl portals (Figure 2.51, Ball-and-stick model of psudopolyrotaxanes). Accordingly, the chemical shifts have assigned to protons as follows; the peaks at 4.7 and 5.5 ppm are due to protons *c* and *d* respectively, which are encapsulated by CB6 as a result shifted upfield; the peak at 6.1 ppm is due to protons *a* which are away from carbonyl portal and the peak at 6.7 ppm belongs to protons *b* because they are close to portal of the CB6, therefore shifted downfield.

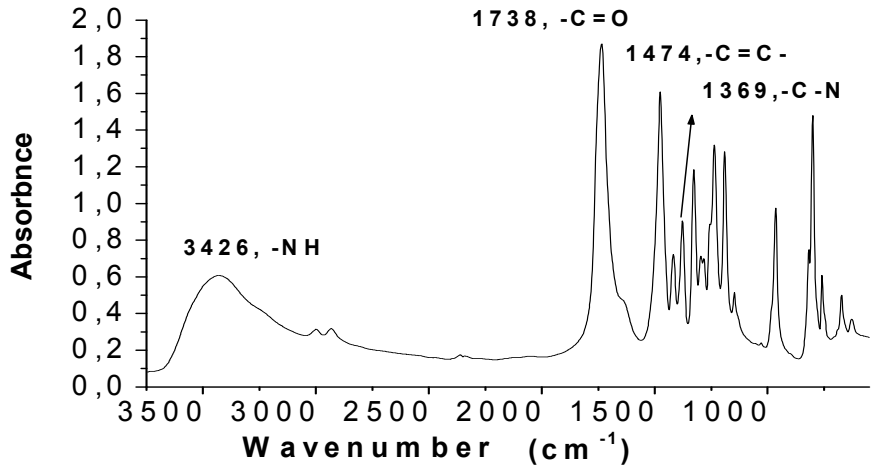

Fig. 2.52- FT-IR spectrum of CB6-encapsulated polypyrrole.

The polymer was also analyzed by other spectroscopic techniques including FT-IR, UV-VIS and fluorescence. FT-IR spectrum of psudopolyrotaxanes shows (Figure 2.52) N-H stretching at 3426 cm^{-1} which is characteristic for PPy. The peak due to C=C stretching was seen at 1474 cm^{-1}. The medium peak at 1369 cm^{-1} is attributed to the C-N(str.) vibration. A strong peak at 1739 cm^{-1} due to C=O stretching confirms the presence of CB6 in the polymer. The solid was stirred in 0.2 M NaCl solution to determine whether CB6 encapsulated the polypyrrole or its presence is

due solely to H-bonding between the protons of polypyrrole and the carbonyl groups of CB6. We assumed that If CB6 was not part of the polymer, it would form a complex with Na ions and remain in solution and polypyrrole would precipitate out. Thus, after treating the polymer with NaCl, we analyzed the solid and the supernatant. The IR spectrum of the solid is similar to before washing--clearly indicating the presence of CB6. The supernatant was evaporated and the IR spectrum of the solid residue shows CB6 peaks. However, this could also indicate the slippage of some CB6 rings from the polymer backbone during washing with salt solution.

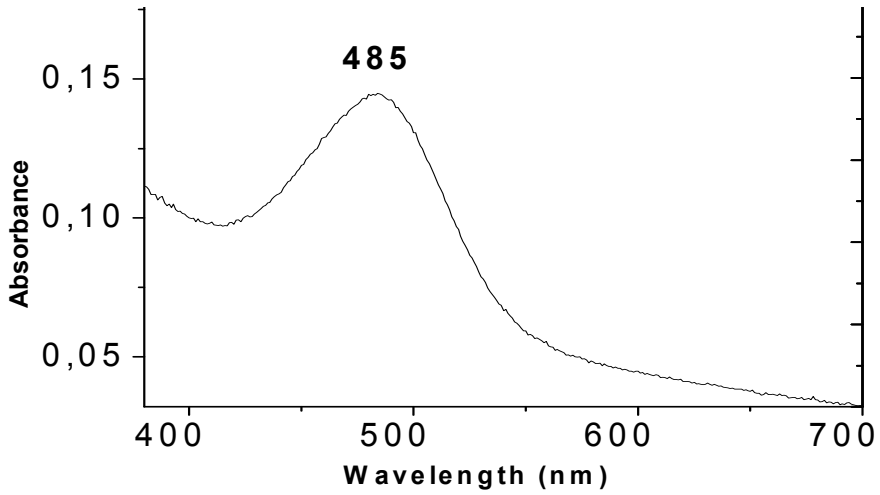

Fig. 2.53- UV-VIS spectrum of CB6-encapsulated polypyrrole in 6N HCl solution.

UV-VIS spectrum of psudopolyrotaxanes exhibits an absorption band at 485 nm due to the π-π* transition which is characteristic for polypyrrole (Figure 2.53).[51, 52]

PL spectrum of psudopolyrotaxanes reveals an emission band at green region (521 nm) (Figure 2.54) when it is excited at 485 nm. This result was also supported by comparing it with the photos taken of the solution of CB6-encapsulated polypyrrole and the irradiation of this solution by UV-light. The acidic solution of PPy-CB6 psudopolyrotaxanes was light brown and showed a green emission under irradiation with UV-light (Figure 2.55a).

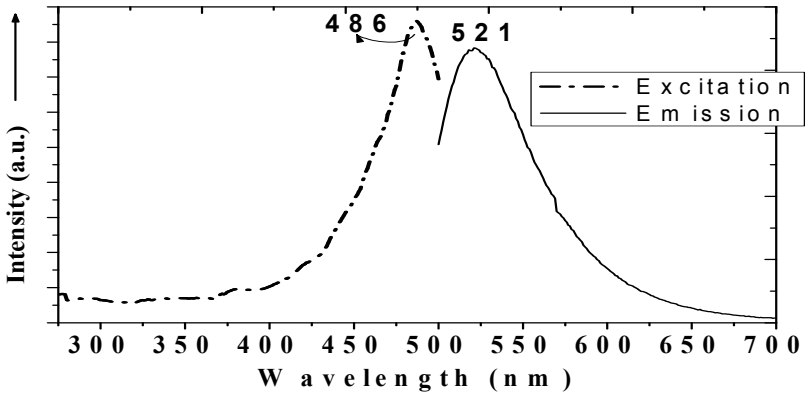

Fig. 2.54- PL spectra of CB6-encapsulated polypyrrole in 6M HCl solution.

On the basis of emission spectrum, we can assume that polypyrrole is threaded by cucurbituril rings to form a pseudopolyrotaxanes. If polymer was not threaded by the rings, there will be no emission due to strong interaction between the polymer chains.

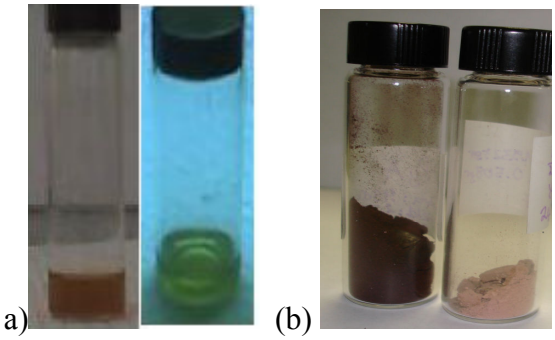

Fig. 2.55- (a) The acidic solution of CB6-encapsulated polypyrrole is light brown and exhibits a green PL under irradiation with UV-light; (b) Polypyrrole (black powder) and CB6-encapsulated polypyrrole (salmon powder).

Figure 2.56 shows the powder XRD patterns of polypyrrole (c), CB6 (b), and psudopolyrotaxanes (a). Polypyrrole was prepared using $FeCl_3$ as an oxidising agent under standard conditions (Figure 2.55b, black powder).[49] The pattern of polypyrrole illustrates that it is a typical non-crystalline amorphous polymer, however CB6, when compared with spectrum 2.56c, has crystal composition because there are three sharp peaks (2θ = 14.8, 23.2, 31.3) in the XRD pattern (Fig. 2.56b). Compared with the parent polymer, the presence of CB6 provides some crystallinity and as a

result regularity to psudopolyrotaxanes as shown in the Figure 2.56a. Similar changes have been observed in polyrotaxanes incorporating CB6 by Tan *et al*. [53]

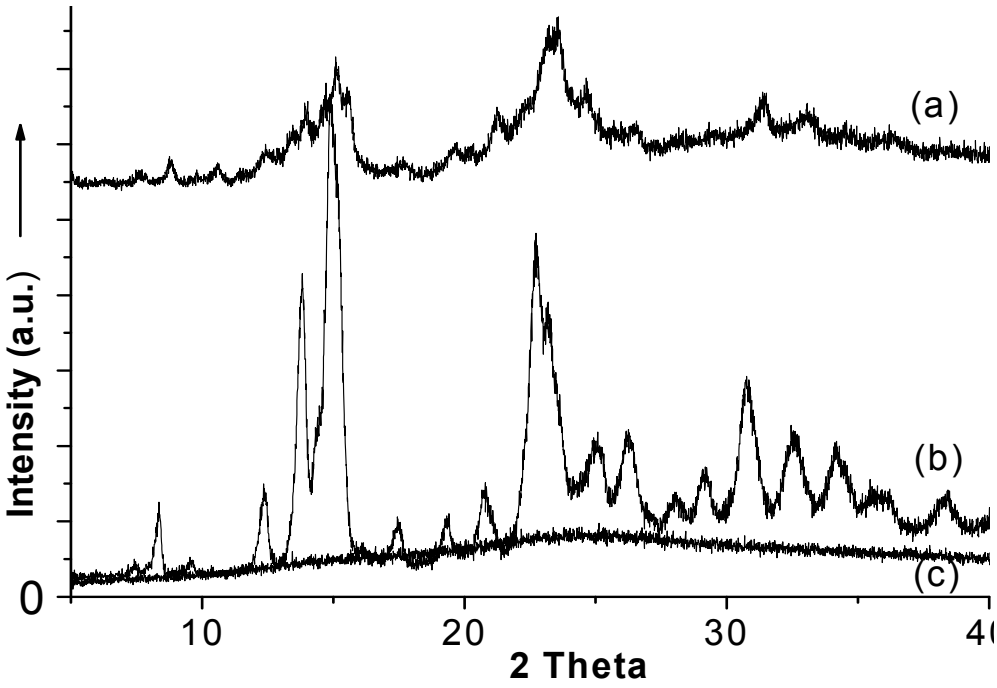

Fig. 2.56- Powder XRD patterns of a) CB6-encapsulated polypyrrole, b) CB6, c) polypyrrole.

CHAPTER 3

CONCLUSION

In this thesis, a series of polyfluorene based copolymers have been synthesized via Suzuki coupling for LED applictions.

Fluorene monomers functionalized with hexyl units have been synthesized. Polyfluorene based polymers have been synthesized through coupling these monomers with the corresponding boronic ester derivatives via Suzuki coupling reaction. Copolymers consisted of repeating units of fluorene-fluorene, fluorene-phenylene and fluorene-thiophene building blocks. Suzuki coupling was an important tool to obtain high yield and soluble polymers.

Our aim was to modify conductive light emitting polymers through supramolecular chemistry to obtain polymers with interesting and different properties than the parent polymers. For example, it was possible to functionalise the C9 of blue light emitting polyfluorene through rotaxanation using cucurbit[6]uril as a macrocycle. For this purpose, we have tried two approaches. First approach involved the preparation of a series of appropriate copolymers whose side chains allowed us to carry out rotaxanation. Post modifications on the hexyl chains by attaching propargylamine or formaton of a triazole ring yielded insoluble polymers through crosslinking of alkyne groups with each other and triazole groups forming networks between each other by strong H-bonding and π-π interactions. Insoluble post-modified polymers disabled us to continue further.

In the second approach, first a fluorene monomer was functionalized with a suitable azide monomer. Then, by addition of alkyne monomer and CB(6), rotaxane was formed via CB(6)-catalysed 1,3 dipolar cycloaddition. The formation of rotaxane was confirmed by the presence of a signal at 6.5 ppm in ^{1}H-NMR spectrum. Further polyrotaxane formation was not achieved due to time restriction. Functionalization

of the fluorene monomer with alkyne monomer yielded insoluble monomers because of crosslinking between the alkyne groups.

In the next part, methods of preparing CB(6)-encapsulated polypyrrole were investigated. It was found that pyrrole was threaded by CB(6) but since this complex was not soluble in water, the polymerisation was tried in NaCl solution. However, this solvent prevented Fe(III) to approach pyrrole as sodium ions coordinate with the portal carbonyl of CB(6). As a result no polymerization was obtained. On the other hand, dissolving the inclusion complex in 6M HCl solution, regardless of the presence of $FeCl_3$ as an oxidising agent, initiated polymer formation with moderate yields. Spectroscopic analyses from FT-IR, UV-Vis, Fluorescence, ^{1}H-NMR confirmed the formation of CB(6)-encapsulated polypyrrole. Furthermore, by encapsulation, separation of the polymer chains was possible and green fluorescence emission was observed.

In the last part, WLED was prepared by a hybrid system by azide functionalized polyfluorene copolymer and inorganic GaN species. Our WLED showed high CRI indexes (>90). Azide groups, decomposed to nitrene groups formed crosslinks allowing the broadening of the emission spectrum. Stability and degradation behaviour of the polymer was studied under heat exposure. It was shown that crosslinking began earlier than formation of fluorenone units.

CHAPTER 4

EXPERIMENTAL SECTION

All reagents and solvents were of the commercial reagent grade and used without further purification except where noted. Pyrrole and aniline were distilled prior to use. Column chromatography was carried out using silica gel (Kieselgel 60, 0.063–0.200 mm). Thin layer chromatography (TLC) was performed on silica gel plates (Kieselgel 60 F254, 1 mm). Nuclear magnetic resonance (NMR) spectra were recorded on a Bruker Avance DPX–400 MHz spectrometer. UV measurements were collected by Cary UV-VIS spectrophotometer. Fluoresence measurements were taken by a Varian Cary Eclipse Fluorimeter. XRD pattern was recorded by Rigaku MiniFlex X-Ray Diffaractometer. FT-IR Spectra were collected by Bruker FT-IR spectrometer. GPC analyses were done by Agilent (HP) GPC apparatus. All reactions were performed under argon.

4.1 Synthesis of 2,7-dibromo-9,9-bis-(6-bromo-hexyl)-9H-fluorene 1

2.7 Dibromofluorene (2.0 g, 6.17 mmol) and tetrabutylammoniumbromide (0.40 g, 1.20 mmol) were suspended in DMSO at rt. The mixture was flushed with nitrogen gas for 30 min. As a result of addition of NaOH (10 mL, % 50) in one portion, a viscous orange solution was observed. Following that 1,6 dibromohexane (9.5 mL, 60 mmol) was added. The reaction mixture was stirred at rt for 2 h. Work-up was done by addition of tert-butyl methyl ether (250 mL) and water (100 mL) to the reaction. The mixture was stirred for 15 min. The organic layer was extracted in tert-butyl methyl ether and washed with water (100 mL), 2N HCl, brine and lastly again with water. After drying over $CaCl_2$ the solvent was evaporated under vacuum. The crude product was purified with column chromatography packed with silica using cylohexane as an eluent. The product was further purified by precipitating the solution in $CHCl_3$ into cold ethanol. Colorless crystals were obtained and dried under vacuum.

Yield: 1.60 g (40%)

Mp: 66-70 ^{o}C

IR (KBr pellet, cm^{-1}): 3025 (-CH, w), 2922 (-CH, s), 2859(-CH, s), 1598(C=C-, w), 1571(C=C-, w)

^{1}H-NMR (400 MHZ, $CDCl_3$) δ_H 7.35-7.2 (m, 6H), 3.34 (t, 4H), 1.95 (m, 4H), 1.7 (m, 4H), 1.20(m, 8H), 0.65(m, 4H)

^{13}C-NMR δ_C 23.6, 27.9, 29.1, 32.8, 33.9, 40.2, 55.9, 121.9, 122.3, 126.9, 131.1, 139.9, 153.1

Elemental Analysis: ($C_{25}H_{30}Br_4$)

Calculated (%) C: 46.19; H: 4.65; Br: 49.16

Found (%) C: 46.69; H: 4.64

R_f: 0.63 (cyclohexane/chloroform 5:5)

4.2 Synthesis of 2,7-Dibromo-9,9-bis-(3-bromo-propyl)-9H-fluorene 2

2,7-Dibromofluorene (1.0 g, 3.08 mmol) and tetrabutylammoniumbromide (0.20 g, 0.60 mmol) were suspended in DMSO (10 mL) at rt. The mixture was flushed with nitrogen gas for 30 min. After addition of NaOH (5mL, %50) in one portion a viscous orange solution was obtained. Following that 1,3-Dibromopropane (6.06 g, 30 mmol) was added. The reaction mixture was stirred at rt for two h. Work-up was done by addition of tert-butyl methyl ether (250 mL) and water (100 mL) to the reaction. The mixture was stirred for a 15 min. The organic layer was extracted in tert-butyl methyl ether and washed with water (100 mL), 2N HCl, brine and lastly again with water. After drying over $CaCl_2$, the solvent was evaporated under vacuum. The orange crude product was purified with column chromatography by elution with a mixture of cyclohexane, chloroform (8/2, v/v) over silica. The product was further purified by recrystallisation from cyclohexane to obtain white fine powder.

Yield: (105 mg, %6)

Mp: 127-129 ^{o}C

IR (KBr pellet, cm^{-1}) 3048 (CH-), 2927(CH-), 1605 (C=C-)

^{1}H-NMR (400 MHZ, $CDCl_3$) δ_H 7.45 (m, 6H), 3.05(t, 4H), 2.06(m, 4H), 1.08 (m, 4H)

^{13}C-NMR δ_C 27.1, 33.7, 38.7, 54.8, 122.2, 122.7, 127.0, 131.7, 139.8, 151.6

R_f: 0.34 (cyclohexane/chloroform, 8/2, v/v)

4.3 Synthesis of 9, 9-Bis-(6-azido-hexyl)-2,7-dibromo-9H-fluorene 3

Sodium azide (0.10 g, 1.54 mmol) and 2,7-dibromo-9,9-bis-(6-bromo-hexyl)-9H-fluorene (0.50 g, 0.77 mmol) were suspended in DMSO (10 mL) and the mixture was heated to 60 ^{o}C for 24 h. A light yellow solution was obtained. The solution was poured into water (40.0 mL) and organic layer was extracted with diethyl ether (50.0 mL X 3). The combined organic layers were washed with water after drying it over $CaCl_2$.The solvent was removed under reduced pressure to obtain a light yellow oil.
Yield: 360 mg (%82)
IR (NaCl plates, cm^{-1}): 3042 (CH-, w), 2927 (CH-, s), 2091(C-N_3, s)
R_f: 0.76 (Cyclohexane/Chloroform 1/1, v/v)

4.4 Synthesis of {6-[2,7-Dibromo-9-(6-prop-2-ynylamino-hexyl)-9H-fluoren-9-yl]-hexyl}-prop-2-ynyl-amine 4

2,7-Dibromo-9,9-bis-(6-bromo-hexyl)-9H-fluorene (100 mg, 0.15 mmol) was dissolved chloroform (4 mL) and added dropwise onto PGA (0.5 mL, excess). A yellow solution was obtained. The reaction was stirred for one d. at rt. 0.1 M NaOH (15 mL) was added and stirred for 2 hours and organic layer was extracted with chloroform (20 mL). Solvent was evaporated and brown oil was tried to dissolve in 0.1 M HCl (25 mL). Organic layer was extracted with chloroform (25 mL) and the solvent was evaporated under reduced pressure to obtain brown film

Yield: 83 mg (%90)
FT-IR (KBr pellet, cm^{-1}): 3382 (-NH, w), 3300 (terminal alkyne, s), 2936 (-CH, s)

4.5 Synthesis of cucurbit[6]uril

Glycoluril (5.68 g, 40 mmol) was suspended in sulphuric acid (20 mL 9 M) and heated to 75 ^{o}C to dissolve. Formaldehyde (7.0 mL from 37 % w/w aq. Sol., 100 mmol) was added into the clear reaction solution. The reaction was kept at 75 ^{o}C for 1 d and at 100 ^{o}C for 12 h. The reaction mixture was heated about 110 ^{o}C. The light orange reaction solution was added into cold water (200mL). Diluted mixture was precipitated into acetone (1L) to obtain white precipitates. The precipitates were collected by suction and washed with water/acetone (200/800 mL). Obtained white precipitates were added into water (200 mL) and stirred for 1 h. The precipitates were filtered and added into hot formic acid (20 mL). Water (120 mL) was added dropwise to obtain precipitates. After letting 1 d, white precipitates were observed. The precipitates were collected and washed with hot water (100 mL). The whole residues of solvents was evaporated under reduced pressure to obtain white fine powder product.

Yield: 3 g (35 %)
Mp: >300 ^{o}C
FT-IR: (KBr pellet, cm^{-1}): 3500 (NH-, m), 2999 (C-H, s), 1738 (C=O, s)
^{1}H-NMR: (400 MHz, 0.2 M NaCl,D_2O) = δ_H 4,46 (12H, d), 5,54 (12H, d), 5,75 (12H, s)

4.6 Addition of bis(pinacolato)diborane to 2,7-Dibromo-9,9-bis-(6-bromo-hexyl)-9H-fluorene 5

Freshly distilled DMF (7 mL) was flushed under argon. Bispinacolatodiborane (430 mg, 1.69 mmol), KOAc (498 mg, 5.08 mmol) and $PdCl_2$(dppf) (41 mg, 0.05 mmol) and 2,7-dibromo-9,9-bis-(6-bromo-hexyl)-9H-fluorene (500 mg, 0.77 mmol) were added. The red reaction mixture was flushed with argon for 15 min. Then, the reaction mixture was refluxed at 80 ^{o}C for overnight. The gray-black reaction mixture was added to cold water (50 mL) and organic layer was extracted with chloroform (30 mL X 4). The solvent was removed under reduced pressure to obtain light yellow crude product. The product was purified with coulumn chromatography packed with silica, and cyclohexane/ethyl acetate (10:1, v/v) as

eluent. The product was obtained as white fine powder after recrystallisation from cyclohexane.

Yield: 240 mg (% 42)

FT-IR (KBr pellet, cm^{-1}): 3062 (-CH, w), 2929 (-CH, s), 1736 (-C=0, s), 1346 (B-0, s)

^{1}H-NMR (400 MHZ, $CDCl_3$) δ_H 7.7-7.3 (m, 6H), 3.8 (t, 4H), 1.95 (m, 4H), 1.7 (m, 4H), 1.36 (s, 24H), 1.20(m, 8H), 0.65(m, 4H)

4.7 Synthesis of Azidoethylamine[42]

2-chloroethylamine hydrochloride (5.0 g, 0.04 mmol) was dissolved in water (50 mL). Sodium azide (2.48 g, 38.0 mmol) was added slowly into the former solution. The solution was refluxed at 70 ^oC for 2 d. Then, the reaction solution was cooled to rt. Addition of NaOH solution (20 mL, 4.4 M) followed by stirring for 2 h. Organic layer was extracted with DCM (50 mL). After drying the organic layer over $CaCl_2$, solvent was evaporated under reduced pressure to obtain light yellow oil.

Yield: 2.50 g (%67)

FT-IR(NaCl plates, cm^{-1}): 3369 (-NH), 2936 (-CH), 2102 (C-N_3)

4.8 Synthesis of Rotaxane

Cucurbit[6]uril (435.0 mg, 0.435 mmol) was dissolved in 6N HCl (15 mL) and stirred for 30 min. (2-Azido-ethyl)-(6-{9-[6-(2-azido-ethylamino)-hexyl]-2,7-dibromo-9H-fluoren-9-yl}-hexyl)-amine (131 mg, 0.198 mmol) in 5 mL of 6N HCl were added into former solution. Lastly propargylammonium salt (40 mg, 0. 435 mmol) was added. The reaction mixture was stirred for 3 d at rt. After evaporation of the solvent under reduced pressure, an orange film was observed. It was dissolved in minimum amount of water and precipitated into acetone (80 mL) for purification. The precipitates were collected via centrifugation at 2500 rpm for 20 min. The collected solids were dissolved in water and filtered by suction. The product was purified by precipitation into acetone to obtain white fine powders.

Yield: 104 mg (% 20)

FT-IR (KBr pellet, cm^{-1}): 3431 (-NH, b), 2929 (-CH, m), 1730 (-C=0, s)

^{1}H-NMR (400 MHZ, D_2O) selected δ_H 7.8-7.5 (m, 6H), 6.5 (s, 2H) 4.0-0.6 (alkyl protons)

4.9 Synthesis of poly[(9,9-Dihexyl-9H-fluorene)-co-alt-(9,9-bis-(6-bromo-hexyl)-9H-fluorene)] P1

2,7-Dibromo-9,9-bis-(6-bromo-hexyl)-9H-fluorene (975 mg, 0.150 mmol) and 9,9-dihexylfluorene-2,7-bis(trimethyleneborate) (754 mg, 0.150 mmol) were suspended in a mixture of degassed THF (15 ml) and H_2O (7 ml). $Pd(PPh_3)_4$ (21 mg) and K_2CO_3 (2.49 g, 18 mmol) were added sequentially. The mixture was degassed again and heated at 80 °C for 48 h under argon and then poured into methanol. The precipitate was collected by filtration and dissolved in chloroform. The solution was washed with water and concentrated under reduced pressure. The concentrated solution was poured into methanol; the solid residue was collected by centrifugation and dissolved in THF. The solution was added into stirred large excess of MeOH. The precipitate was collected by filtration and dried under vacuum to obtain yellowish powder.

Yield: 1.1 g 64%.

IR (KBr pellet, cm^{-1}):3019 (CH-, w), 2923 (CH-, s), 1600(C=C-, w), 1558(C=C-, w), 727(C-Br, m),

^{1}H-NMR (400 MHZ, $CDCl_3$) δ_H 7.85 (m, 12H), 3.32 (t, 4H, J=6 Hz), 2.16 (m, 4H), 1.71 (m, 4H), 1.22(m, 24H), 0.84(m, 14H)

^{13}C-NMR δ_c 140.5, 140.2, 139.9, 126.1, 121.1, 119.7, 54.7, 54.6, 39.6, 32.9, 31.8, 30.6, 28.8, 28.2, 26.9, 23.0, 21.6, 13.1

Mn:$8.90*10^3$ g/mol

Mw:$3.59*10^4$ g/mol

UV λmax : 384 nm (in Chlorofom)

PL λmax : 417 nm (in Chlorofom)

4.10 Synthesis of poly[(9,9-Dihexyl-9H-fluorene)-co-alt-(9,9-bis-(6-azido-hexyl)-9H-fluorene)] P2

Poly[(9,9-Dihexyl-9H-fluorene)-co-alt-(9,9-bis-(6-bromo-hexyl)-9H-fluorene)] **P1** (300 mg, 0.36 mmol) and NaN_3 (60 mg, 1.08 mmol) were suspended in dry DMF (5 ml) and heated at 60 °C for 24 h. The mixture was poured into water (20 mL) and extracted with diethyl ether (50 mLx3). The combined organic layer was washed with water, dried over $CaCl_2$ and concentrated under reduced pressure. The residue was precipitated into methanol. The precipitate was collected by centrifugation and dried under vacuum to obtain yellow solid.

Yield: 205 mg, 75%.

IR (KBr pellet, cm^{-1}): 3065(CH-), 2935 (CH-), 2859(CH-), 2100 (-N_3), 1613(C=C-), 1571(C=C-).

^{1}H-NMR (400 MHZ, $CDCl_3$) δ_H 7.75 (m, 12H), 3.16 (m, 4H,), 2.16 (m, 4H), 1.46 (m, 4H), 1.22(m, 24H), 0.82(m, 14H)

Mn:$3.68*10^3$ g/mol

Mw: 2.04×10^4 g/mol

UV λmax : 386 nm (in Chlorofom)

PL λmax : 417 nm (in Chlorofom)

4.11 Synthesis of poly[9,9-bis-(6-bromo-hexyl)-9H-fluorene-co-1,4-phenylene] P3

2,7-dibromo-9,9-bis-(6-bromo-hexyl)-9H-fluorene (500 mg, 0.77 mmol), 1–4 phenyl diboronic acid (125 mg, 0.76 mmol), $PdCl_2$ (dppf) (11 mg, 0.01 mmol), K_2CO_3 (1.275 g, 9.23 mmol) were dissolved in degassed THF (10 mL) and H_20 (5 mL) mixture and degassed with argon for 30 min. The reaction mixture was stirred at 80 ^oC for 3 d. The organic layer was extracted with chloroform (250 mL). It washed with water, brine, dried over $CaCl_2$ and concentrated under reduced pressure. Yellowish powder was obtained after further purification by precipitation into methanol (200 mL) three times.

Yield: 408 mg (% 94)

IR (KBr pellet, cm^{-1}): 3024 (CH-, w), 2929 (CH-, s) 1606(C=C-, w), 1518(C=C- w), 727 (C-Br, m)

^{1}H-NMR (400 MHZ, $CDCl_3$) δ_H 7.65 (m, 10H), 3.32 (t, 4H, J=3 Hz), 2.04 (m, 4H), 1.64 (m, 4H), 1.21(m, 8H), 0.80(m, 4H)

Mn:$1.37*10^3$ g/mol

Mw:$1.19*10^4$ g/mol

UV λmax: 366 nm (in THF)

PL λmax: 410 nm (in THF)

4.12 Synthesis of poly[9,9-bis-(6-azido-hexyl)-9H-fluorene-co-1,4-phenylene] P4

Poly[9,9-bis-(6-bromo-hexyl)-9H-fluorene-co-1,4-phenylene] **P3** (222 mg, 0.40 mmol) and sodium azide (54 mg, 0.83 mmol) were suspended in DMSO (10 mL) and heated at 60 ^oC for 2 d.

The mixture was poured into water (20 mL) and extracted with chloroform (50 mLx3). The combined organic layer was washed with water, dried over $CaCl_2$ and concentrated under reduced pressure. The residue was precipitated into methanol. The precipitate was collected by centrifugation and dried under vacuum to obtain yellowish powder.

Yield: 121 mg (62 %)

IR (KBr pellet, cm^{-1}): 3026 (CH-, w), 2928 (CH-, s), 2093(C-N_3, s), 1596(C=C-, w)

^{1}H-NMR (400 MHZ, $CDCl_3$) δ_H 7.35 (m, 8H), 3.25 (m, 4H), 1.98 (m, 4H), 1.57 (m, 4H), 1.21 (m, 8H), 0.75 (m, 4H)

Mn:$2.41*10^3$ g/mol

Mw:$1.46*10^4$ g/mol

UV λmax : 366 nm (in Chloroform)

PL λmax : 410 nm (in Chloroform)

4.13 Synthesis of poly[9,9-bis-(6-bromo-hexyl)-9H-fluorene-co-2,5-thienylene] P5

2,7-dibromo-9,9-bis-(6-bromo-hexyl)-9H-fluorene (800 mg, 1.23 mmol), thiophenediboronic acid (253.5 mg, 1.476 mmol), TBAB (20 mg, 0. 062 mmol), were suspended in a mixture of degassed THF (20 mL), H_2O (10 mL). $PdCl_2$ (dppf) (20 mg, 0. 025 mmol) and K_2CO_3 (2.04 g, 14.76 mmol) were added sequentially. The mixture was degassed again and heated at 60 °C for 2 d. The mixture was extracted with chloroform (100 mL) and the organic layer was washed with water (50 mL), brine and dried over $CaCl_2$. The organic layer was concentrated under reduced pressure and precipitated into methanol (200 mL). The yellow-brown precipitates were collected by centrifugation at 900 rpm for 30 min. Purification by precipitation into methanol and then collecting were repeated for three times to obtain brown powder.

Yield: 437 mg (62 %)
IR (KBr pellet, cm^{-1}): 3064 (CH-, w), 2925 (CH-, s) 1604(C=C-, w), 1568(C=C-, w), 730 (C-Br, m)
^{1}H-NMR (400 MHZ, $CDCl_3$) δ_H 7.35 (m, 8H), 3.20 (m, 4H), 1.97 (m, 4H), 1.58 (m, 4H), 1.08 (m, 8H), 0.60(m, 4H)
Mn:$6.98*10^2$ g/mol
Mw:$1.97*10^3$ g/mol
UV λmax : 400 nm (in Chloroform)
PL λmax : 464 nm (in Chloroform)

4.14 Synthesis of poly[9,9-Dihexyl-9H-fluorene] P6

9,9-Dihexyl-2,7-dibromofluorene (250 mg, 0.50 mmol), 9,9-Dihexylfluorene-2,7-bis(trimethyleneborate) (255 mg, 0.50 mmol), TBAB (8.10 mg, 0. 026 mmol) were suspended in degassed Toluene (10 mL). $Pd(PPh_3)_4$ (11.8 mg, 0.01 mmol) and K_2CO_3 (841 mg, 6.10 mmol) were added sequentially. The mixture was degassed again and heated at 60 °C for 2 d and then poured into methanol. The precipitate was collected by filtration and dissolved in chloroform. The solution was washed with

water and concentrated under reduced pressure. The concentrated solution was poured into methanol; the solid residue was collected by centrifugation and dissolved in dichloromethane. The solution was added into stirred large excess of MeOH. The precipitate was collected by filtration and dried under vacuum to obtain yellow powder.

Yield: 216 mg (% 64)

IR (KBr pellet, cm^{-1}): 3031 (CH-, w), 2929 (CH-, s) 1606(C=C-, w)

UV λmax: 373 nm (in Dichloromethane)

PL λmax: 418 nm (in Dichloromethane)

4.15 Synthesis of poly[(9,9-Dihexyl-9H-fluorene)-co-alt-(9,9-bis-6-(azidoethylamino)-hexyl-9H-fluorene)] P7

P1 (110 mg, 0.024 mol) was added into azidoethylamine (1.106 g, 0.012 mol) and heated gently about 30 ^{o}C. THF (3 mL) was added and the solution was stirred for 3 d. The mixture was poured into water and the organic layer was extracted with chloroform (20 mL). Yellow powder was obtained after evaporation of the solvent under reduced pressure.

Yield: 105 mg (94 %)

FT-IR (KBr pellet, cm^{-1}): 3327 (-NH, b), 3053 (-CH, w), 2929 (-CH, s), 2099 (C-N_3, s)

4.16 Synthesis of CB6-Py inclusion complex

Cucurbit(6)uril (100 mg, 0.100 mmol) was dissolved in 3 mL 0.1M NaCl solution. Pyrrole (7 μL, 0.110 mmol) in 1 mL of water was added to obtain a clear solution. After about 15 minutes clear solution became cloudy and viscous. The mixture was stirred overnight and the solid was separated by centrifugation. The white fine powder was dried under vacuum overnight.

Yield: 75 mg (% 70)

IR (KBr pellet, cm^{-1}): 3426 (-NH), 1702 (-C=0)

^{1}H NMR (400 MHz, 0.2 M NaCl in D_2O): δ_H 6.79 (m, 1H), 6.13 (m, 1H), 5.93 (t, 1H, $^{3}J_{HH}$= 1.9 Hz) 5.70 (m, 12H, CB6), 5.50 (m, 12H, CB6) 5.25 (t, 1H, $^{3}J_{HH}$= 1.9 Hz), 4.21 (m, 12H, CB6)

4.17 Polymerisation of Complex via Acid Catalysis

CB6-Py inclusion complex (50 mg, 0.05 mmol) was dissolved in 3 mL 6M HCl and an aqueous solution of $FeCl_3.6H_20$ (13 mg, 0.05 mmol) was added; light yellow clear solution was obtained which was stirred at rt overnight. The colour of the reaction solution turned into light brown. It was poured into acetone (30 mL). Salmon-coloured precipitates were collected via centrifugation and dried under vacuum overnight

Yield: 36 mg, 72%

IR (KBr pellet, cm^{-1}): 3426 (-NH), 1702 (-C=0)

^1H NMR (400 MHz, DMSO/D_2O): δ_H 6.7 (m, 2H), 6.1 (m, 2H), 5.70 (m, 12H, CB6), 5.5 (m, 1H), 5.4 (m, 12H, CB6), 4.7 (m, 1H), 4.2 (m, 12H, CB6)

UV λmax : 490 nm (in 6N HCl)

PL λmax : 521 nm (in 6N HCl)

REFERENCES

1- Shirakawa, H.; Louis, E.J.; MacDiarmid, A.G.; Chiang, C.K; Heeger, A.J.; *J Chem Soc Chem Comm.*, 1977,579

2- Burroughes, J. H.; Bradley, D. D. C.; Brown A. R., Marks, R. N.; Mackay, K.; Friend, R. H.; Burns, P. L.; Holmes, A. B.; *Nature*, 1990, 347, 539–541

3- Kraft, A.; Grimsdale, A. C.; Holmes, A. B.; *Angew. Chem. Int. Ed.*, 1998, 37, 402

4- Friend, R. H.; Gymer, R. W.; Holmes, A. B.; Burroughes, J. H.; Marks, R. N.; Taliani, C.; Bradley, D. C. C.; Dos Santos, D. A.; Brdas, J. L.; Lgdlund, M.; Salaneck, W. R.; *Nature*, 1999, 397, 121

5- Bernius, M.T.; Inbasekaran, M.; O'Brien, J.; Wu, W.; *Adv. Mater.*, 2000, 12, 1737

6- Mitschke, U.; Bauerle, P. J. J.; *Mater. Chem.*, 2000, 10

7- Sariciftci, N.S.; Braun, D.; Zhang, C.; Sardanov, V.; Heeger, A.J.; Stucky, G.; Wudl, F.; *Appl. Phys. Lett.,* 1993, 62, 585

8- McQuade, D.T.; Pullen, A. E.; Swager, T. M.; *Chem. Rev.*, 2000, 100, 2537-2574

9- Tessler, N.; Denton, G. J.; Friend, R. H.; *Nature*,1996, 382, 695-697

10- http://www.cdtltd.co.uk/technology/36.asp

11- Leclerc, M.; *Journal of Polymer Science: Part A: Polymer Chemistry*, 2001, vol. 39, 2867-2873

12- Lakowicz, J. R.; Principles of Fluorescence Spectroscopy, 2nd ed. (Kluwer Academic, Dordrecht/Plenum, New York, 1999), p. 11

13- List, E. J. W.; Gaal, M.; Guentner, R.; de Freitas, P. S.; Scherf, U.; *Synth. Met.*, 2003, 139, 759

14- Lemmer, U.; Heun, S.; Mahrt, R.F.; Scherf, U.; Hopmeier, M.; Siegner, U.; Göbel, E.O.; Müllen, K.; Bässler, H.; *Chem. Phys. Lett.*, 1996, 240, 373

15- Zhao, W.; Cao, T.; White, J.M.; *Advanced Functional Materials*, 2004, 14, 783

16- Denton, G. J.; Tessler, N.; Harrison, N.T.; Friend, R.H.; *Phys. Rev. Lett.*, 1997, 78, 733

17- P.Einzel, T. Bein, J. Phys. Chem.1989, 93, 6270

18- Kim, B. H.; Jung, J. H.; Kim, J. W.; Choi, H. J.; Joo, J.; *Synth. Met.*, 2001, 121, 1311

19- Wu, Q.; Xue, Z.; Qi, Z.; Wang, F.; *Polymer,* 2000, 41, 2029-2032

20- (a) Yeh, J.M.; Chin, C.P.; Chang, S.; *Journal of Applied Polymer Science,* 2003,vol. 88, 3264–3272 (b) Anuar, K.; Murali, S.; Fariz, A.; Ekramul, H. N. M. M.; *Materialsscience (Medziagotyra),* 2004, vol. 10, no. 3

21- Yoshida, K.; Shinomura, T.; Ito, K.; Hayakawa, R.; *Lagmuir*, 1999, 15, 910-913

22- Shinomura, T.; Yoshida, K.; Ito, K.; Hayakawa, R.; *Polym. Adv. Technol.* , 2000, 11, 837- 839

23- Lagrost, C.; Ching, K.I.C.; Lacroix, J.C.; Aeiyach, S.; Jouini, M.; Lacaze, P.C.; Tanguy, J. J.; *Mater. Chem.*, 1999, 10, 2351- 2358

24- Takashima, Y.; Oizumi, Y.; Sakamoto, K.; Miyauchi, M.; Kamitori, S.; Harada, A.; *Macromolecules*, 2004, 37, 3962 – 3964

25- Boogaard, M. V. D.; Bonnet, G.; Hof, P.V.; Wang, Y.; Brochon, C.; Hutten, P. V.; Lapp, A.; Hadziioannou, G.; *Chem. Mater.*, 2004, 16, 4383 – 4385

26- Storsberg J.; Ritter, H.; Pielartzik, H.; Groenendaal, L.; *Adv. Mater.*, 2000, no.8, 12

27- McGehee, M. D.; Heeger, A. J.; *Advanced Materials*, 2000, 12, 1655.

28- Cacialli, F.; Wilson, J. S.; Michels, J. J.; Daniel, C.; Silva, C.; Friend, R.H.; Severin N, Samori P, Rabe JP, O'Connell J, Taylor PN, Anderson H.L., *Nature Materials*, 2002, 1, 160-164

29- Marsitzky, D.; Vestberg, R.; Blainey, P.; Tang, B.T.; Hawker, C. G.; Carter, K. R.; Am, J.; *Chem. Soc.*, 2001, 123, 6965 – 6972

30- Tiftik, H. B.; Masters Thesis, May 2007.

31- Setayesh, S.; Grimsdale, A. C.; Weil, T.; Enkelmann, V.; Mullen, K.; Meghdadi, F.; List, E. J. W.; Leising, G.; *JACS*, 2001, vol. 123, no.5, 946-953

32- Behrend, R.; Meyer, E.; Rusche, F.; *Justus Liebigs Ann. Chem.*, 1905, *339*, 1-37.

33- Sun, Y.; Giebink, N. C.; Kanno, H.; Ma, B.; Thomson, M. E.; Forrest, S. R.; *Nature*, 2006, 440, 908–912

34- Lee, S. K.; Hwang, D. H.; Jung, B. J.; Cho, N. S.; Lee, J.; Lee, J. D.; Shim, H. K.; *Adv. Funct. Mate*r.; 2005, 15, 1647-1655.

35- Luo, J.; Li, X.; Hou, Q.; Peng, J. B.; Yang, W.; Cao, Y.; *Adv. Mater.*, 2007, 19, 1113- 1117

36- Liu, J.; Zhou, Q. G.; Cheng, Y. X.; Geng, Y. H.; Wang, L. X.; Ma, D. G.; Jing, X. B.; Wang, F. S.; *Adv. Fuct. Mater.*, 2006, 16, 957- 965

37- Mock, W. L.; Pierpont J.; *J. Chem. Soc., Chem. Commun*., 1990, 1509 - 1511

38- Liu, J.; Xie, Z. Y.; Cheng, Y. X.; Geng, Y. H.; Wang, L. X.; Jing, X. B.; Wang, F. S.; *Adv. Mater.*, 2007, 19, 531-535.

39- Hide, F.; Kozodoy, P.; DenBaars, S. P.; Heeger, A. J.; *Appl. Phys. Le tt.*, 1997, 70, 2664

40- Guha, S.; Haight, R.A.; Bojarczuk, N. A.; Kisker, D. W.; *J. Appl. Phys*, 1997, 82, 4126

41- Heliotis, G.; Stavrinou, P.N.; Bradley, D.D.C.; Gu, E.; Griffin, C.; Jeon, C.W.; Dawson, M.D.; *Applied Physics Letters*, 2005, 87, 103505

42- Ben-Efraim, D. A.; *Tetrahedron*, 1973, 29, 4111.

43- Miyaura, N.; Suzuki, A.; *Chem. Rev.,* 1995, 95, 2457- 2483

44- Murray, K. A.; Holmes, A. B.; Moratti, S. C.; Rumbles, G.; *J. Mater. Chem*., 1999, *9*, 2109.

45- Pogantsch, A.; Wenzl, F. P.; List, E. J. W.; Leising, G.; Grimsdale,A. C.; Müllen, K.; *Adv. Mater.*, 2002, 14, 1061- 1064

46- McNeill, R.; Siudak, R.; Wardlaw, J. H.; Weiss, D. E.; *Aust. J. Chem.*, 1963, 16, 1056- 75

47- Skotheim, T. A.; Elsenbaumer, R. L.; *Handbook of Conducting Polymers*, 2nd ed. (Ed: J. R. Reynolds), Marcel Dekker, New York 1998

48- Song, H. K.; Tayhas G.; Palmore, R.; *Adv. Mater.,* 2006, 18, 1764- 1768.

49- a) Hawkins, S. J.; Ratcliffe, N. M.; *J. Mater. Chem.*, 2000, 10, 2057 b) Dias, H. V. R.; Fianchini, M. ; Rajapakse, R. M. G. ; *Polymer*, 2006, 47. 7349 c) Nabid, M. R. ; Entezami, A. A. ; *J. Applied Polymer Science*, 2004, 94, 254

50- a) Jeon, Y. M.; Kim, J.; Whang, D.; Kim, K.; *J. Am. Chem. Soc.*, 1996, 118, 9790 b) Whang, D.; Heo,J.; Park, J. H.; Kim, K.; *Angew. Chem. Int. Ed.*, 1998, 37, 78 c) Tarmyshov, K. R.; Muller-Plathe, F.; J. *Phys. Chem. B*, 2006, 110, 14463

51- Patil, A. O.; Heeger, A. J.; Wudl, F.; *Chem. Rev*., 1988, 88, 183

52- Bufon, C. C. C.; Vollmer, J.; Heinzel, T.; Espindole, P.; John, H.; Heinze, J.; *J. Phys. Chem. B*, 2005, 109, 19191

53- Hou, Z. S.; Tan, Y. B.; Kim, K.; Zhou, Q. F.; *Polymer*, 2006, 47, 5267

54- Li, J.; Yan, D.; *Macromolecules,* 2001, 34, 1542.

55- a)Huyal, I. O.; Koldemir Ü; Ozel T., Nizamoglu S.; Tuncel D.; Demir H. V.; White Light Emission with High Color Rendering Index > 90 from Single-Layer Azide Functionalized Polyfluorene-Copolymer on Near-UV Light Emitting Diode (in preparation) b) Huyal, I. O.; Ozel, T.; Nizamoğlu, S.; Koldemir, U.; Tuncel, D.; Demir, H. V.; Conference on Lasers and Electro-Optics (CLEO) and Quantum Electronics and Laser Science Conference (Quels), Baltimore, 2007.

56- Tuncel, D.; Koldemir, U. Synthesis of Cucurbituril-Encapsulated Polypyrrole.(submitted)

57- http://www.olympusmicro.com/primer/techniques/fluorescence/fret/fretintro.html